Digital Comprehensive Summaries of Uppsala Dissertations
from the Faculty of Pharmacy 335

Theranostic Targeting of GRPR and PSMA in Prostate Cancer

AYMAN ABOUZAYED

ACTA UNIVERSITATIS
UPSALIENSIS
2023

ISSN 1651-6192
ISBN 978-91-513-1828-8
urn:nbn:se:uu:diva-501391

UPPSALA
UNIVERSITET

Dissertation presented at Uppsala University to be publicly examined in Fåhræussalen, Rudbecklaboratoriet, Dag Hammarskjölds Väg 20, 752 37, Uppsala, Friday, 1 September 2023 at 10:00 for the degree of Doctor of Philosophy (Faculty of Pharmacy). The examination will be conducted in English. Faculty examiner: PD Dr. Cristina Müller (Center for Radiopharmaceutical Sciences, the Paul Scherrer Institute).

Abstract

Abouzayed, A. 2023. Theranostic Targeting of GRPR and PSMA in Prostate Cancer. *Digital Comprehensive Summaries of Uppsala Dissertations from the Faculty of Pharmacy* 335. 94 pp. Uppsala: Acta Universitatis Upsaliensis. ISBN 978-91-513-1828-8.

This thesis is based on five original articles that investigated the theranostics of prostate cancer by gastrin-releasing peptide receptor (GRPR) and prostate-specific membrane antigen (PSMA) targeting. GRPR and PSMA are two extensively evaluated prostate cancer cell markers due to their overexpression in the majority of prostate cancer samples. Theranostic targeting of GRPR and PSMA is an attractive strategy to improve the management of prostate cancer patients.

Papers I and II focused on the dual targeting of GRPR and PSMA. The effect of linker modification on the affinity for GRPR and PSMA and the pharmacokinetic profile was evaluated. In Paper III, the effect of the GRPR antagonist RM26 conjugation to an albumin-binding domain on the pharmacokinetic profile and its potential use in therapy was investigated. Paper IV focused on developing a GRPR antagonist that was suitable for single-photon emission computed tomography (SPECT) using technetium-99m. In Paper V, the GRPR antagonist developed in Paper IV was translated into a phase I clinical trial to assess safety and dosimetry.

Modifying the linkers in GRPR and PSMA heterodimers can largely impact the affinity for both targets. This modification influenced the in vivo targeting specificity and biodistribution, with [^{125}I]I-BO530 in Paper I and [^{111}In]In-BQ7812 in Paper II outperforming other analogues. Our findings in Paper III indicated that the conjugation of an albumin-binding domain to RM26 increased the blood concentration of the radiotracer. This increase led to elevated and stable tumour uptake of [^{111}In]In-DOTA-ABD-RM26 after several days of injection. However, [^{111}In]In-DOTA-ABD-RM26 was also increasingly taken up by various healthy organs. The GRPR antagonist [^{99m}Tc]Tc-maSSS-PEG$_2$-RM26, studied in Paper IV, showed high specificity and affinity for GRPR. This resulted in elevated GRPR-mediated uptake. Additionally, maSSS-PEG$_2$-RM26 could be radiolabelled via a straightforward radiolabelling protocol. Clinical evaluation of [^{99m}Tc]Tc-maSSS-PEG$_2$-RM26 in prostate and breast cancer patients (Paper V) demonstrated the safety and tolerability of the radiotracer, with favourable dosimetry and no side effects.

In conclusion, this thesis evaluated different tools for the theranostic targeting of GRPR and PSMA. The findings warrant further investigation to optimise the reported radiotracers.

Keywords: prostate cancer, gastrin-releasing peptide receptor (GRPR), prostate-specific membrane antigen (PSMA), nuclear medicine, molecular imaging, radiotracers, theranostics

Ayman Abouzayed, Department of Medicinal Chemistry, Box 574, Uppsala University, SE-75123 Uppsala, Sweden.

ISSN 1651-6192
ISBN 978-91-513-1828-8
URN urn:nbn:se:uu:diva-501391 (http://urn.kb.se/resolve?urn=urn:nbn:se:uu:diva-501391)

وَأَنْ لَيْسَ لِلْإِنْسَانِ إِلَّا مَا سَعَى

To my beloved family

List of Papers

This thesis is based on the following papers, which are referred to in the text by their Roman numerals.

I. **Abouzayed**, **A**.*, Yim, C.B.*, Mitran, B., Rinne, S.S., Tolmachev, V., Larhed, M., Rosenström, U., Orlova, A. (2019) Synthesis and Preclinical Evaluation of Radio-Iodinated GRPR/PSMA Bispecific Heterodimers for the Theranostics Application in Prostate Cancer. *Pharmaceutics*, 11(7):358

II. Lundmark, F.*, **Abouzayed**, **A**.*, Mitran, B., Rinne, S.S., Varasteh, Z., Larhed, M., Tolmachev, V., Rosenström, U., Orlova, A. (2020) Heterodimeric Radiotracer Targeting PSMA and GRPR for Imaging of Prostate Cancer–Optimization of the Affinity towards PSMA by Linker Modification in Murine Model. *Pharmaceutics*, 12(7):614

III. **Abouzayed**, **A**., Tano, H., Nagy, Á., Rinne, S.S., Wadeea, F., Kumar, S., Westerlund, K., Tolmachev, V., Karlström, A.E., Orlova, A. (2020) Preclinical Evaluation of the GRPR-Targeting Antagonist RM26 Conjugated to the Albumin-Binding Domain for GRPR-Targeting Therapy of Cancer. *Pharmaceutics*, 12(10):977

IV. **Abouzayed**, **A**., Rinne, S.S., Sabahnoo, H., Sörensen, J., Chernov, V., Tolmachev, V., Orlova, A. (2021) Preclinical Evaluation of ^{99m}Tc-Labeled GRPR Antagonists maSSS/SES-PEG_2-RM26 for Imaging of Prostate Cancer. *Pharmaceutics*, 13(2):182

V. Chernov, V., Rybina, A., Zelchan, R., Medvedeva, A., Bragina, O., Lushnikova, N., Doroshenko, A., Usynin, E., Tashireva, L., Vtorushin, S., **Abouzayed**, **A**., Rinne, S.S., Sörensen, J., Tolmachev, V., Orlova, A. (2023) Phase I Trial of [^{99m}Tc]Tc-maSSS-PEG_2-RM26, a Bombesin Analogue Antagonistic to Gastrin-Releasing Peptide Receptors (GRPRs), for SPECT Imaging of GRPR Expression in Malignant Tumors. *Cancers (Basel)*, 15(6):1631

* Equal contribution

Reprints were made with permission from the respective publishers.

List of Publications Not Included in this Thesis

I. Lundmark, F.*, **Abouzayed**, **A**.*, Rinne, S.S., Timofeev, V., Sipkina, N., Naan, M., Kirichenko, A., Vasyutina, M., Ryzhkova, D., Tolmachev, V., Rosenström, U., Orlova, A. (2023) Preclinical Characterisation of PSMA/GRPR-Targeting Heterodimer [^{68}Ga]Ga-BQ7812 for PET Diagnostic Imaging of Prostate Cancer: A Step towards Clinical Translation. *Cancers (Basel)*, 15(2):442

II. Rinne, S.S., Yin, W., Borras, A.M., **Abouzayed**, **A**., Leitao, C.D., Vorobyeva, A., Löfblom, J., Ståhl, S., Orlova, A., Gräslund, T. (2022) Targeting Tumor Cells Overexpressing the Human Epidermal Growth Factor Receptor 3 with Potent Drug Conjugates Based on Affibody Molecules. *Biomedicines*, 10(6):1293

III. Lundmark, F., Olanders, G., Rinne, S.S., **Abouzayed**, **A**., Orlova, A., Rosenström, U. (2022) Design, Synthesis, and Evaluation of Linker-Optimised PSMA-Targeting Radioligands. *Pharmaceutics*, 14(5):1098

IV. Rinne, S.S., Leitao, C.D., **Abouzayed**, **A**., Vorobyeva, A., Tolmachev, V., Ståhl, S., Löfblom, J., Orlova, A. (2021) HER3 PET Imaging: ^{68}Ga-Labeled Affibody Molecules Provide Superior HER3 Contrast to ^{89}Zr-Labeled Antibody and Antibody-Fragment-Based Tracers. *Cancers (Basel)*, 13(19):4791

V. Rinne, S.S., **Abouzayed**, **A**., Gagnon, K., Tolmachev, V., Orlova, A. (2021) ^{66}Ga-PET-imaging of GRPR-expression in prostate cancer: production and characterization of [^{66}Ga]Ga-NOTA-PEG$_2$-RM26. *Sci Rep*, 11(1):3631

VI. Güler, R., Svedmark, S.F., **Abouzayed**, **A**., Orlova, A., Löfblom, J. (2020) Increasing thermal stability and improving biodistribution of VEGFR2-binding affibody molecules by a combination of in silico and directed evolution approaches. *Sci Rep*, 10(1):18148

* Equal contribution

VII. Vorobyeva, A., Bezverkhniaia, E., Konovalova, E., Schulga, A., Garousi, J., Vorontsova, O., **Abouzayed**, **A**., Orlova, A., Deyev, S., Tolmachev, V. (2020) Radionuclide Molecular Imaging of EpCAM Expression in Triple-Negative Breast Cancer Using the Scaffold Protein DARPin Ec1. *Molecules*, 25(20):4719

VIII. Deyev, S.M., Vorobyeva, A., Schulga, A., **Abouzayed**, **A**., Günther, T., Garousi, J., Konovalova, E., Ding, H., Gräslund, T., Orlova, A., Tolmachev, V. (2020) Effect of a radiolabel biochemical nature on tumor-targeting properties of EpCAM-binding engineered scaffold protein DARPin Ec1. *Int J Biol Macromol*, 145:216–225

IX. Rinne, S.S., Dahlsson Leitao, C., Gentry, J., Mitran, B., **Abouzayed**, **A**., Tolmachev, V., Ståhl, S., Löfblom, J., Orlova, A. (2019) Increase in negative charge of ^{68}Ga/chelator complex reduces unspecific hepatic uptake but does not improve imaging properties of HER3-targeting affibody molecules. *Sci Rep*, 9(1):17710

X. Mitran, B., Varasteh, Z., **Abouzayed**, **A**., Rinne, S.S., Puuvuori, E., De Rosa, M., Larhed, M., Tolmachev, V., Orlova, A., Rosenström U. (2019) Bispecific GRPR-Anatonistic Anti-PSMA/GRPR Heterodimer for PET and SPECT Diagnoistic Imaging of Prostate Cancer. *Cancers (Basel)*, 11(9):1371

XI. Oroujeni, M.*, **Abouzayed**, **A**.*, Lundmark, F., Mitran, B., Orlova, A., Tolmachev, V., Rosenström, U. (2019) Evaluation of Tumor-Targeting Properties of an Antagonistic Bombesin Analogue RM26 Conjugated with a Non-Residualizing Radioiodine Label Comparison with a Radiometal-Labelled Counterpart. *Pharmaceutics*, 11(8):380

* Equal contribution

Contents

Introduction 13
Prostate Cancer 13
Anatomy of the Prostate 14
Progression to Malignancy 14
Diagnosis of Prostate Cancer 16
Prostate-Specific Antigen Screening 16
Digital Rectal Examination and Biopsy 17
Gleason Grading System 17
Imaging of Prostate Cancer 18
Staging of Prostate Cancer 18
Radionuclide-Based Molecular Imaging of Prostate Cancer 19
Radiotracers Used in Prostate Cancer Imaging 21
Management of Prostate Cancer 22
Localised Prostate Cancer 22
Locally Advanced Prostate Cancer 23
Metastatic Prostate Cancer 23
Prostate-Specific Membrane Antigen 25
Chemical Structures of Tracers Targeting PSMA 30
Gastrin-Releasing Peptide Receptor 32
Chemical Structures of Tracers Targeting GRPR 36
Dual Targeting of GRPR and PSMA in Prostate Cancer 38
Selection of a Suitable Radionuclide 39
Selection of a Suitable Chelator and Linker 40
Selection of a Suitable Targeting Ligand 40
Strategies to Improve Tumour Uptake and Pharmacokinetics 41
Binding to Serum Albumin 41
Reduction of Undesirable Accumulation of Radioactivity 41

Aims of this Thesis 43

Paper I 44
Synthesis and Preclinical Evaluation of Radio-Iodinated GRPR/PSMA Bispecific Heterodimers for the Theranostics Application in Prostate Cancer 44
Background and Aim 44
Results and Discussion 44

Conclusion 49

Paper II 50
Heterodimeric Radiotracer Targeting PSMA and GRPR for Imaging of Prostate Cancer–Optimization of the Affinity towards PSMA by Linker Modification in Murine Model 50
Background and Aim 50
Results and Discussion 50
Conclusion 54

Paper III 55
Preclinical Evaluation of the GRPR-Targeting Antagonist RM26 Conjugated to the Albumin-Binding Domain for GRPR-Targeting Therapy of Cancer 55
Background and Aim 55
Results and Discussion 55
Conclusion 58

Paper IV 59
Preclinical Evaluation of ^{99m}Tc-Labeled GRPR Antagonists maSSS/SES-PEG$_2$-RM26 for Imaging of Prostate Cancer 59
Background and Aim 59
Results and Discussion 60
Conclusion 62

Paper V 63
Phase I Trial of [^{99m}Tc]Tc-maSSS-PEG$_2$-RM26, a Bombesin Analogue Antagonistic to Gastrin-Releasing Peptide Receptors (GRPRs) for SPECT Imaging of GRPR Expression in Malignant Tumors 63
Background and Aim 63
Results and Discussion 64
Conclusion 67

Concluding Remarks 68

Ongoing and Future Studies 70

Appendix 71

Acknowledgements 72

References 76

Abbreviations

% IA/g	Percentage of injected activity per gram
ABD	Albumin-binding Domain
ADT	Androgen deprivation therapy
AR	Androgen receptor
AUC	Area under the curve
BBN	[Leu^{13}]Bombesin
CDR	Cancer detection rate
CT	Computed tomography
DNA	Deoxyribonucleic acid
DOTA	1,4,7,10-tetraazacyclododecane-1,4,7,10-tetraacetic acid
DRE	Digital rectal examination
DUPA	2-[3-(1,3-dicarboxypropyl)ureido]pentanedioic acid
EBRT	External beam radiation therapy
EDTA	Ethylenediaminetetraacetic acid
FCH	Fluoromethylcholine
FDA	Food and Drug Administration
FDG	Fluorodeoxyglucose
FDHT	16β-fluoro-5α-dihyrotestosterone
FECH	Fluoroethylcholine
FMISO	Fluoromisonidazole
FSPG	(4*S*)-4-(3-fluoropropyl)-L-glutamic acid
GRP	Gastrin-releasing peptide
GRPR	Gastrin-releasing peptide receptor
HSA	Human serum albumin
IC_{50}	Half-maximal inhibitory concentration
K_D	Equilibrium dissociation constant
log*D*	Octanol-water distribution coefficient
mCRPC	Metastatic castration-resistant prostate cancer
MDP	Methylene diphosphonate
mpMRI	Multiparametric magnetic resonance imaging
MRI	Magnetic resonance imaging
NAAG	N-acetyl-L-aspartyl-L-glutamate
NOTA	1,4,7-triazacyclononane-1,4,7-triacetic acid
p.i	Postinjection
PEG	Polyethyleneglycol

PET	Positron emission tomography
PI-RADS	Prostate imaging reporting and data system
PIN	Prostatic intraepithelial neoplasia
PSA	Prostate-specific antigen
PSMA	Prostate-specific membrane antigen
RCP	Radiochemical purity
SPECT	Single-photon emission computed tomography
SUV	Standardised uptake value
$t_{1/2}$	Half-life
TNM	Tumour-lymph node-metastasis
TPUS-Bx	Transperineal ultrasound-guided biopsy
TRUS-Bx	Transrectal ultrasound-guided biopsy

Introduction

Prostate Cancer

Prostate cancer is the second most commonly diagnosed cancer in men, resulting in more than 1.4 million new cases and over 370,000 deaths in 2020 [1]. Several factors increase the risk of developing prostate cancer. These risk factors include age, with the risk of developing prostate cancer increasing with age, and family history, with men having a family member previously diagnosed with prostate cancer being at twofold higher risk of developing the disease. One more major risk factor is race, with African Americans being at higher risk of developing prostate cancer. Lifestyle choices may also contribute to developing prostate cancer.

A man with an elevated risk of developing prostate cancer is recommended to take periodic blood tests for early detection. If prostate cancer is suspected, the person undergoes several tests that can include physical examination and biopsy of the prostate. Imaging is then necessary to determine the extent of the disease and provide the best possible treatment regimen.

There are several treatment options to manage prostate cancer patients based on the Gleason score of the malignant tissue and the stage of the disease. The age and health status of the patient are also taken into consideration when choosing the optimal treatment. Watchful waiting, active surveillance, radical prostatectomy, hormonal therapy, brachytherapy, chemotherapy, immunotherapy, palliative treatment, external beam radiation therapy and radionuclide therapy are the major treatment options available for prostate cancer patients.

Anatomy of the Prostate

The human prostate has the shape of an inverted cone, with its base situated by the urinary bladder and its apex contacting the penile urethra. It is located inferior to the urinary bladder, superior to the perineal membrane, and anterior to the rectum[2]. The prostate can be divided into an anterior lobe, a median lobe, lateral lobes, and a posterior lobe.

In the previous century, John E. McNeal established the widely accepted histological zone division of the prostate gland (Figure 1), in which it can be divided into a peripheral zone, which constitutes approximately 70% of the gland; a transition zone, which surrounds part of the urethra; and a central zone, which makes up the base of the prostate gland[3–5]. The prostate also includes anterior fibromuscular stroma and is surrounded by a fibrous layer called a capsule.

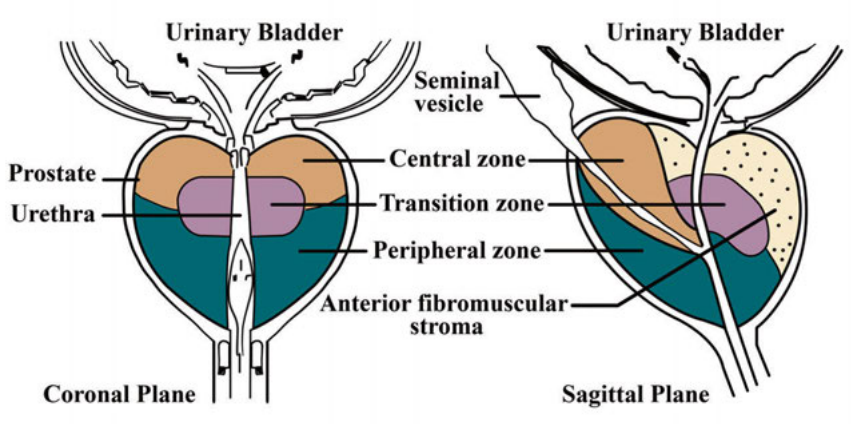

Figure 1. Schematic illustration of the human prostate gland.

Progression to Malignancy

Among the different benign lesions of the prostate, prostatic intraepithelial neoplasia (PIN) is considered a precursor for prostate cancer[6]. PIN is a confined neoplastic proliferation of epithelial cells of the prostate, and it can be divided into low- and high-grade PIN, with the latter being highly associated with invasive disease[7,8]. PIN can develop into localised prostate cancer, which can progress to advanced prostate cancer with local invasion and then to metastatic prostate cancer (Figure 2).

The most common site of prostate cancer metastases is bone (84.4% of patients with metastatic prostate cancer), followed by distant lymph nodes (10.6%), liver (10.2%), and thorax (9.1%), and to a lower extent, metastases

can be found in the brain, digestive system, retroperitoneum, kidneys, and adrenal glands[9]. In the 1990s, the term oligometastatic cancer was proposed as an intermediate cancer stage that is characterised by a low number of metastases and may be approached with curative intent[10].

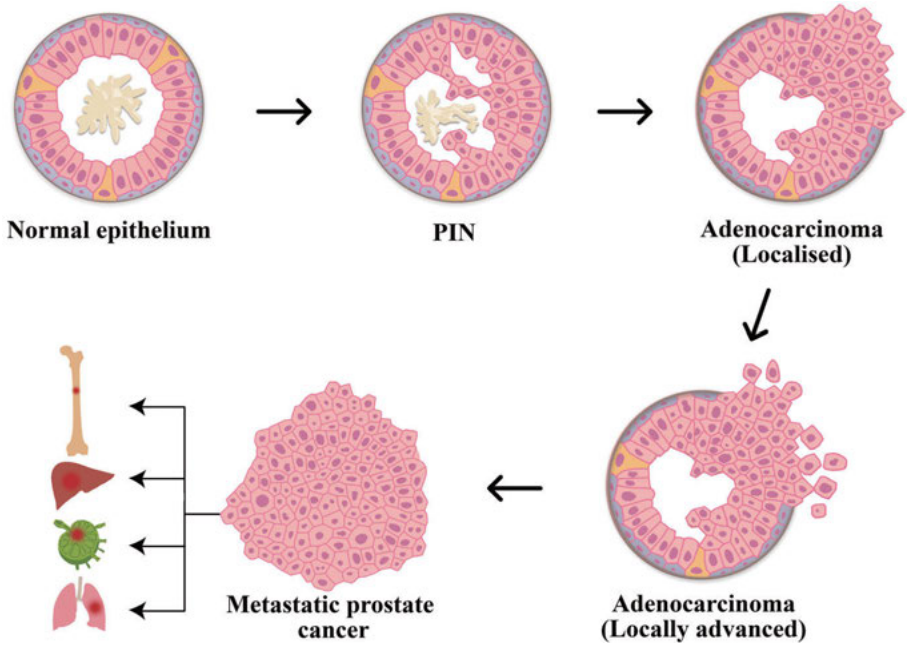

Figure 2. Progression of prostate cancer and main sites of metastases. *Adapted from Wang et al., 2018, Genetics and biology of prostate cancer, under CC BY-NC 4.0, (https://doi.org/10.1101/gad.315739.118)*.

Prostate cancer is a heterogeneous disease and is often multifocal and multizonal[11]. The majority of prostate cancers (>70%) originate in the posterior region of the peripheral zone. Approximately 10–20% of prostate cancers arise from the transition zone, and a small percentage arise from the central zone[12,13]. While prostate cancer originates primarily in the peripheral zone, benign prostatic hyperplasia arises from the transition zone[14,15]. The location of prostate cancer origin may be of substantial value. For example, a study suggested that peripheral zone prostate cancers may lead to worse clinical outcomes than prostate cancers originating in the transition zone[16].

The vast majority of prostate cancers are adenocarcinomas, which include two subtypes: acinar adenocarcinoma, which constitutes the majority of prostate cancer types, and ductal adenocarcinoma, which tends to spread more quickly than acinar adenocarcinoma. Other types of prostate cancers include squamous cell carcinoma, transitional cell carcinoma, neuroendocrine carcinoma and sarcomas[17].

Diagnosis of Prostate Cancer

Patients with prostate cancer are usually asymptomatic during the early stages of the disease. Patients with localised or locally advanced prostate cancer may experience urinary obstruction, haematuria, and haematochezia, among other symptoms. In metastatic prostate cancer, pelvic or lumbar pain may become the main symptom in addition to lethargy and weight loss. A patient with prostate cancer usually presents with an elevated prostate-specific antigen (PSA) level in blood. Detection of high PSA levels is often followed by a digital rectal examination (DRE). If the prostate gland feels suspicious during the DRE, the patient will then undergo ultrasound-guided biopsy, before or after multiparametric magnetic resonance imaging (mpMRI), to assess the state of the prostate gland and confirm malignancy. Depending on the tumour stage, PSA value, and Gleason score, the patient can undergo other imaging methods such as positron emission tomography (PET), single-photon emission computed tomography (SPECT) and bone scans for further assessment and deciding on the optimal treatment plan[18].

Prostate-Specific Antigen Screening

PSA is a glycoprotein produced by the epithelium of the prostate and released into the circulation. Serum PSA exists in free and complexed forms, and their concentrations in blood can be estimated using a simple, commercially available test. Prostate cancer is associated with a decreased free PSA and an increased total PSA. Therefore, PSA screening is widely used for the early detection of prostate cancer to achieve a better therapeutic outcome. A high total PSA value will prompt referral to a urologist for further evaluation.

The feasibility and availability of PSA blood tests allow for guidance on when prostate biopsies are necessary. These tests also serve as an important tool to monitor the response to treatment and diagnose recurrent prostate cancer[19]. However, there are several limitations to PSA blood tests, such as poor sensitivity and specificity. Moreover, many prostate cancer patients have low total PSA values, as some prostate cancer types do not elevate the PSA levels in blood. Additionally, PSA levels in the blood can increase under many conditions that include, but are not limited to, increasing age and several nonmalignant prostatic conditions, such as prostatitis and benign prostatic hyperplasia. Despite the limitations, PSA screening is recommended for high-risk groups, as the benefits outweigh the limitations. There is an ongoing criticism against PSA screening indicating that it can result in unnecessary overdiagnosis and overtreatment[20].

Digital Rectal Examination and Biopsy

A patient with elevated blood PSA levels undergoes a DRE. Since the majority of prostate cancers begin in the peripheral zone (the majority of the posterior area of the prostate), it is possible for the urologist to detect a palpable nodule that may be prostate cancer. A suspicious DRE will prompt a referral for an mpMRI and needle biopsy to further evaluate the prostate. Transrectal ultrasound-guided biopsy (TRUS-Bx) and transperineal ultrasound-guided biopsy (TPUS-Bx) are commonly used biopsy procedures, during which multiple tissue samples of the prostate are acquired to increase the likelihood of detecting malignant tissue. Histochemical and immunohistochemical assays are used to study the morphological characteristics of the acquired tissue and detect the presence of specific proteins that may aid in the planning for treatment.

There are several disadvantages to TRUS-Bx, including increased rates of serious infection after the procedure and severe rectal bleeding. Several studies have compared TRUS-Bx and TPUS-Bx in terms of cancer detection rate (CDR) and the complications arising from the procedures. One study found no significant difference in CDR between the two methods. However, TRUS-Bx led to a significantly higher percentage of major complications, such as sepsis and rectal bleeding, than TPUS-Bx (4.3% vs. 0.6%, respectively, $P<0.05$), while the duration of TPUS-Bx was longer and the procedure was more painful than TRUS-Bx[21]. Another study demonstrated that TPUS-Bx was more effective with regard to CDR in the anterior zones of the prostate than TRUS-Bx[22]. Overall, TPUS-Bx has an acceptable CDR and is recommended as a safer alternative to TRUS-Bx[23,24]. The sensitivity of TRUS-Bx and TPUS-Bx remain low, and the procedures are invasive with the risk of severe complications. Additionally, metastatic prostate cancer cannot be confirmed by biopsies. Therefore, other imaging modalities, discussed later in this text, aid in the diagnosis and staging of prostate cancer.

The obtained biopsy tissues are studied and graded via the widely used Gleason grading system to confirm malignancy and categorise the patients.

Gleason Grading System

Donald F. Gleason developed and refined the Gleason grading system to describe the histologic appearance of prostate cancer. The system uses a scale of 1 to 5, with Gleason pattern 1 describing well-differentiated prostate cancer, and pattern 5, the highest grade, describes poorly differentiated prostate cancer[25]. One Gleason grade is assigned to the most predominant pattern (primary grade), and another Gleason grade is assigned to the second most predominant pattern (secondary grade). Therefore, a Gleason grade can theoretically range from 2 to 10. However, due to several limitations, the Gleason grading system has been revised with grades starting from a 3 + 3 Gleason score, and a newer grading classification was designed to more accurately reflect the biology of

prostate cancer[26]. Higher Gleason scores of prostate cancers are associated with worse clinical outcomes[27]. Table A1 (in the Appendix) illustrates a recently revised grading system classifying patients into 5 grade groups, offering several advantages over the original Gleason classification. For example, it offers a more refined classification system, as it is documented that a Gleason score of 4 + 3 has a significantly worse prognosis than a Gleason score of 3 + 4 [28].

Imaging of Prostate Cancer

Multiparametric MRI combines anatomic sequences with at least two functional sequences. The use of mpMRI before biopsies may result in preventing a large percentage of primary biopsies[29]. The prostate imaging reporting and data system (PI-RADS) is a reporting tool designed to standardise prostate MRI image acquisition techniques and interpretation, with a general aim to decrease the number of unnecessary biopsies. Several versions of PI-RADS were developed for optimization[30]. An elevated PI-RADS score (which ranges between 1–5) was found to be strongly correlated with a higher CDR[31].

The combination of mpMRI and TRUS-Bx provides more information than biopsy of suspicious tissue alone. More cases of clinically significant prostate cancer are detected by the combination of MRI and TRUS-BX than by TRUS-Bx alone[32,33], with a large number of patients receiving a different treatment regimen based on the findings[34].

Computed tomography (CT) can be used for the detection of nodal and distant metastases, but it is not the primary imaging modality for prostate cancer due to its lack of molecular information and inferior soft-tissue contrast[35]. MRI can also be used to assess nodal, bone marrow, soft tissue and visceral metastases. However, MRI sensitivity can be inferior to that of radionuclide-based imaging methods for the detection of prostate cancer metastases[36]. Radionuclide-based imaging modalities include SPECT and PET, which are discussed on the next page.

Staging of Prostate Cancer

Accurate and precise staging of prostate cancer is important to provide the best management option to prolong the survival of patients. The Whitmore-Jewett staging system is a prostate cancer staging system that was introduced and modified in the previous century and used the ABCD stage system[37,38]. However, due to several limitations in the Whitmore-Jewett staging system, the TNM (tumour-lymph node-metastasis) staging system is the most commonly used system for staging prostate cancer, offering a better stratification of newly diagnosed patients. The TNM system provides information on the size and extent of the primary tumour, the invasion of nearby lymph nodes

and whether the cancer has metastasised, as shown in Table A2 in the Appendix[39,40].

Radionuclide-Based Molecular Imaging of Prostate Cancer

Molecular imaging is defined as the "visualisation, characterisation, and measurement of biological processes at the molecular and cellular levels in humans and other living systems" [41], and molecular imaging relies on the use of agents to "visualise, characterise, and measure biological processes in living systems" [41]. There are several methods that implement the concept of molecular imaging, and the methods that are elaborated on this thesis are SPECT and PET.

Radionuclide-based molecular imaging utilises the photons that are emitted during the decay of a radionuclide or that result from an annihilation reaction after an emitted positron collides with an electron. The emitted photons are detected by scanners and registered. Radiotracers are often intravenously injected either in the form of radionuclides that are taken up by a specific organ of the body or in the form of radiolabelled ligands (Figure 3A) that follow a particular biological function or bind to a specific cell marker. Based on the detected radiation, an image is generated illustrating the distribution of the radiotracer. For accurate image interpretation, SPECT and PET images are often combined with images generated using other imaging methods, typically CT and MRI, to provide anatomical context for the nuclear imaging data.

At a predetermined time-point after injecting the radiotracer, SPECT or PET imaging (Figure 3B and 3C) is performed to detect where the radiotracer has accumulated. SPECT relies on single-photon detection and uses physical collimators to reject photons outside a small angular range. PET, on the other hand, does not require physical collimators. Instead, it relies on the simultaneous detection of two annihilation photons resulting from a positron decay event. Therefore, PET exhibits higher sensitivity than SPECT[42].

Recent advances in SPECT have improved its resolution. This, in addition to the wider availability of SPECT scanners (approximately 27,180 SPECT scanners vs. approximately 5,672 PET scanners worldwide by the first quarter of 2023 [43]), warrants the continuous development of SPECT-suitable radiotracers to provide wide outreach to patients.

Both PET and SPECT are commonly used in the imaging of prostate cancer. PET and SPECT radiotracers can be used to target different processes, such as tumour metabolism and proliferation, prostate cancer cell receptors, such as the gastrin-releasing peptide receptor (GRPR), or antigens, such as the prostate-specific membrane antigen (PSMA). Bone scans to detect bone metastases are also a common application of PET and SPECT radiotracers[44].

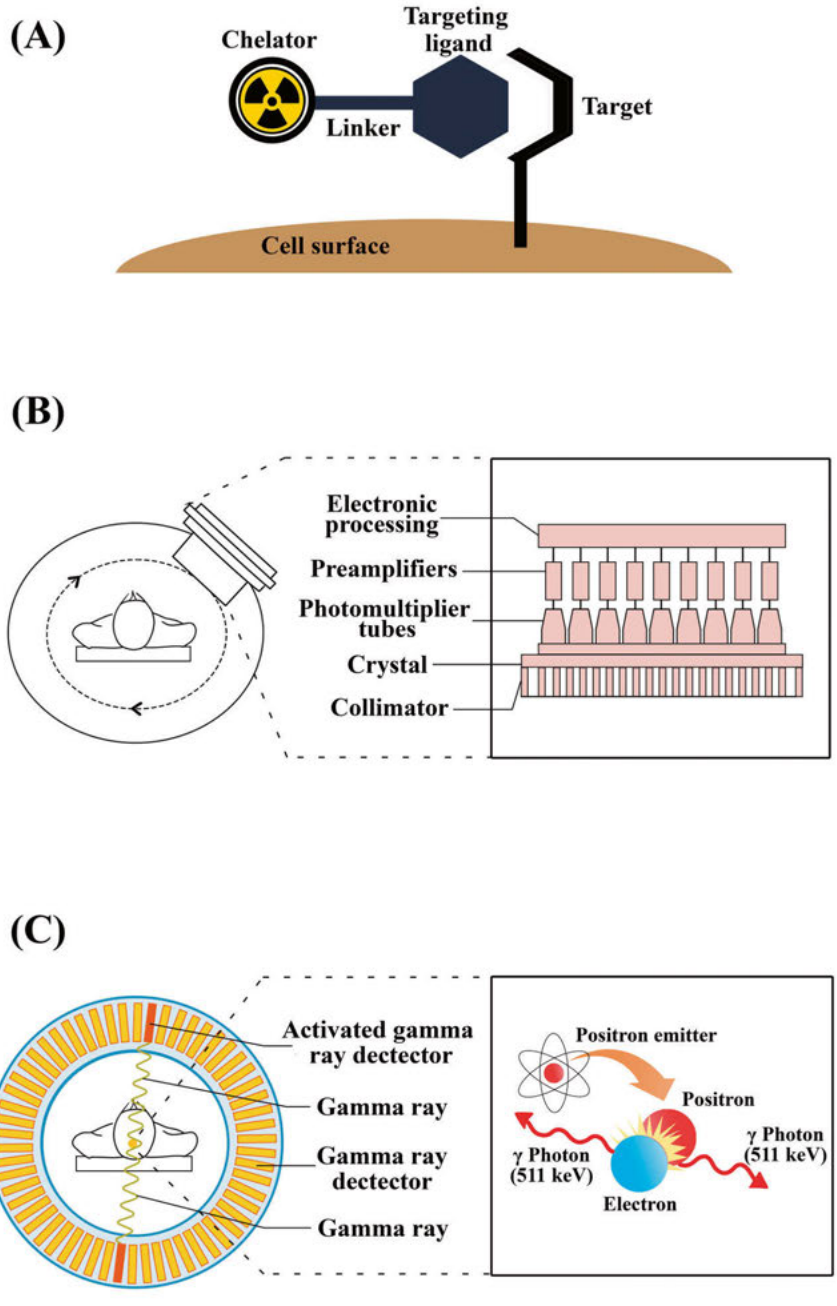

Figure 3. A schematic illustration of the (**A**) radiotracer, (**B**) single-head SPECT scanner, and (**C**) PET scanner.

Radiotracers Used in Prostate Cancer Imaging

The Warburg effect first highlighted the increased glucose uptake by tumour cells. Years later, the glucose analogue [^{18}F]-fluorodeoxyglucose ([^{18}F]FDG) was developed and is widely used for imaging the increased rate of glucose uptake in cancer patients[45,46]. Different clinical trials have assessed the use of [^{18}F]FDG in the imaging of prostate cancer, and the general conclusion was that [^{18}F]FDG has low sensitivity for detecting true positive prostate tumours[47]. However, in certain groups of patients with more aggressive prostate tumours, it may have some utility[48].

One of the established characteristics of cancer is the elevation of choline uptake[49]. Consequently, choline was radiolabelled with carbon-11 and fluorine-18 and evaluated for imaging prostate cancer. [^{11}C]Choline demonstrated higher sensitivity than [^{18}F]FDG in detecting prostate tumours[50]. However, [^{11}C]choline and [^{18}F]choline have limited use in primary tumour detection and staging due to their low sensitivities and specificities[51]. Other notable radiotracers that were evaluated for imaging prostate cancer include [^{11}C]methionine, [^{18}F]fluciclovine, [^{11}C]acetate, [^{18}F]FMISO, [^{18}F]FSPG, and [^{18}F]FDHT.

Individuals with high-risk prostate cancer are recommended to undergo bone scans to detect any bone metastases, as bone is the most common site of prostate cancer metastasis. The most notable and commonly used example is [^{99m}Tc]Tc-methylene-diphosphonate ([^{99m}Tc]Tc-MDP) whole-body bone scintigraphy, which is widely available, affordable, and has excellent sensitivity[52]. After injection, [^{99m}Tc]Tc-MDP is chemisorbed onto the hydroxyapatite crystals and accumulates where bone metastases are present[53]. [^{18}F]NaF is a PET radiotracer that was developed several decades ago for imaging bone metastases and regained use with the spread of PET scanners. A clinical trial showed that [^{18}F]NaF had higher sensitivity for detecting bone metastases than [^{99m}Tc]Tc-MDP[54].

The theranostic method of targeting prostate cancer cell receptors and antigens with the right radiopharmaceutical has advantages. This approach involves the use of an imaging radiopharmaceutical that detects positive expression of a receptor or antigen on the tumour cells. Thereafter, a therapeutic radiopharmaceutical can be used to target the same receptor or antigen and irradiate and kill the tumour cells. Two of the most prominent prostate cancer cell markers are PSMA and GRPR, and both targets will be discussed in more detail in the subsequent sections of this thesis.

Management of Prostate Cancer

There are several options available for managing patients with prostate cancer. The most suitable treatment option is selected based on the stage of the disease, which can be localised, locally advanced, or metastatic prostate cancer. In addition to the stage, several other factors are taken into consideration to ensure that the patient receives the best possible therapeutic option while maintaining a good quality of life. The patient's age, medical condition, and personal preference can majorly influence the choice of treatment. Therefore, the treatment regimen is tailored to each patient.

Localised Prostate Cancer

Localised prostate cancer is defined as cancer that is confined within the prostate, without metastases or invasion of seminal vesicles. For localised prostate cancer patients of an advanced age or with comorbidities, watchful waiting may be the recommended approach for management. Watchful waiting is the least aggressive management option, during which the patient is monitored for the development of symptoms without frequent testing. Active surveillance is another option that can be recommended for men with low-grade localised prostate tumours. It involves regular retesting, with the patients routinely undergoing PSA blood tests, DREs, biopsies, and/or MRI scans to monitor the status of the tumour to decide if a therapeutic intervention with curative intent is necessary[55].

Curative intervention of localised prostate cancer is recommended, especially for individuals with intermediate- and high-risk prostate cancer, to prevent the disease from metastasising and avoid aggressive treatment options. Radical prostatectomy is offered for healthy men with long life expectancies. However, it is associated with a risk of complications such as urinary incontinence and impotence, which majorly affect the quality of life, and patients may opt for an alternative choice of treatment.

Brachytherapy is a treatment option in which low- or high-radiation-dose seeds are implanted to irradiate the tumour. Iodine-125 ($t_{½}$ = 59.4 d), palladium-103 ($t_{½}$ = 17.0 d), and caesium-131 ($t_{½}$ = 9.7 d) are examples of radioisotopes used in low-dose brachytherapy, while iridium-192 ($t_{½}$ = 73.8 d) is the most commonly used radioisotope in high-dose brachytherapy[56]. Another available treatment option is cryotherapy, which involves cryoablation of tumours by using low temperatures (usually below -40 °C) to kill malignant cells[57]. Another thermoablative treatment option is high-intensity focused ultrasound. It involves focusing ultrasound waves at the targeted prostate tumour, and the accumulation of ultrasound waves result in an elevated temperature, which leads to cellular damage[58]. External beam radiation therapy (EBRT) is also a commonly used treatment option for localised prostate cancer. It entails the delivery of fractionated radiation doses to destroy malignant

cells[59]. EBRT can be categorised into photon and proton therapy, with the latter having the advantage of sparing more healthy tissue, utilising the characteristic Bragg peak[60]. Patients with intermediate- or high-risk localised tumours can also be offered hormone therapy as a neoadjuvant or an adjuvant treatment to control the disease.

Overall, patients with localised prostate cancer have a favourable prognosis with 5-year survival rates exceeding 99%, and the survival rates are not significantly different between patients undergoing active surveillance, radical prostatectomy, or EBRT. However, lower incidences of progression and metastases are more closely associated with patients undergoing radical prostatectomy and EBRT than with patients undergoing active surveillance[61]. It has also been shown that men with long life expectancies suffering from localised prostate cancer had long-standing benefits from radical prostatectomy compared with watchful waiting, gaining an additional 2.9 years of life on average[62].

Locally Advanced Prostate Cancer

The term locally advanced prostate cancer is used to describe cancer that has spread beyond the prostate to nearby regions without distant metastases. Multimodal treatment is recommended for locally advanced prostate cancer, with the main options for treatment being radical prostatectomy, hormone therapy such as androgen deprivation therapy (ADT), and EBRT. Clinical trials have demonstrated that patients receiving combination therapy have improved overall survival compared with that of patients receiving a single treatment option[63–65]. The duration of ADT in combination therapy impacts survival, and compared with short-term ADT, long-term ADT results in longer overall survival[66].

Metastatic Prostate Cancer

Approximately 5% of prostate cancer patients have distant metastasis[67]. ADT is the first-line treatment for metastatic prostate cancer since the prostate gland depends on androgens for development and growth. ADT includes gonadotropin-releasing hormone agonists and antagonists and bilateral orchiectomy, with the goal of achieving castration levels of testosterone. The majority of patients on ADT still have progressive cancer, and the disease is then termed metastatic castration-resistant prostate cancer (mCRPC). The first signal of castration resistance is often the rise of serum PSA levels, which are typically androgen-responsive. The expression of androgen receptors (ARs) is upregulated in samples of CRPC patients undergoing ADT, and therefore, newer classes of drugs can be used for effective treatment. Potent AR antagonists can effectively block AR, and examples of AR antagonists are enzalutamide, apalutamide, and darolutamide. The use of enzalutamide after chemotherapy

improved the median overall survival versus placebo after chemotherapy in patients with mCRPC[68]. Apalutamide and darolutamide improved the survival of patients with metastatic castration-sensitive prostate cancer[69,70]. Abiraterone is another drug that can be effective at this stage by inhibiting the synthesis of androgens[71,72], and the use of abiraterone was shown to improve the median overall survival[73].

Chemotherapy plays an important role in the treatment of mCRPC, with docetaxel and cabazitaxel being the most commonly used chemotherapeutic agents that improve the median overall survival of patients with mCRPC[74,75]. Immunotherapy is another option for managing patients with mCRPC, with Sipuleucel-T being the most prominent example, as it was found to improve the median overall survival[76].

The use of radiopharmaceuticals in managing patients with mCRPC is an emerging approach with promising results. The Food and Drug Administration (FDA) recently approved [^{177}Lu]Lu-PSMA-617 for the treatment of mCRPC. This treatment approach relies on the detection of PSMA-expressing tumours using PSMA-targeting radiotracers such as [^{68}Ga]Ga-PSMA-11 or [^{18}F]PSMA-1007. Subsequently, the beta-emitter PSMA-targeting [^{177}Lu]Lu-PSMA-617 can be used for targeting and irradiating these PSMA-expressing tumours. The use of [^{177}Lu]Lu-PSMA-617 was shown to prolong overall survival and imaging-based progression-free survival when added to standard care compared with standard care alone[77].

Bone is the most common site of prostate cancer metastases, and bone metastases lead to increased mortality rates. Therefore, there is a necessity to improve bone health and alleviate pain resulting from bone metastases. Denosumab is an antibody that increases bone mineral density, and its use delays the initial skeletal-related events[78]. The alpha-emitter radium-223 is a bone-seeking radionuclide that prolongs the time to the initial skeletal-related events and the median overall survival[79].

Many patients with mCRPC have a poor prognosis, and the 5-year survival rate of prostate cancer patients with distant metastases is low compared with that of patients with localised or locally advanced prostate cancers[80]. Despite the advances made in providing alternative treatment options, much work is still needed to further prolong the overall survival and improve the quality of life for these patients. One successful and very promising approach is the theranostic targeting of PSMA.

Prostate-Specific Membrane Antigen

Prostate-specific membrane antigen (PSMA, also known as glutamate carboxypeptidase II, folate hydrolase 1, N-acetylated α-linked acidic dipeptidase, or N-acetyl-L-aspartyl-L-glutamate peptidase) was first discovered in the prostate in the 1980s through the murine monoclonal antibody 7E11-C5.3 [81]. PSMA is a type II transmembrane protein made of 750 amino acids (707 extracellular, 24 transmembrane, and 19 intracellular amino acids[82]) that is mainly expressed in the prostate and the proximal renal tubules. It has lower expression in the salivary glands, brain, and small intestine, among other tissues[83–85]. In the healthy prostate, PSMA is expressed in the luminal epithelial cells. It is also expressed in PIN, hyperplastic and malignant prostate cells[86]. PSM' is a spliced variant of PSMA that has higher expression in the normal prostate than that of PSMA, whereas PSMA expression levels increase as the cells progress to the malignant state[87,88] and continues to increase as the disease progresses. PSMA is also highly expressed in the vast majority of prostate cancer samples[89–91]. Additionally, PSMA is expressed in the endothelial cells of the neovasculature of tumours but not in the vasculature of normal tissues[92]. PSMA has an internalisation signal that enables the internalisation of ligands[93], and it has been found that antibodies that bind to PSMA increase the rate of PSMA internalisation[94].

[^{111}In]In-Capromab pendetide (also known as ProstaScint®) is based on 7E11-C5.3 and was the first FDA-approved radiopharmaceutical for the molecular imaging of prostate cancer. It targets an intracellular epitope of PSMA[95] and therefore effectively binds only to damaged cells. This selective binding resulted in poor performance of ProstaScint® in the imaging of prostate cancer, and its production was discontinued in 2018, with several new PSMA-targeting radiotracers outperforming ProstaScint® in clinical settings[96]. Another notable monoclonal antibody is J591, which was developed in the late 1990s and targets the extracellular domain of PSMA, thus enabling the targeting of viable prostate cancer cells[97]. J591 can be used for SPECT and PET imaging and is currently under evaluation for radionuclide therapy[98–100]. In addition to these antibodies, several small molecules were developed to target PSMA with high affinity and specificity. Examples of these molecules are highlighted in the following paragraphs, and the chemical structures of several of them are shown in Figure 4 on Pages 30 and 31.

One of the identified functions of PSMA in the brain is that it hydrolyses N-acetyl-L-aspartyl-L-glutamate (NAAG) into N-acetyl-aspartate and glutamate. Therefore, it was hypothesised that the inhibition of PSMA may be effective in achieving neuroprotection by preventing glutamate excitotoxicity through decreasing the levels of glutamate and increasing the levels of NAAG. In the early 1990s, several PSMA inhibitors were subsequently developed based mainly on NAAG or glutamate derivatives, but they were weak inhibitors and lacked specificity[101,102].

More research was needed to further evaluate PSMA and the design of its inhibitors. It was established that a template for a potent inhibitor should utilise both the C-terminal glutamate recognition site and the divalent zinc atoms at the active site of PSMA. One of the most potent and selective PSMA inhibitors was then developed in the mid-1990s and termed 2-PMPA (2-(phosphonomethyl)pentanedioic acid)[103], which is the most notable example of phosphonate-based PSMA inhibitors. Despite the high potency of 2-PMPA, it was too hydrophilic to reach the brain, and it also had poor oral bioavailability. Several thiol-based PSMA inhibitors were developed and evaluated; an example is 2-(3-mercaptopropyl)pentanedioic acid (2-MPPA), which showed selectivity for PSMA but relatively low potency[104].

Another class of PSMA inhibitors is urea-based inhibitors, which mimic NAAG in their design and have two amino acids that are joined by urea linkage. The design utilises the aspartate and glutamate binding sites, while urea acts as the zinc-binding group. Urea-based low molecular weight PSMA inhibitors were first developed in the early 2000s, showing high affinity to the extracellular domain of PSMA[105]. Kozikowski et al. developed inhibitors based on 2-[3-(1,3-dicarboxypropyl)ureido]pentanedioic acid (DUPA)[105], which serves as the basis of many PSMA urea-based inhibitors available today[106]. Some of the first urea-based PSMA inhibitors that were radiolabelled to evaluate their potential use in PET and SPECT imaging include [^{11}C]DCMC and [^{125}I]DCIT[107,108]. Both radiotracers showed specific PSMA uptake in prostate cancer xenografts.

Structural modifications in the linkers of urea-based inhibitors aimed to benefit from the spacious accessory hydrophobic pocket and the arene-binding site within the entrance funnel to the active binding site of PSMA[106,109], in order to modify the pharmacokinetics to improve the detection of prostate tumours. These structural modifications resulted in numerous PSMA-targeting radiotracers with favourable binding properties and pharmacokinetics. Notable examples will be mentioned in the subsequent paragraphs.

Several urea-based radiotracers were developed for radiohalogenation[110], with [^{123}I]MIP-1072 and [^{123}I]MIP-1095 standing out as prominent PSMA-targeting radiotracers. Preclinical studies demonstrated the ability of radioiodinated urea-based small compounds to bind specifically to PSMA in vitro and in vivo. Both [^{123}I]MIP-1072 and [^{123}I]MIP-1095 were internalised in LNCaP cells (PSMA^{+}), and [^{123}I]MIP-1095 had higher LNCaP tumour uptake than [^{123}I]MIP-1072 with 29.1 ± 15.1% of injected activity per gram (%IA/g) at 24 h postinjection (p.i)[111]. Clinical evaluation of [^{123}I]MIP-1072 and [^{123}I]MIP-1095 indicated that the radiotracers were able to identify PSMA-expressing lesions in the prostate gland and distant metastases at early time points, and they also had favourable pharmacokinetic profiles[112]. MIP-1095 was then radiolabelled with iodine-124 and iodine-131 to assess its safety and estimate the dosimetry for PET imaging and therapy, respectively[113].

[^{131}I]MIP-1095 was evaluated for repeated treatment of prostate cancer patients. However, administration of second or third doses resulted in more frequent and intense adverse events, in addition to being less effective than the first dose[114].

Other urea-based PSMA inhibitors were designed to be radiolabelled with technetium-99m for SPECT imaging, showing high affinity for PSMA in vitro and in vivo. They can also chelate rhenium-188 if therapy is applicable[115,116]. [^{99m}Tc]Tc-MIP-1404 (also known as trofolastat) is an example of such radiotracers. In a clinical study, it identified more bone metastases than standard bone scans[117]. Another example is [^{99m}Tc]Tc-PSMA-I&S, which contains an amino acid-based chelator formed of mercaptoacetyl tri-serine for radiolabelling with technetium-99m[118]. [^{99m}Tc]Tc-PSMA-I&S identified PSMA-expressing lesions and demonstrated favourable dosimetry[119,120].

In recent years, PET-PSMA has become the major player in the imaging of prostate cancer patients, with several radiotracers gaining wide recognition, including [^{18}F]DCFBC, [^{18}F]DCFPyL, [^{18}F]PSMA-1007, [^{68}Ga]Ga-PSMA-11, [^{68}Ga]Ga-PSMA-I&T, and [^{68}Ga]Ga-PSMA-617.

[^{18}F]DCFBC utilises the favourable characteristics of fluorine-18 to identify PSMA-expressing prostate tumours during PET imaging. It localised in PSMA-expressing tumour xenografts in mice[121], and in a clinical trial, it detected more clinically significant high-grade malignant prostate tumours than MRI, although the sensitivity of MRI for detecting primary prostate tumours was higher[122]. [^{18}F]DCFPyL (also known as piflufolastat, or PYLARIFY®) is a commercially available, FDA-approved radiotracer for PSMA-expressing prostate tumour imaging. PET/CT imaging using [^{18}F]DCFPyL could detect more lesions than conventional imaging methods[123]. This radiotracer is also useful in men with biochemically recurrent prostate cancer, as it can lead to a change in the treatment strategy of patients[124].

[^{68}Ga]Ga-PSMA-11 (also known as gallium-68 gozetotide, LOCAMETZ®, or Illuccix®) is another FDA-approved PSMA-targeting radiotracer. It is arguably the most commonly used radiotracer in clinical settings today for PSMA-expressing prostate cancer imaging. [^{68}Ga]Ga-PSMA-11 was first reported in 2012, showing favourable characteristics in preclinical studies[125]. Early clinical studies showed that [^{68}Ga]Ga-PSMA-11 was superior to [^{18}F]FECH in detecting prostate tumours[126]. [^{68}Ga]Ga-PSMA-11 was shown to have a high CDR that significantly increased with high PSA levels[127]. It was also superior to the standard imaging routine in preoperative lymph node staging[128].

One of the most successful PSMA-targeting radiotracers is PSMA-617. The DOTA chelator in the structure of PSMA-617 allows radiolabelling with gallium-68 for PET imaging and lutetium-177 or actinium-225 for therapy. The only PSMA-targeting radiotherapeutic tracer that has received FDA approval to date is [^{177}Lu]Lu-PSMA-617 (also known as lutetium-177 vipivotide tetraxetan, or Pluvicto™). PSMA-617 was first reported in 2015. Preclinical

evaluation of PSMA-617 showed feasible labelling with gallium-68 and lutetium-177. The affinity of PSMA-617 for PSMA was reported to be higher than that of PSMA-11, and it also demonstrated favourable biodistribution with higher tumour uptake at 24 h p.i in tumour-bearing mice[129]. Administration of [^{177}Lu]Lu-PSMA-617 in humans is safe and generally tolerable[130]. [^{177}Lu]Lu-PSMA-617 also leads to favourable therapeutic outcomes in many patients with PSMA-expressing mCRPC[77]. Labelling of PSMA-617 with the alpha-emitter actinium-225 shows great potential in therapy; however, this therapeutic approach is still experimental, and the effects of using actinium-225 are yet to be fully uncovered. [^{18}F]PSMA-1007 was developed based on the structure of PSMA-617 to be its diagnostic pair[131,132]. [^{18}F]PSMA-1007 showed lower urinary bladder accumulation than [^{68}Ga]Ga-PSMA-11, a favourable characteristic for better detection of primary prostate tumours[133]. However, compared with imaging with [^{68}Ga]Ga-PSMA-11, imaging with [^{18}F]PSMA-1007 may lead to more false-positive readings[134].

PSMA inhibitors classes other than urea-based inhibitors have also been evaluated in early phase clinical trials, showing promising results. A notable example is the phosphoramidate-based PSMA inhibitor [^{18}F]CTT1057, which demonstrated favourable dosimetry and pharmacokinetic profiles[135]. Nevertheless, urea-based PSMA inhibitors comprise the majority of PSMA-targeting radiotracers today.

Despite the success of PSMA-targeting radiotracers, they do not cover the entirety of prostate cancers[136]. Additionally, PSMA expression is lower in the early stages of prostate cancer and is suppressed in advanced and aggressive neuroendocrine prostate cancers[137,138].

Some pitfalls may arise from the use of PSMA-targeting radiotracers. For example, [^{68}Ga]Ga-PSMA-11 demonstrated high CDR even in patients with low levels of serum PSA, but elevated uptake of [^{68}Ga]Ga-PSMA-11 was documented in the cervical, celiac, and sacral ganglia. This elevated uptake may be misinterpreted for lymph node metastases, which may lead to incorrect staging and selection of treatment options[139,140]. Another pitfall may be present in patients with Paget disease, as several reports have associated elevated uptake of PSMA-targeting radiotracers, such as [^{68}Ga]Ga-PSMA-11 and [^{18}F]DCFPyL, with Paget disease rather than bone metastases. This may also lead to misinterpretation and incorrect management[141,142]. Treatment with [^{177}Lu]Lu-PSMA-617 is associated with several adverse events, one of which is xerostomia, as a result of the elevated uptake in the salivary glands.

Moreover, many PSMA-expressing prostate tumours were shown to be resistant to [^{177}Lu]Lu-PSMA-617 therapy, which may be attributed to the characteristics of lutetium-177. The use of other radionuclides, such as terbium-161, lead-212, or actinium-225, may deliver higher doses to PSMA-expressing tumours[143–146].

The aforementioned examples of PSMA-targeting pitfalls necessitate the targeting of other antigens or receptors that are overexpressed in prostate cancer to further improve diagnostic efficacy and subsequent therapeutic options. One such target is the gastrin-releasing peptide receptor.

Chemical Structures of Tracers Targeting PSMA

2-PMPA

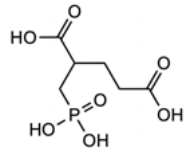

2-MPPA

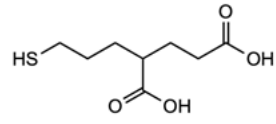

DCMC

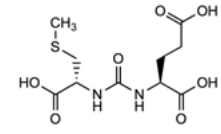

DCIT

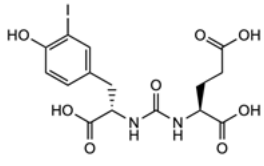

DCFBC

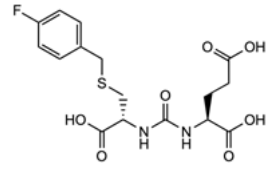

DCFPyL

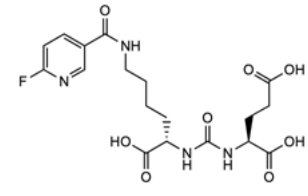

MIP-1072

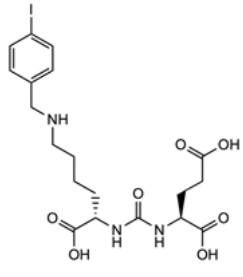

MIP-1404

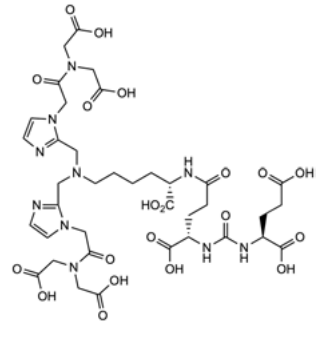

MIP-1095

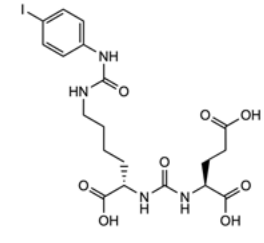

PSMA-I&S

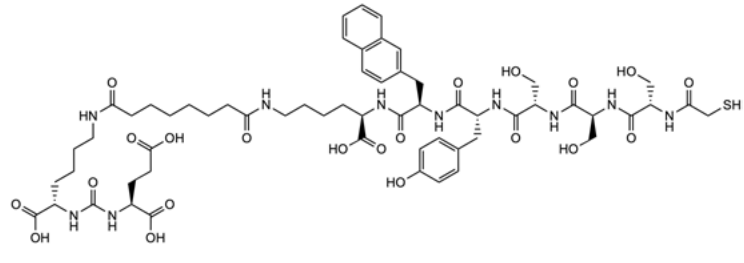

PSMA-I&T

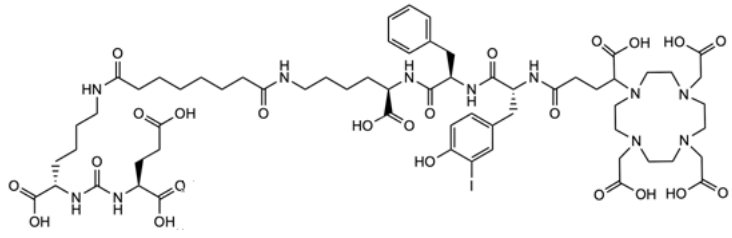

CTT1075

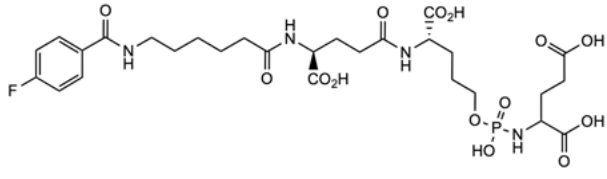

PSMA-11

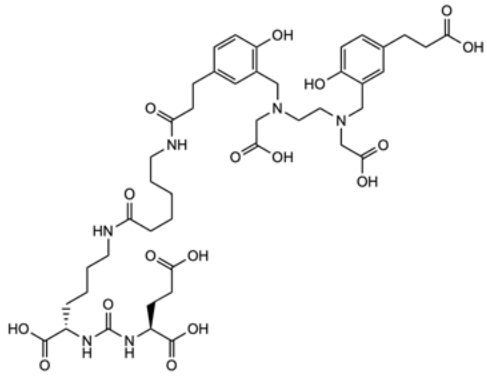

PSMA-617

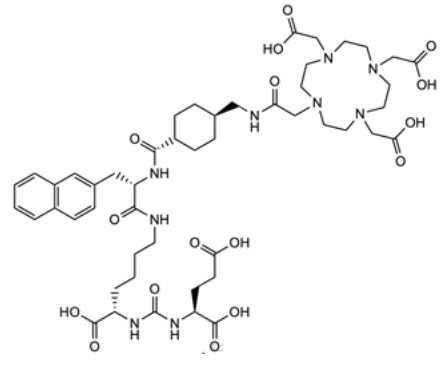

PSMA-1007

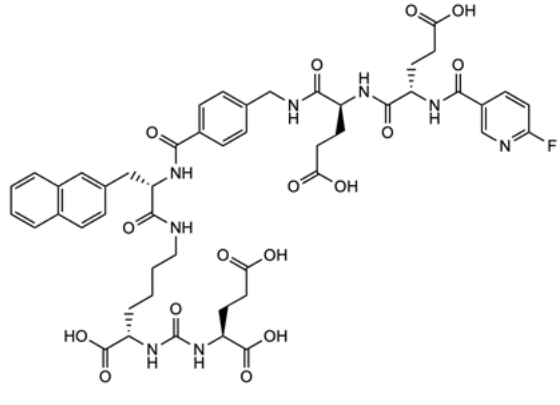

Figure 4. The chemical structures of several PSMA-targeting tracers.

Gastrin-Releasing Peptide Receptor

Gastrin-releasing peptide receptor (GRPR, also known as bombesin type 2 receptor) is a 384-amino-acid seven-transmembrane G-protein coupled receptor that was first identified in the late 1980s[147,148]. The identification of GRPR was preceded by the isolation of [Leu^{13}]bombesin (BBN), which is a tetradecapeptide isolated in the early 1970s from the European frog *Bombina bombina*[149]. Early evaluation of bombesin indicated a smooth muscle stimulation effect in addition to increased release of gastrin; however, the mechanism of action was not uncovered at the time[150,151]. A few years later, the gastrin-releasing peptide (GRP) was isolated from the porcine stomach and was found to be a 27 amino acid peptide that shares the same seven C-terminal amino acids, which regulate biological activity, with BBN[152–155]. Subsequent studies helped in identifying the target for GRP, GRPR, to which it binds with high affinity[147,156,157]. GRPR regulates several functions, such as gastric acid secretion, gastrointestinal motility, pancreatic secretion, and itch transmission[158–161].

The expression of GRPR in normal human tissues is the highest in the pancreas, while low GRPR expression is found in the stomach, brain, and adrenal cortex[162]. The normal prostate lacks GRPR expression, and most hyperplastic prostate cells also lack GRPR[163]. Interestingly, GRPR expression has been documented in various malignancies, including prostate, breast, colon, uterine, and ovarian cancer[164–169]. GRPR is overexpressed in the majority of primary prostate tumours (63–100%) and high-grade PIN[163,170,171], as well as in 85.7% of lymph node and 52.9% of bone metastases[172]. The expression of GRPR is androgen-dependent[173] and is higher in PIN and early-stage prostate cancer than in the late stages. Additionally, the expression is higher in well-differentiated than in poorly differentiated malignant tumours, as it was found to be inversely correlated with the Gleason score[163,174,175]. These findings propose GRPR as an attractive target for early-stage and oligometastatic prostate cancer.

Most GRPR-targeting radiotracers are based on the structure of BBN (*p*Glu^{1}-Gln^{2}-Arg^{3}-Leu^{4}-Gly^{5}-Asn^{6}-Gln^{7}-Trp^{8}-Ala^{9}-Val^{10}-Gly^{11}-His^{12}-Leu^{13}-Met^{14}-NH_2), with conjugations designed on the N-terminus, as the sequence on the C-terminus is crucial for binding site recognition. The chemical structures of some of the GRPR-targeting tracers are shown in Figure 5 on Pages 36 and 37. Some of the early developed radiotracers comprised the whole structure of BBN with few modifications in some amino acids. The general hypothesis was that GRPR activation by agonists would lead to high internalisation and the retention of radioactivity after lysosomal degradation, resulting in high tumour uptake[176]. Notable examples of such GRPR-agonistic radiotracers are [^{111}In]In-DOTA-[Pro^{1}, Tyr^{4}]BBN and [^{111}In]In-DTPA-[Pro^{1}, Tyr^{4}]BBN, which showed elevated GRPR-specific uptake[177,178]. However, the use of larger peptides may result in lower serum stability as they become more prone to the action of different proteases. It has been demonstrated that the

use of truncated peptides can significantly improve metabolic stability and simultaneously improve affinity to the targeted receptor[179]. Many truncated BBN analogues with agonistic functions have been developed and evaluated in preclinical and clinical studies. Remarkable examples of these radiotracers include [^{99m}Tc]Tc-RP527, which was evaluated in a clinical study on patients with breast and prostate cancer. [^{99m}Tc]Tc-RP527 was able to identify GRPR-expressing tumours in both groups without causing adverse events[180]. Another example is [^{177}Lu]Lu-AMBA, which showed high affinity for GRPR with high retention in PC-3 cells (GRPR^{+}), which effectively resulted in favourable therapeutic outcomes in tumour-bearing mice[181]. [^{68}Ga]Ga-AMBA also showed better visualisation of prostate and breast cancer xenografts in nude mice than [^{18}F]FCH and [^{18}F]FDG, respectively[182,183]. Clinical evaluation of [^{68}Ga]Ga-AMBA showed that the radiotracer could identify GRPR-expressing lesions and that it caused minor adverse events, such as tachycardia and abdominal discomfort[184]. However, the evaluation of [^{177}Lu]Lu-AMBA in a phase I clinical trial on mCRPC patients was associated with severe adverse effects linked to the activation of GRPR, which ultimately resulted in the discontinuation of the trial[185,186].

As mentioned earlier, the activation of GRPR regulates multiple functions. Additionally, it was demonstrated that GRPR activation stimulates tumour proliferation and growth[187,188] and that GRPR antagonists inhibit tumour growth[189,190]. Despite the general consensus that GRPR agonists are highly retained in tumour cells after internalisation, it has been recently demonstrated that GRPR antagonists have a similar, if not better, performance in vivo, as they retain high affinity for GRPR[191,192]. Therefore, the use of antagonistic GRPR-targeting radiotracers can be beneficial, as they have a favourable pharmacokinetic profile and can visualise GRPR-expressing tumours while evading the undesirable effects related to GRPR activation.

There are several classes of BBN-based GRPR antagonists that aim to improve stability while maintaining high potency; an example is the desMet^{14} analogues. One such analogue is [D-Phe^{6}]BBN(6–13)-ethylamide, which was first reported in the early 1990s and was shown to be highly potent[193]. One of the first radiotracers to be developed based on this class of GRPR antagonists is [^{99m}Tc]Tc-DB1, which showed favourable pharmacokinetics and elevated tumour-to-nontumour ratios in a preclinical evaluation[194]. Another example of this class is [^{68}Ga]Ga-SB3, which was developed to mimic [^{99m}Tc]Tc-DB1 but with a DOTA chelator incorporated. [^{68}Ga]Ga-SB3 could visualise GRPR-expressing tumours in breast and prostate cancer patients and was well tolerated[195,196]. However, a study showed that SB3, radiolabelled with indium-111, is prone to degradation by neprilysin, which is one of the major proteases. This degradation may affect tumour uptake, as lower levels of the intact radiotracer are available in circulation[197]. In later years, [^{99m}Tc]Tc-DB1 was further modified to prolong the retention in GRPR-expressing tumours by replacing Gly^{11} with Sar^{11} (N-methylated Gly, the radiotracer is named [^{99m}Tc]Tc-DB15). This

substitution was found to increase resistance to the proteolytic activity of neprilysin. [^{99m}Tc]Tc-DB15 was translated into an early-phase clinical trial and showed high safety and tolerability while visualising GRPR-expressing tumours[198].

Another class of GRPR antagonists was based on modification of the amino acids at positions 13 and 14 of BBN. For example, an analogue based on Ac-GRP(20–25) or Ac-[His^{7}]BBN(7–12) with Leu^{13} and Met^{14} on the C-terminus of BBN being replaced by NH-CH[CH_2-$CH(CH_3)_2$]$_2$ demonstrated high affinity for GRPR[199]. Employing the C-terminal sequence of this analogue while modifying the N-terminal structure provided the basis of the GRPR-targeting moiety ([D-Phe^{6}]BBN(6–12)) of the notable radiotracer [^{68}Ga]Ga-NeoB (NeoB is also known as NeoBOMB1). It visualised GRPR-expressing tumour xenografts, and repeated cycles of its theranostic pair [^{177}Lu]Lu-NeoB were tolerable in a preclinical study[200,201]. Clinical evaluation of [^{68}Ga]Ga-NeoB indicated safety and tolerability, and GRPR-expressing tumours were clearly visualised[202]. Both [^{68}Ga]Ga-NeoB and [^{177}Lu]Lu-NeoB are undergoing further clinical evaluation.

The substitution of Asn^{6}, Leu^{13}, and Met^{14} in BBN(6–14)-NH_2 with D-Phe^{6}, Sta^{13} (Sta: 3*S*,4*S*-4-amino-3-hydroxy-6-methyl-heptanoic acid), and Leu^{14} resulted in the highly potent GRPR antagonist JMV594 (D-Phe-Gln-Trp-Ala-Val-Gly-His-Sta-Leu-NH_2 [203], also referred to as RM26). JMV594 serves as the basis of many of the antagonistic GRPR-targeting radiotracers available today. Our group has extensively worked on using JMV594 in the development of radiotracers for imaging GRPR-expressing tumours. Linking JMV594 to a suitable chelator via a polyethylene glycol (PEG) linker resulted in wide selection of antagonistic GRPR-targeting radiotracers with high affinity and favourable pharmacokinetics[204–206]. A notable example is [^{68}Ga]Ga-NOTA-PEG_2-RM26, which showed promising characteristics in preclinical studies[207]. More recently, our group translated [^{68}Ga]Ga-NOTA-PEG_2-RM26 into an early-phase clinical trial and it showed great promise. The data from this study are yet to be published. [^{68}Ga]Ga-NOTA-PEG_3-RM26 was evaluated in clinical trials and was deemed safe and well tolerated. Additionally, [^{68}Ga]Ga-NOTA-PEG_3-RM26 performed better than an agonistic GRPR-targeting radiotracer in detecting primary prostate tumours and lymph node metastases, and it had favourable dosimetry[208].

One of the early radiotracers based on JMV594 is [^{111}In]In-RM1, which demonstrated favourable pharmacokinetics and elevated tumour uptake in mice. In a direct comparison with the GRPR agonist [^{111}In]In-AMBA, the radiolabelled GRPR antagonist RM1 was superior in terms of tumour uptake, and clearly visualised tumours[192]. Modifying the linker between the chelator and JMV594 in RM1 resulted in one of the most evaluated GRPR-targeting radiotracers to date, RM2 [209]. The incorporation of a positively charged 4-amino-1-carboxymethyl piperidine linker in RM2 resulted in an improved affinity in comparison with RM1. [^{68}Ga]Ga-RM2 (also known as BAY 86-7548)

and [^{111}In]In-RM2 demonstrated favourable pharmacokinetics and clear visualisation of GRPR-expressing xenografts during PET/CT and SPECT/CT imaging[209]. The first clinical study of [^{68}Ga]Ga-RM2 was performed on prostate cancer patients, and the results showed high sensitivity, specificity, and accuracy for detecting primary prostate cancer (88%, 81%, and 83%, respectively)[210]. More clinical evaluations of [^{68}Ga]Ga-RM2 in prostate and breast cancer patients supported [^{68}Ga]Ga-RM2 as a promising GRPR-targeting radiotracer[211–214]. Additionally, [^{68}Ga]Ga-RM2 outperformed [^{18}F]FDG in the imaging of oestrogen-positive breast cancer[215]. Its theranostic pair, [^{177}Lu]Lu-RM2 (also known as BAY 1017858), was evaluated in an early phase clinical trial showing great promise[216].

Other notable antagonistic GRPR-targeting radiotracers include [^{68}Ga]Ga-ProBOMB1, which demonstrated favourable pharmacokinetics and dosimetry in a preclinical study[217].

Research on targeting GRPR for the management of prostate cancer is expanding with great potential, but there is still more to learn. A limitation to targeting GRPR is, similar to PSMA, not all prostate tumours overexpress GRPR. In fact, a larger percentage of prostate cancer samples are GRPR-negative. The absence of GRPR expression may result in other targeted radiotracers effectively competing with GRPR-targeting radiotracers. However, given the high expression of GRPR in PIN and in the majority of primary prostate tumours, GRPR-targeted therapy may play a major role in the future of prostate cancer management either alone or as a complement to other types of targeted therapy, such as PSMA-targeted radionuclide therapy.

Chemical Structures of Tracers Targeting GRPR

[Leu^{13}]Bombesin

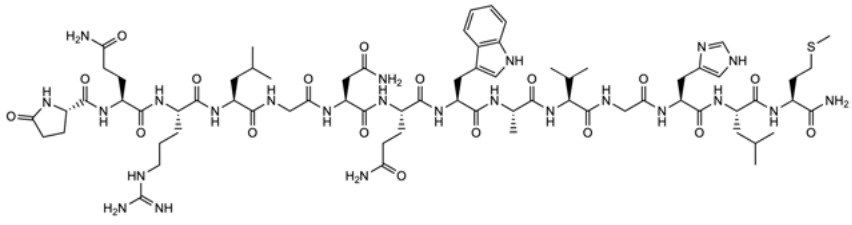

RP527

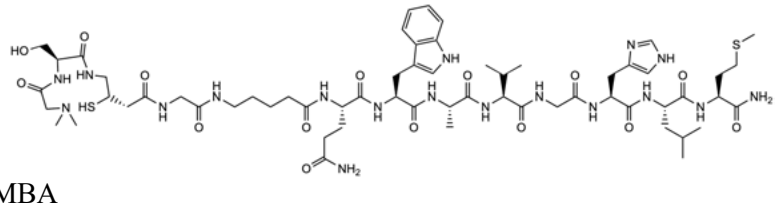

AMBA

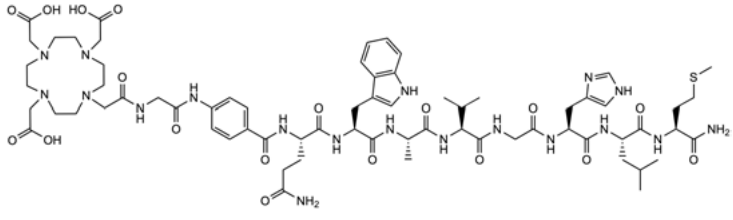

DB1

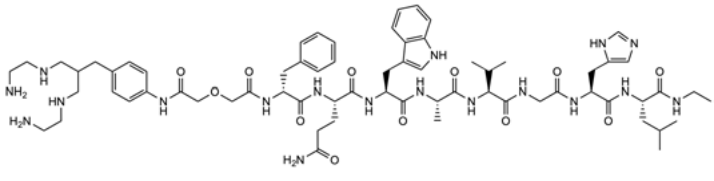

SB3

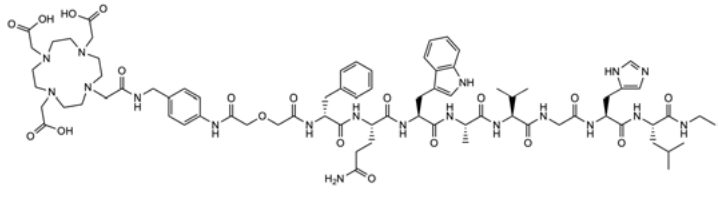

DB15

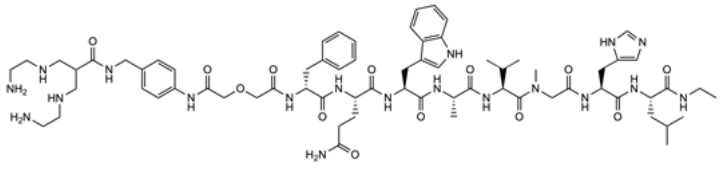

NeoB

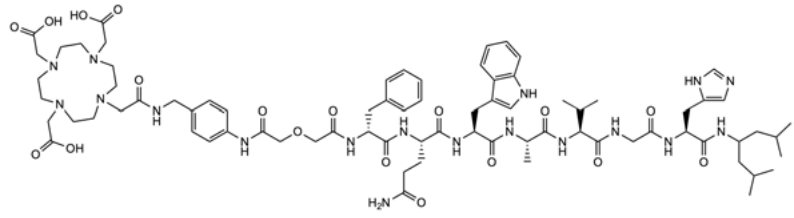

ProBOMB1

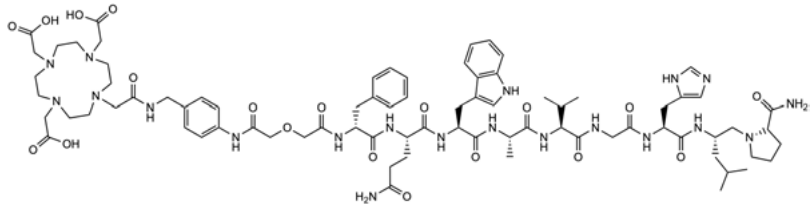

NOTA-PEG$_2$-RM26

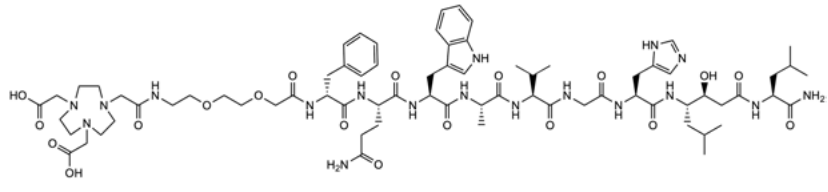

RM1

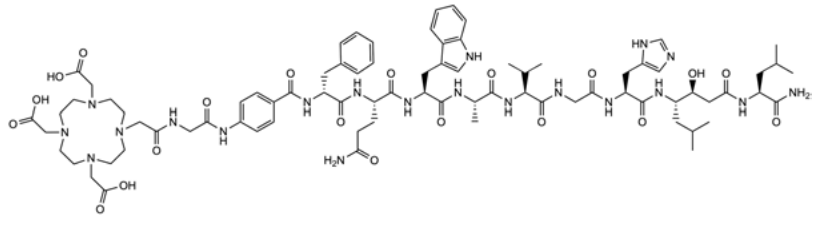

RM2

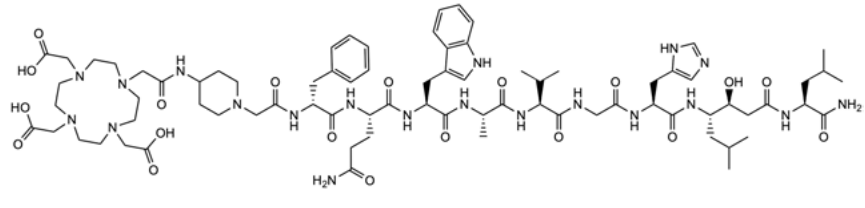

Figure 5. The chemical structures of several GRPR-targeting tracers.

Dual Targeting of GRPR and PSMA in Prostate Cancer

Thus far, research has shown that targeting GRPR is promising for detecting the early stages of prostate cancer. One specific potential application for GRPR targeting is the management of oligometastatic prostate cancer. There is compelling evidence that GRPR is overexpressed in the early stages of the disease and in the majority of lymph node and bone metastases, which comprise the main sites for prostate cancer metastases. In contrast, PSMA targeting is more extensively evaluated as a result of its overexpression in most prostate cancers, especially in mCRPC. The role of GRPR targeting in prostate cancer can be seen as complementary to PSMA targeting.

A number of studies have compared PSMA- and GRPR-targeting radiotracers in prostate cancer patients[218–222]. The majority of findings suggest that PSMA-targeting radiotracers are superior in identifying prostate cancer. This finding is supported by PSMA-expressing lesions that were missed by GRPR-targeting radiotracers due to the lack of GRPR expression or the lower standardised uptake values (SUVs) for GRPR-targeting radiotracers than for PSMA-targeting radiotracers. Conversely, the findings also point to PSMA-negative lesions that were detected by GRPR-targeting radiotracers and confirmed by immunohistochemical analysis as true malignancies, especially in the earlier stages of prostate cancer. Additionally, in some early-stage prostate cancers, GRPR-targeting radiotracers may show higher uptake than radiotracers targeting PSMA. These findings support the need for GRPR-targeted therapy but may also cause a radiation burden to patients if two different radiotracers are needed to visualise lesions that overexpress PSMA and lesions that overexpress GRPR within the same patient.

A possible strategy to overcome this issue is to target both PSMA and GRPR with a single radiotracer. An ideal heterodimer that targets PSMA and GRPR with high specificity and affinity may improve the sensitivity of detecting prostate cancer. It may also cover the different stages of the disease, given the PSMA and GRPR expression patterns in prostate cancer. It is also not difficult to imagine that a theranostic pair may further improve the therapeutic outcome achieved by the existing treatment options.

Several PSMA- and GRPR-targeting radiotracers have been developed and reported in recent years. The design of such radiotracers mainly comprises a urea-based PSMA-targeting moiety and a BBN-based GRPR-targeting moiety that are linked together to a chelator for labelling with a suitable radionuclide. Many research groups, including ours, have investigated this attractive concept by evaluating and reporting a number of heterodimers. The first heterodimers were reported in 2014 and demonstrated high specificity and affinity for both PSMA and GRPR. Despite the suboptimal pharmacokinetics of these heterodimers, they established the dual-targeting concept[223,224]. In the following years, more heterodimers were developed and evaluated, strengthening the hypothesis of dual targeting of GRPR and PSMA[225–228]. One heterodimer was

also evaluated in an early-phase clinical trial and demonstrated favourable dosimetry[229].

Our group has evaluated this promising approach, and two papers in this thesis discuss the results of novel PSMA- and GRPR-targeting radiolabelled heterodimers.

Selection of a Suitable Radionuclide

Choosing a radionuclide depends on whether the tracer is used for SPECT or PET imaging or for radionuclide therapy. For imaging, the radionuclide of choice should have a half-life that covers the biological half-life of the tracer and the intended time of imaging, as well as long enough to allow for production and quality control after radiolabelling. Not all molecules can withstand harsh radiolabelling conditions. Therefore, the selected radionuclide/radiolabelling chemistry should suit the properties of the molecule to be radiolabelled.

Ideally, the branching fraction of the emitted gamma or positron should be as high as possible (pure emitters), allowing for sensitive detection by SPECT or PET, while needing less scanning time and lower injected radioactivity. The energies of the gammas emitted by SPECT-suitable radionuclides should be high enough to penetrate through the tissue and reach the scanner but not too high to cause 'noise' in the resulting image after interaction with surrounding matter. In the case of PET-suitable radionuclides (positron emitters), the lower the energy is, the better, as the positron will then travel a shorter distance before annihilation.

Technetium-99m ($t_{½}$ = 6 h), iodine-123 ($t_{½}$ = 13 h) and indium-111 ($t_{½}$ = 2.8 d) are three examples of radionuclides suitable for SPECT imaging. Carbon-11 ($t_{½}$ = 20 min), gallium-68 ($t_{½}$= 68 min), fluorine-18 ($t_{½}$ = 110 min), zirconium-89 ($t_{½}$ = 3.3 d), and iodine-124 ($t_{½}$ = 4.2 d) are examples of radionuclides suitable for PET imaging.

The optimal radionuclide should also be cost-effective. For a radionuclide to be cost-effective, there must be an abundance of the parent nuclide and feasible production of the desired radionuclide in high quantities to allow for management of multiple patients with a single production.

The selection of a therapeutic radionuclide depends on the short range and the high linear energy transfer of the emitted particles, for example, β^- or α particles. These features will cause DNA damage and death of the targeted cells while sparing healthy tissues. A relatively long half-life of the radionuclide, along with favourable pharmacokinetics of the radiotracer, would maximise the therapeutic effect and lower the number of treatment cycles. Examples of therapeutic radionuclides include yttrium-90 ($t_{½}$ = 2.7 d), lutetium-177 ($t_{½}$ = 6.6 d), iodine-131 ($t_{½}$ = 8 d), actinium-225 ($t_{½}$ = 9.9 d), and radium-223 ($t_{½}$ = 11.4 d).

Selection of a Suitable Chelator and Linker

Most radionuclides need a moiety that they can bind to radiolabel a tracer. For example, radiometals require chelators, which chelate them and at the same time conjugate them to a ligand that targets a specific protein. An additional advantage is that radiometal-chelator complexes can be highly retained intracellularly after internalisation of the radiotracer. There is a wide selection of chelators that are compatible with the different properties of radionuclides and form stable complexes to minimise the presence of free radionuclides, which is undesirable as they can reduce the imaging contrast (tumour-to-nontumour ratios) or lead to false-positive findings. The net charge of the radionuclide-chelator complex and its position in the molecule have been shown to influence the pharmacokinetics of radiotracers, and therefore, careful selection of a suitable chelator is necessary to achieve a better-performing radiotracer[230]. Moreover, the moiety for radiolabelling can influence the residualising properties of radiohalogens. For example, the use of *N*-succinimidyl 4-guanidinomethyl-3-[^{125}I]iodobenzoate significantly improved the retention of iodine-125 compared with that with the use of nonresidualising moieties[231].

Apart from connecting the targeting moiety to the radionuclide, the function of linkers or spacers extends to modulating the affinity, lipophilicity, and pharmacokinetic profiles of the radiotracers. The use of linkers in BBN analogues radiolabelled with indium-111 resulted in a dramatic increase in affinity for GRPR compared with that of the BBN analogue without a linker to the chelator[232]. Several studies have shown that the use of PEG linkers in many radiotracers improves the affinity and tumour uptake while decreasing renal uptake[233–235].

Selection of a Suitable Targeting Ligand

An optimal ligand should have, among other properties, high specificity and affinity for the target, that is, to enable high tumour uptake while injecting low amounts of the ligand[236].

The selection of ligand in a radiotracer also depends on the intended purpose of use. For example, diagnostic radiotracers ideally should undergo rapid clearance from the body while being highly retained at the target. This allows for early imaging. Similar properties are also desirable for therapeutic radiotracers to deliver high doses to malignant tumours while simultaneously minimising the exposure of healthy tissues to radiation[237]. In comparison with antibodies and large proteins, low-molecular-weight ligands exhibit rapid clearance from blood and nontarget tissues and better tumour penetration[238,239]. Additionally, they are cheaper and easier to produce, can withstand harsh labelling conditions, and exhibit little to no immunogenicity.

Therefore, the majority of the radiotracers used for targeting PSMA and GRPR comprise small molecules or peptides of rather low molecular weight as their ligand for targeting.

Strategies to Improve Tumour Uptake and Pharmacokinetics

There are several strategies that can be employed to enhance tumour uptake for better diagnostic and therapeutic outcomes. Other strategies focus on protecting healthy organs from toxicity caused by elevated uptake of radioactivity. A number of these strategies will be highlighted in the following sections.

Binding to Serum Albumin

Human serum albumin (HSA, 66.5 kDa) is the most abundant protein in human plasma and has a half-life of approximately 19 days. Therefore, designing radiotracers that bind to albumin can improve and prolong the uptake in the targeted tumours as a result of the increased blood concentration. This concept has been utilised for decades, and increased tumour uptake and enhanced pharmacokinetic profiles has been shown with albumin-binding tracers[240]. A number of studies have evaluated the incorporation of albumin-binding moieties in PSMA-targeting radiotracers. For example, the incorporation of moieties such as 4-(p-iodophenyl)butyric acid, Evans blue, and ibuprofen in the structure of [^{177}Lu]Lu-PSMA-617 resulted in significantly increased tumour uptake and ultimately a higher area under the curve (AUC) for tumour activity uptake. This increased uptake resulted in an improved response to treatment in tumour-bearing mice[241–243]. Radiotracers that bind to albumin may influence the treatment regimen by injecting lower activities and/or subjecting the patients to fewer treatment cycles while potentially achieving the same therapeutic outcome as that of [^{177}Lu]Lu-PSMA-617 without an albumin-binding moiety.

Reduction of Undesirable Accumulation of Radioactivity

An ideal pharmacokinetic profile of a radiotracer would reflect a high tumour uptake and low activity in other tissues. However, this is not always the case, and many radiotracers are highly taken up by excretory organs, such as the kidneys. Additionally, it is common that the expression of the targeted protein is found in healthy tissues. The accumulation of radioactivity in healthy tissues may give rise to tolerable adverse events or, in some cases, severe toxicity.

Radionuclide therapy of PSMA-expressing mCRPC often causes xerostomia as a result of radioactivity accumulation in the salivary glands. Different

strategies to reduce PSMA-targeting radiotracer uptake in salivary glands are currently under investigation. One strategy aims to cause vasoconstriction by external cooling to reduce uptake; however, the effect of external cooling was found to be mild and insufficient[244].

Botulinum toxin A can be injected into the salivary glands of patients with neurologic disorders to control sialorrhea[245,246]. In the case of PSMA-targeting radiotracers, the use of botulinum toxin A was found to significantly reduce [^{68}Ga]Ga-PSMA-11 uptake to a large extent[247].

A common complication of radionuclide therapy is nephrotoxicity. The renal uptake of PSMA-targeting radiotracers is mediated by the kidneys being the main excretory organ and by endogenous PSMA expression in the proximal tubules of kidneys. The renal uptake of PSMA-targeting radiotracers can be reduced in tumour-bearing mice by using excess amounts of unlabelled PSMA inhibitors such as 2-PMPA or PSMA-11. Optimising the dose and time of administration of unlabelled PSMA inhibitors is essential to avoid the reduction of radiotracer uptake in PSMA-expressing tumours[248,249].

Other strategies that can be employed for nephroprotection and for improving pharmacokinetics include the coinjection of positively charged amino acids, the use of cleavable linkers, and pretargeting.

The anionic nature of megalin in the kidneys enhances the transport of cationic proteins[250]. Therefore, positively charged amino acids such as lysine and arginine can significantly decrease the renal uptake of radiotracers, as they compete with the radiotracers for the anionic binding sites[251].

The use of cleavable linkers that are cleaved specifically by brush border enzymes in the proximal tubule cell membrane may result in radiometabolites that are rapidly excreted into urine[252].

Another promising strategy to improve pharmacokinetics and minimise background radioactivity is pretargeting. In this approach, an unlabelled molecule is administered to bind to the targeted protein. After a period of time that allows the distribution, binding, and clearance of the unlabelled molecule from blood, the radiotracer, which is designed to have rapid clearance, is injected to bind to the unlabelled molecule which is bound to the targeted protein. This approach was shown to minimise radioactivity uptake in healthy tissues for protein-based agents, such as affibody molecules and monoclonal antibodies[253,254].

Aims of this Thesis

The general aim of this thesis was to develop and evaluate novel radiotracers for targeting PSMA and GRPR in prostate cancer to improve its diagnosis and therapy.

The specific aims of the studies were to:

- Evaluate dual targeting of PSMA and GRPR using heterodimers that can be radioiodinated for SPECT and PET imaging and for therapy (**Paper I**).

- Improve the affinity towards PSMA in PSMA- and GRPR-targeting heterodimers by modifying the linkers (**Paper II**).

- Investigate the effect of conjugating an albumin-binding domain to the GRPR antagonist RM26 on targeting GRPR-expressing prostate cancer (**Paper III**).

- Evaluate SPECT-suitable GRPR antagonists based on RM26 for imaging of GRPR-expressing malignant tumours in a preclinical study (**Paper IV**) and translate the best performing radiotracer into a phase I clinical trial to assess its safety and tolerability in prostate and breast cancer patients (**Paper V**).

Paper I

Synthesis and Preclinical Evaluation of Radio-Iodinated GRPR/PSMA Bispecific Heterodimers for the Theranostics Application in Prostate Cancer

Background and Aim

The targeting of PSMA has been established for theranostic approaches in prostate cancer, with several FDA-approved radiopharmaceuticals being used, such as [^{68}Ga]Ga-PSMA-11, [^{18}F]DCFPyL, and [^{177}Lu]Lu-PSMA-617 [255]. The targeting of GRPR for the management of prostate cancer is being extensively evaluated in preclinical and early-phase clinical studies, and it is showing great promise. Recently, a few radiometal-based heterodimers have been evaluated for dual targeting of GRPR and PSMA, and they have shown great potential[223,224].

The aim of this study was to develop a dual-targeting heterodimer to cover a wide spectrum of prostate cancers by targeting both GRPR and PSMA. The use of radioiodine would permit SPECT (iodine-123) and PET (iodine-124) imaging, as well as therapy (iodine-131), without changing the structure of the heterodimer.

Three heterodimers (Figure 6) were developed to target GRPR by using the GRPR antagonist RM26 and to target PSMA by using the PSMA inhibitor PSMA-617. The three heterodimers differed in the linkers between the PSMA-targeting moiety and the rest of the structure to modify lipophilicity. We aimed to characterise all three heterodimers in vitro, evaluate their in vivo targeting specificity, and select the best-performing heterodimer for further evaluation in vivo.

Results and Discussion

The heterodimers BO530, BO535, and BO536 were radiolabelled with iodine-125 with good radiochemical purities (RCPs). Purification using solid-phase extraction cartridges resulted in over 95% purity. The radiolabelled heterodimers were highly stable when incubated with human serum at 37 °C. The octanol-water distribution coefficient (log*D*) values showed that the most hydrophilic heterodimer among the three was [^{125}I]I-BO530, the heterodimer with

the hydrophilic linker, while the least hydrophilic heterodimer was [^{125}I]I-BO535, the heterodimer with the hydrophobic linker.

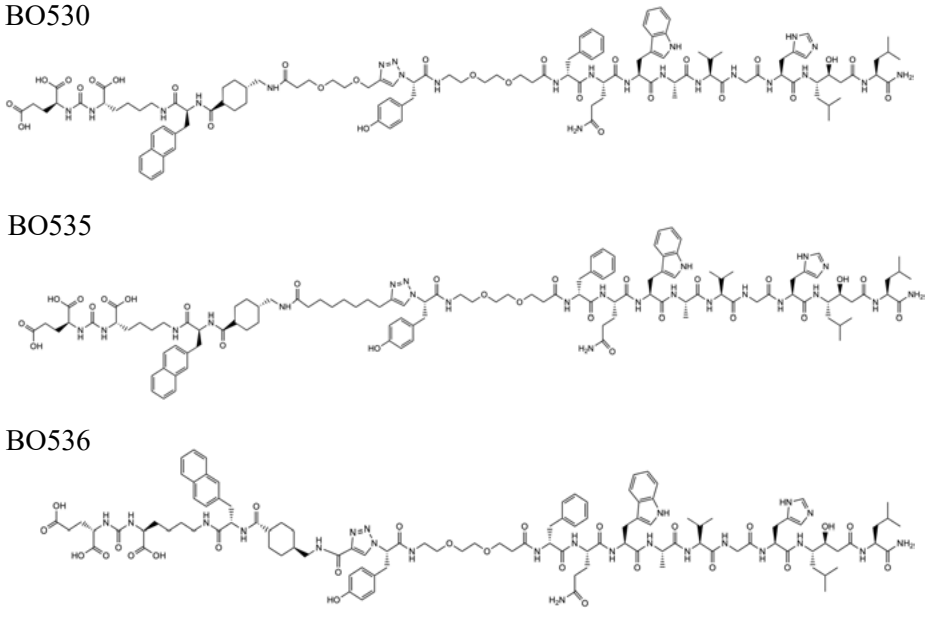

Figure 6. The chemical structures of the heterodimers BO530, BO535, and BO536.

The in vitro binding assays (Figure 7) demonstrated a significant reduction in heterodimer uptake upon blocking GRPR in PC-3 cells (GRPR$^+$), upon blocking PSMA in LNCaP cells (PSMA$^+$), and after blocking GRPR, PSMA, or both targets in PC-3 PIP cells (PSMA$^+$, GRPR$^+$), thus demonstrating that all three radioiodinated heterodimers bound to GRPR and PSMA with high specificity.

There was a high retention of radioactivity in PC-3 PIP cells (Figure 8A) from the three heterodimers after 24 h of incubation. To test the role of ligand-target interactions in retention, [^{125}I]I-BO530 was further evaluated in PC-3 and LNCaP cells (Figure 8B), and the results showed a decrease of approximately 86% in cell-associated radioactivity in PC-3 cells (GRPR$^+$) and a decrease of approximately 40% in LNCaP cells (PSMA$^+$) after 24 h of incubation. This finding indicated that the high cellular retention may be regulated by interacting with PSMA rather than GRPR.

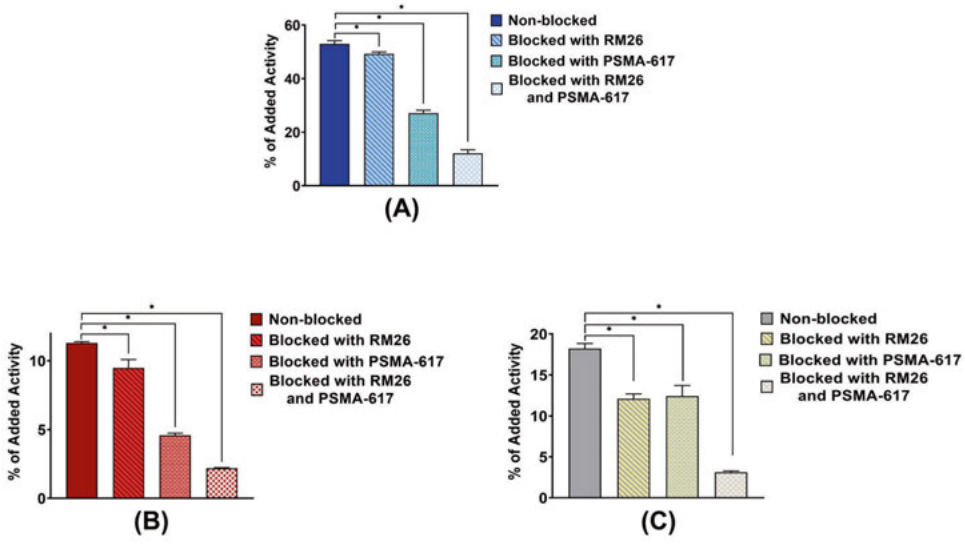

Figure 7. The results of the in vitro GRPR and PSMA binding of (**A**) [^{125}I]I-BO530, (**B**) [^{125}I]I-BO535, and (**C**) [^{125}I]I-BO536 in PC-3 PIP (PSMA^{+}, GRPR^{+}) cells. The data are presented as the mean values, and the error bars represent the standard deviation. * Indicates a statistically significant difference with a P value less than 0.05.

The half-maximal inhibitory concentration (IC_{50}) values (Figures 8C and 8D) to GRPR for BO530, BO535, and BO536 were 13 ± 3 nM, 20 ± 2 nM, and 6 ± 2 nM, respectively. The IC_{50} values to PSMA were 98 ± 13 nM, 100 ± 10 nM, and 80 ± 7 nM for BO530, BO535, and BO536, respectively. These results indicated that the affinity of the heterodimers for GRPR was higher than that for PSMA, and BO536 was more potent for both GRPR and PSMA than BO530 and BO535.

To further evaluate and select the best-performing heterodimer among the three, the targeting specificity was tested in Balb/c nu/nu mice bearing either PC-3 (GRPR^{+}) or LNCaP (PSMA^{+}) tumours (Figure 9). The results from the GRPR-targeting groups showed that pancreatic uptake (due to endogenous expression of GRPR) significantly decreased for all three heterodimers upon blocking GRPR. However, a significant reduction in PC-3 tumour uptake was only demonstrated for [^{125}I]I-BO530. The results from the PSMA-targeting groups showed a significant reduction in kidney uptake (due to PSMA expression in proximal tubules of kidneys) upon blocking of PSMA for all three heterodimers, while a significant reduction in LNCaP tumours was only evident for [^{125}I]I-BO530 and [^{125}I]I-BO536.

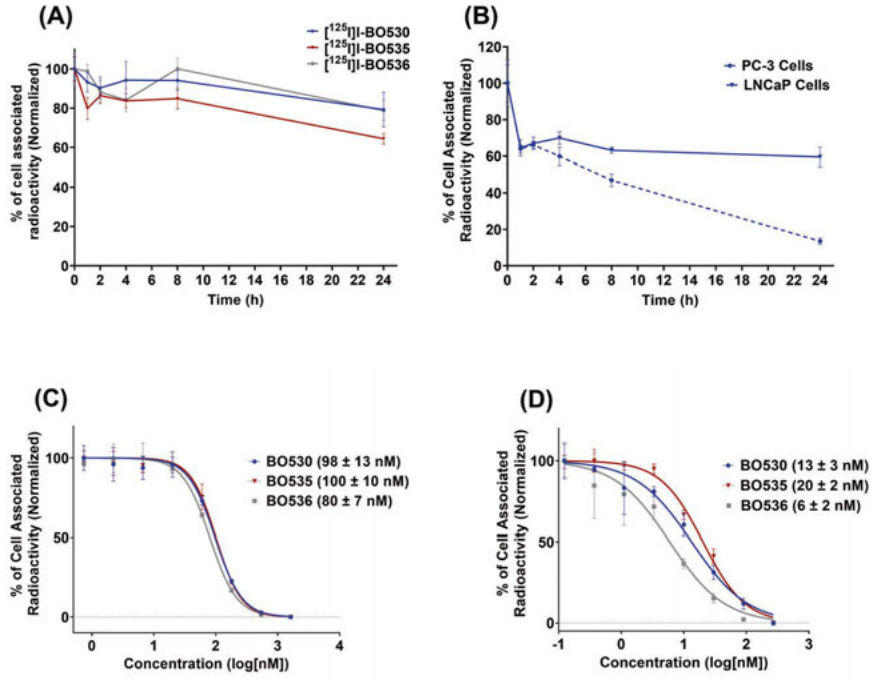

Figure 8. In vitro assays showing (**A**) the cellular retention of activity of the radiolabelled heterodimers in PC-3 PIP (PSMA$^+$, GRPR$^+$) cells, (**B**) the cellular retention of activity of [^{125}I]I-BO530 in PC-3 (GRPR$^+$) and LNCaP (PSMA$^+$) cells, and the IC_{50} of the three heterodimers for (**C**) PSMA and (**D**) GRPR. The error bars represent the standard deviation.

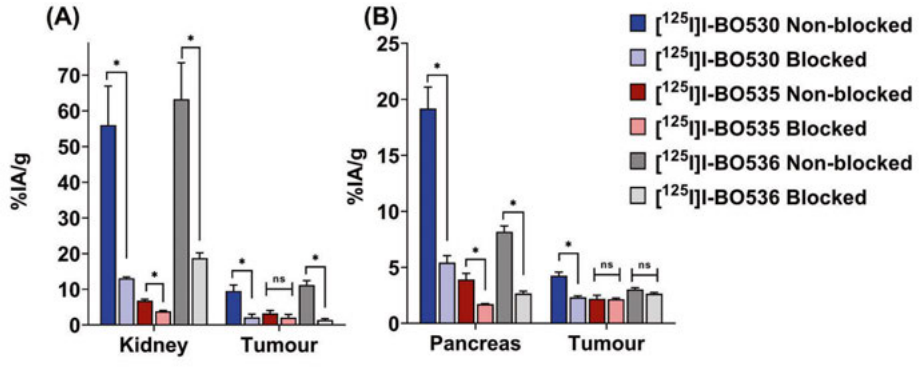

Figure 9. The in vivo targeting specificity study in Balb/c nu/nu mice bearing (**A**) LNCaP (PSMA$^+$) and (**B**) PC-3 (GRPR$^+$) tumours at 1 h p.i. The data are presented as the mean values, and the error bars represent the standard deviation. ^{ns} indicates no statistically significant difference, and * indicates a statistically significant difference with a P value less than 0.05.

Given the previous findings, the heterodimer [^{125}I]I-BO530 was selected for further evaluation in vivo. The biodistribution over time in Balb/c nu/nu mice bearing PC-3 PIP (PSMA^{+}, GRPR^{+}) tumours was studied, and the results are shown in Figure 10. At 1 h p.i, elevated uptake in various organs was observed, with the highest uptake being in the kidneys, and the tumour uptake was also high. The uptake in the kidneys and tumour further increased at 3 h p.i due to the initially elevated concentration in blood. At 24 h p.i, the uptake in most organs nearly diminished, while the uptake in the kidney decreased fivefold. Tumour uptake remained high, exceeding the uptake in all other tissues. At the last studied time point, 72 h p.i, the uptake in tumours only decreased twofold. Rough estimation of the AUC showed a 10-fold higher dose in the kidneys than in the tumour. Therefore, more work needs to be done to lower the kidney uptake. The data indicated that imaging at early time points may not be feasible, as the tumour-to-nontumour ratios were not high. The microSPECT/CT images, shown in Figure 11, corroborated the biodistribution profile, with the greatest contrast being at 72 h p.i.

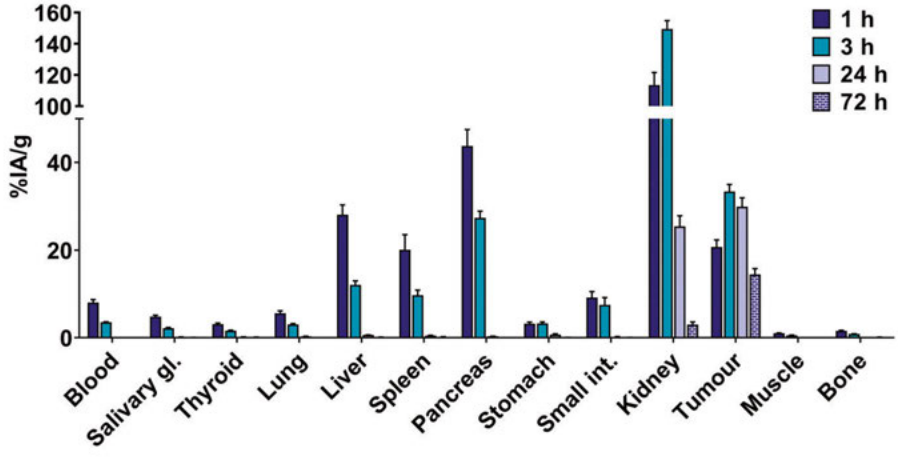

Figure 10. The biodistribution of [^{125}I]I-BO530 in Balb/c nu/nu mice bearing PC-3 PIP (PSMA^{+}, GRPR^{+}) tumours. The data are presented as the mean values, and the error bars represent the standard deviation.

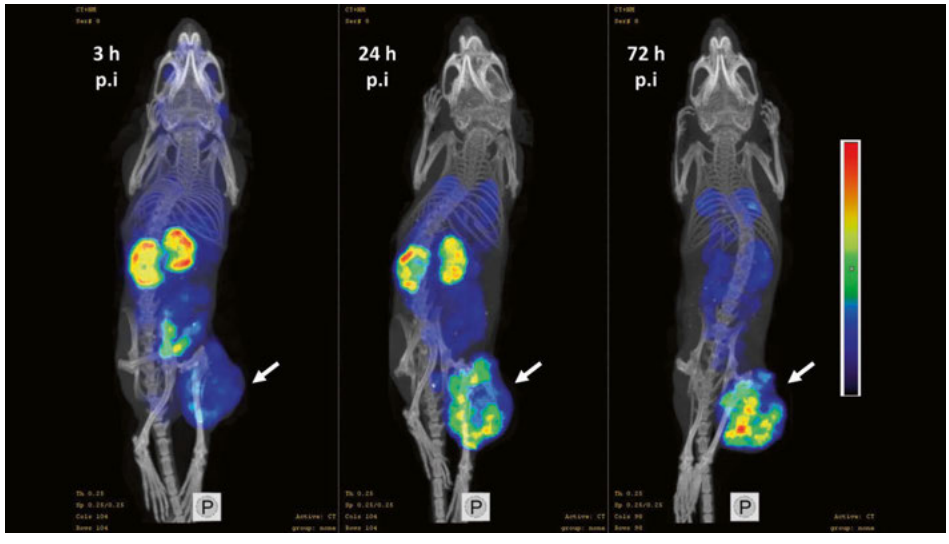

Figure 11. MicroSPECT/CT images of [^{125}I]I-BO530 in Balb/c nu/nu mice bearing PC-3 PIP (PSMA^{+}, GRPR^{+}) tumours. The white arrows point to the tumours.

Conclusion

This study reported the synthesis and preclinical evaluation of a promising GRPR and PSMA dual-targeting radioiodinated heterodimer. [^{125}I]I-BO530 showed high in vitro and in vivo specificity for GRPR and PSMA, with elevated and well-retained uptake in tumours. Further work on [^{125}I]I-BO530 is needed to reduce renal uptake and achieve an optimal pharmacokinetic profile for imaging.

Paper II

Heterodimeric Radiotracer Targeting PSMA and GRPR for Imaging of Prostate Cancer–Optimization of the Affinity towards PSMA by Linker Modification in Murine Model

Background and Aim

In Paper I, we reported the development and preclinical evaluation of three radioiodinated heterodimers for dual targeting of PSMA and GRPR in vitro and in vivo. Our group also previously developed and reported the preclinical evaluation of another heterodimer, NOTA-DUPA-RM26 (BQ7800), that is suitable for labelling with radiometals[225]. The heterodimer BQ7800 was radiolabelled with indium-111 and had rapid blood clearance and low kidney uptake. The affinity of [^{111}In]In-BQ7800 for GRPR was high; however, it had low affinity for PSMA, which resulted in rapid clearance from PC-3 PIP tumours.

The aim of this paper was to synthesise, radiolabel, and characterise three heterodimers (BQ7810, BQ7812, and BQ7813) based on BQ7800, with modifications in the linker between the PSMA-targeting moiety and the rest of the structure to improve the affinity for PSMA and at the same time evaluate the effect of a shorter PEG linker between the GRPR-targeting moiety and the rest of the structure on the properties of the heterodimers. The chemical structures are shown in Figure 12.

Results and Discussion

The three heterodimers were radiolabelled with indium-111 with high RCPs (>99%). The labelling stability was high, with minimal release of activity after incubation with excess EDTA. [^{111}In]In-BQ7812 and [^{111}In]In-BQ7813 bound to GRPR and PSMA with high specificity, which was reflected by the significant reduction in radioactivity uptake after blocking GRPR in PC-3 (GRPR^{+}) cells, PSMA in LNCaP (PSMA^{+}) cells, and both GRPR and PSMA in PC-3 PIP (PSMA^{+}, GRPR^{+}) cells. In the case of [^{111}In]In-BQ7810, however, blocking of PSMA in LNCaP cells showed a tendency for decreased radioactivity,

but the difference was not statistically significant. This finding indicated an early sign of poor PSMA affinity for [^{111}In]In-BQ7810. Nevertheless, this heterodimer bound to GRPR with high specificity, as reflected by the significant reduction in radioactivity uptake in PC-3 cells after GRPR saturation.

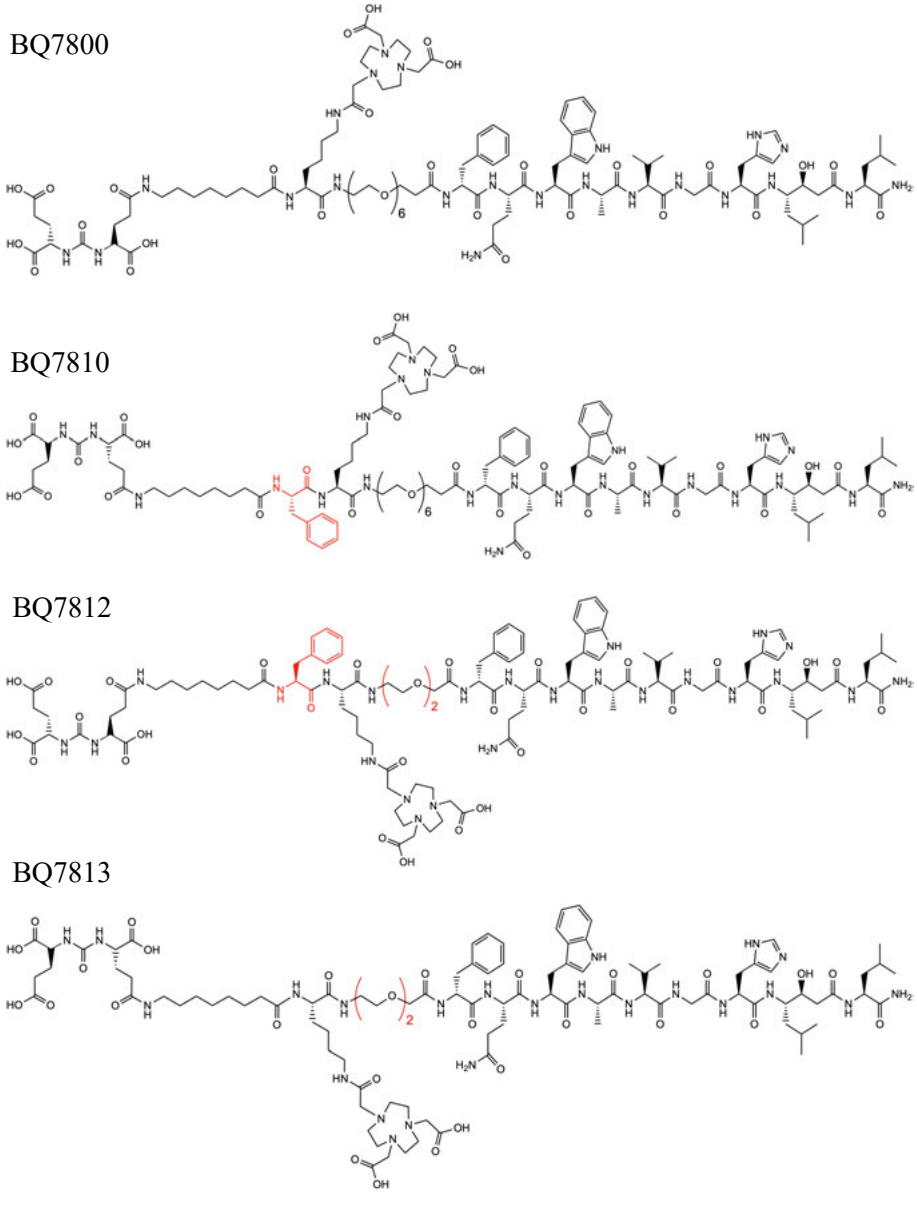

Figure 12. The chemical structures of the reference heterodimer BQ7800 and the developed derivatives BQ7810, BQ7812, and BQ7813.

The internalisation of all three radiolabelled heterodimers was slow, and the octanol-water distribution coefficient indicated that [^{111}In]In-BQ7813 was the most hydrophilic, while [^{111}In]In-BQ7812 was the most lipophilic of the three heterodimers, which corresponded to the structural modifications.

The IC_{50} values indicated that all three heterodimers had high affinity for GRPR, in agreement with the reference heterodimer ^{nat}In-BQ7800. However, the values showed that only ^{nat}In-BQ7812 had improved affinity for PSMA in comparison with the reference heterodimer (102 ± 80 nM for ^{nat}In-BQ7812 vs. 921 ± 363 nM for ^{nat}In-BQ7800). These results demonstrated that the incorporation of a phenylalanine along with the use of a shorter PEG linker was responsible for the overall improved affinity for PSMA.

The aforementioned findings led to the selection of [^{111}In]In-BQ7812 for further evaluation in vivo. It was evaluated in Balb/c nu/nu mice bearing PC-3 PIP tumours, showing significantly decreased [^{111}In]In-BQ7812 tumour uptake upon blocking GRPR and PSMA, as seen in Figure 13. Additionally, pancreatic uptake was significantly reduced upon blocking GRPR. There was a strong tendency for decreased renal uptake, although the difference between PSMA-blocked and nonblocked groups was not statistically significant.

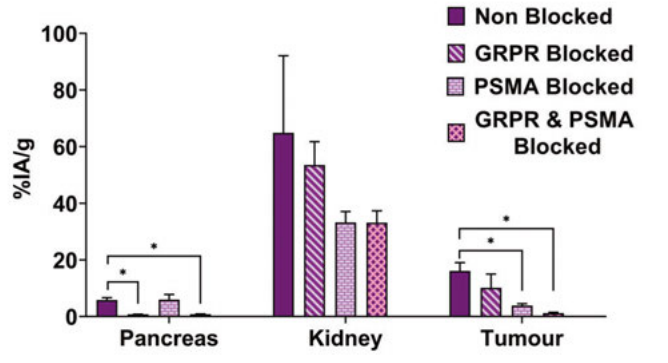

Figure 13. The in vivo targeting specificity of [^{111}In]In-BQ7812 in Balb/c nu/nu mice bearing PC-3 PIP (PSMA^{+}, GRPR^{+}) tumours at 1 h p.i. The data are presented as the mean values, and the error bars represent the standard deviation. * Indicates a statistically significant difference with a P value less than 0.05.

The biodistribution of [^{111}In]In-BQ7812 over time in mice bearing PC-3 PIP tumours (Figure 14) indicated elevated kidney uptake at 1 h p.i that was followed by tumour uptake. At 3 h p.i, the radioactivity uptake nearly diminished in all tissues except for the kidney, liver, and tumour. The radioactivity uptake in all tissues continued to clear at the last studied time point. The tumour-to-nontumour ratios were the highest at 3 h p.i, and the microSPECT/CT images (Figure 15) were in agreement with the pharmacokinetic profile.

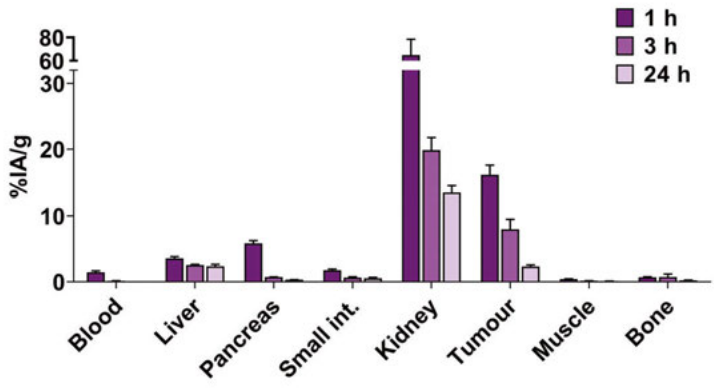

Figure 14. The biodistribution of [^{111}In]In-BQ7812 in Balb/c nu/nu mice bearing PC-3 PIP (PSMA^{+}, GRPR^{+}) tumours. The data are presented as the mean values, and the error bars represent the standard deviation.

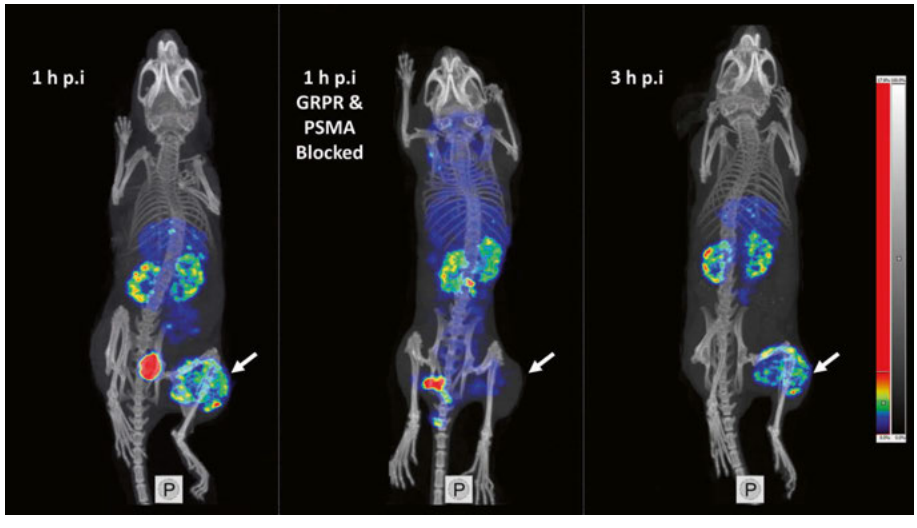

Figure 15. MicroSPECT/CT images of [^{111}In]In-BQ7812 in Balb/c nu/nu mice bearing PC-3 PIP (PSMA^{+}, GRPR^{+}) tumours. The white arrows point to the tumours.

The comparison between the biodistribution of [^{111}In]In-BQ7812 and the reference heterodimer [^{111}In]In-BQ7800 in mice bearing PC-3 PIP tumours at 1 h p.i (Figure 16) indicated significantly higher kidney and tumour uptake for [^{111}In]In-BQ7812 than for [^{111}In]In-BQ7800 due to the dramatic improvement in affinity for PSMA. Additionally, the liver uptake was significantly higher for [^{111}In]In-BQ7812 as a result of the increased lipophilicity due to the incorporated phenylalanine and the shorter PEG linker.

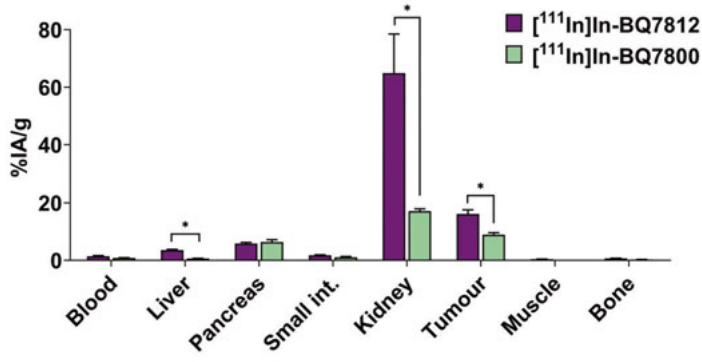

Figure 16. Comparison between the biodistribution of [^{111}In]In-BQ7812 and [^{111}In]In-BQ7800 in Balb/c nu/nu mice bearing PC-3 PIP (PSMA^{+}, GRPR^{+}) tumours at 1 h p.i. The data are presented as the mean values, and the error bars represent the standard deviation. * Indicates a statistically significant difference with a P value less than 0.05.

Conclusion

In this study, we reported the preclinical evaluation of a promising PSMA and GRPR dual-targeting heterodimer that was based on the previously reported heterodimer BQ7800. A few structural modifications led to a significant improvement in affinity for PSMA, which ultimately resulted in a significantly higher tumour uptake. More work is necessary to further improve the pharmacokinetic profile for the heterodimer to be considered for theranostic applications.

Paper III

Preclinical Evaluation of the GRPR-Targeting Antagonist RM26 Conjugated to the Albumin-Binding Domain for GRPR-Targeting Therapy of Cancer

Background and Aim

Targeting GRPR may be useful in the treatment of early stages of prostate cancer and in patients with oligometastatic disease. In recent years, a phase I clinical trial was conducted to evaluate the safety and dosimetry of the GRPR antagonist [^{177}Lu]Lu-RM2 for potential future use in radionuclide-based treatment of GRPR-expressing prostate cancer. Treatment using [^{177}Lu]Lu-RM2 was shown to be safe and well tolerated. It also clears rapidly from blood, and therefore, multiple cycles may be needed to deliver effective doses to tumours.

One strategy to increase drug efficacy is the incorporation of moieties that bind to albumin, which in turn increases the blood concentration and may result in higher tumour uptake over a longer time. This may reduce the number of cycles needed to deliver the appropriate therapeutic doses to tumours while decreasing the resulting adverse events. The albumin-binding domain ABD035 has femtomolar affinity for HSA[256]. Its conjugation to proteins led to increases in in vivo half-life and tumour uptake[257], the constructs were also safe and nonimmunogenic, and their use in humans did not cause adverse effects[258].

The aims of this study were to conjugate the GRPR antagonist RM26 to the albumin-binding domain ABD035 and to evaluate the conjugate in vitro and in vivo to assess the possibility of using it in the treatment of GRPR-expressing prostate cancer.

Results and Discussion

DOTA-ABD-RM26 was radiolabelled with indium-111 with good RCP (63 ± 3%). The purity was over 99% after purification on a size-exclusion column. The binding of [^{111}In]In-DOTA-ABD-RM26 to GRPR was significantly reduced upon blocking GRPR using DOTA-ABD-RM26 in the presence or absence of HSA. The internalisation of [^{111}In]In-DOTA-ABD-RM26 in PC-3 cells was low after 24 h of incubation. The IC_{50} (Figure 17) of ^{nat}In-DOTA-

ABD-RM26 was 30 ± 3 nM and increased to 49 ± 5 nM in the presence of HSA, while it was 4.5 ± 0.7 nM for ^{nat}In-DOTA-RM26. This indicated that while its binding to GRPR was preserved, the conjugation of RM26 to ABD035 led to a lower affinity for GRPR.

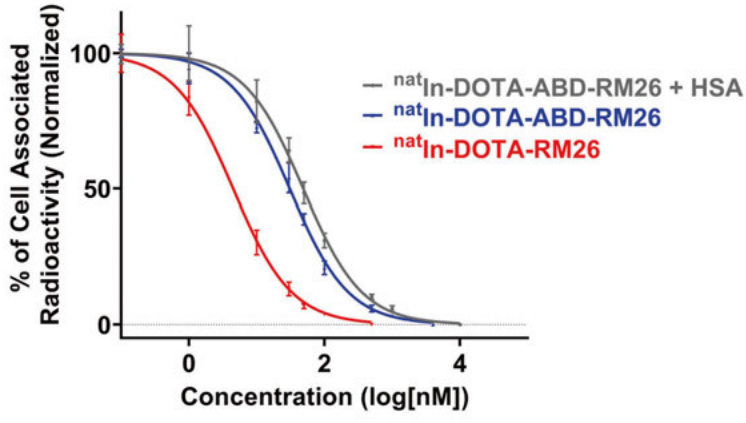

Figure 17. The IC_{50} data of ^{nat}In-DOTA-RM26, ^{nat}In-DOTA-ABD-RM26, and ^{nat}In-DOTA-ABD-RM26 in the presence of HSA in PC-3 ($GRPR^+$) cells. The error bars represent the standard deviation.

In vivo, the GRPR-targeting specificity of [^{111}In]In-DOTA-ABD-RM26 was evaluated in Balb/c nu/nu mice bearing PC-3 tumour xenografts. Despite the compromised affinity of [^{111}In]In-DOTA-ABD-RM26 for GRPR, blocking GRPR resulted in a significant reduction in its uptake in tumours. The biodistribution of [^{111}In]In-DOTA-ABD-RM26 and [^{111}In]In-DOTA-RM26 in PC-3 tumour-bearing mice, shown in Figure 18, demonstrated higher [^{111}In]In-DOTA-ABD-RM26 uptake in blood and many organs. However, the PC-3 tumour and pancreatic ($GRPR^+$) uptake of both radiotracers were similar.

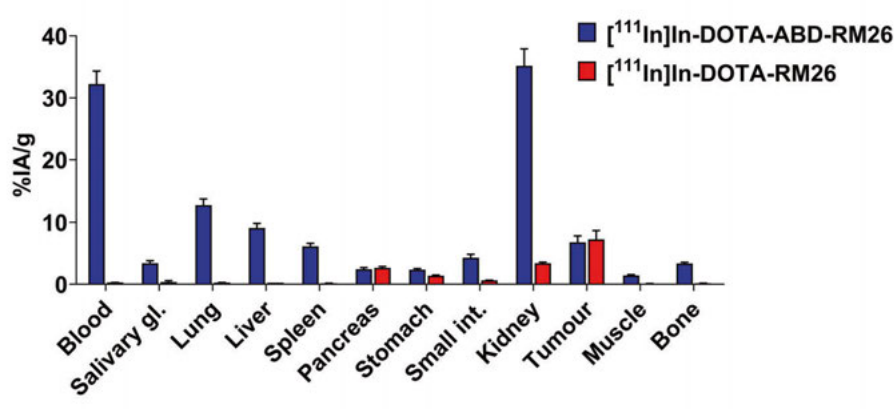

Figure 18. Comparison between the biodistribution of [^{111}In]In-DOTA-ABD-RM26 and [^{111}In]In-DOTA-RM26 in Balb/c nu/nu mice bearing PC-3 (GRPR^{+}) tumours at 1 h p.i. The data are presented as the mean values, and the error bars represent the standard deviation. A statistically insignificant difference in radioactivity uptake was only evident for the pancreas and tumour.

The biodistribution of [^{111}In]In-DOTA-ABD-RM26, shown in Figure 19, at 1 h p.i showed a high concentration of radioactivity in blood (32 ± 4% IA/g). This was accompanied by elevated uptake of radioactivity in the kidneys (35 ± 6% IA/g), while uptake in the PC-3 tumours was 7 ± 2% IA/g. The uptake of radioactivity in the blood decreased by more than 3-fold at 24 h p.i, while the uptake in the tumour increased to 11 ± 2% IA/g. At 144 h p.i, the uptake in blood continued to decrease, the uptake in kidneys decreased 2-fold, and the tumour uptake remained stable (10 ± 1% IA/g). However, the uptake of radioactivity in most other organs was also stable with little difference from the uptake at 24 h p.i.

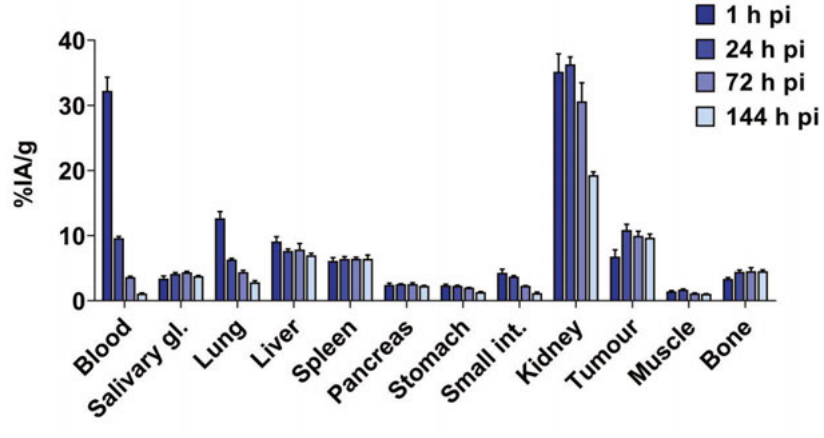

Figure 19. The biodistribution of [^{111}In]In-DOTA-ABD-RM26 in Balb/c nu/nu mice bearing PC-3 (GRPR^{+}) tumours. The data are presented as the mean values, and the error bars represent the standard deviation.

The conjugation of the GRPR antagonist RM26 to ABD035 ultimately resulted in stable tumour uptake even after 6 d p.i as a result of the high radioactivity concentration in blood. Moreover, the conjugate preserved the GRPR targeting feature, despite the lowered affinity from the parental GRPR antagonist RM26. However, elevated kidney uptake that exceeded the tumour uptake was evident in the biodistribution at all studied time points. This is unusual because it has been demonstrated previously that the conjugation of ABD035 to small proteins led to a dramatic decrease in renal reabsorption and because RM26 was shown to exhibit low renal reabsorption. An explanation of the high renal reabsorption at late time points can be corrupted affinity of the conjugate to albumin, which directs the dissociated fraction to renal clearance. There was evidence of radiolabel instability in vivo, reflected by elevated uptake in several organs, such as the liver and bone, even after 6 d p.i.

Conclusion

In this proof-of-principle study, the conjugation of ABD035 to RM26 resulted in elevated activity concentration in blood, which in turn resulted in high and stable uptake in GRPR-expressing tumours after 6 d of injection. Despite this, the elevated uptake in other organs, most notably the kidney and bone, abolishes the potential use of [^{111}In]In-DOTA-ABD-RM26 in radionuclide therapy. Structural modifications are needed to improve the biodistribution profile for radionuclide therapy. One potential use of the conjugate can be to deliver cytotoxic drugs to GRPR-expressing tumours.

Paper IV

Preclinical Evaluation of ^{99m}Tc-Labeled GRPR Antagonists maSSS/SES-PEG$_2$-RM26 for Imaging of Prostate Cancer

Background and Aim

The availability of PET scanners is increasing worldwide as a result of their increased resolution compared with that of SPECT scanners. However, SPECT scanners are more widely available worldwide than PET scanners (over four times the number of PET scanners)[43]. Several advances have been made in SPECT technology, such as cadmium-zinc-telluride detectors, resulting in much improved sensitivity and spatial resolution[259].

The overexpression of GRPR is found in the majority of primary prostate cancer samples and lymph node and bone metastases, in addition to elevated expression in several other malignancies.

Among the SPECT-suitable radionuclides is technetium-99m, which is the most commonly used radionuclide in diagnostic nuclear medicine owing to its favourable properties and feasibility of production. It has been previously demonstrated that the use of peptide-based chelators, such as mercaptoacetyl-tri-glycine or tri-serine, enables the radiolabelling of agents with technetium-99m while preserving affinity[118,260]. The use of such chelators allows for the formulation of single-vial kits for single-step radiolabelling using freshly eluted pertechnetate ($^{99m}TcO_4^-$) [261], which in turn simplifies clinical translation and use. Previous studies showed that the use of serine instead of glycine in chelators resulted in reduced release of technetium-99m in vivo, which was reflected by the lower radioactivity uptake in the stomach and salivary gland[262].

In this study, we aimed to develop two GRPR antagonists based on RM26 that contain peptide-amino-acid-based chelators for radiolabelling with technetium-99m. The two antagonists maSSS-PEG$_2$-RM26 and maSES-PEG$_2$-RM26 (Figure 20) were radiolabelled with freshly eluted $^{99m}TcO_4^-$, characterised in vitro and in vivo, and directly compared, with the main aim of providing a radiotracer with a straightforward radiolabelling protocol for the clinical imaging of GRPR-expressing prostate tumours using the widely available SPECT scanners.

maSSS-PEG$_2$-RM26

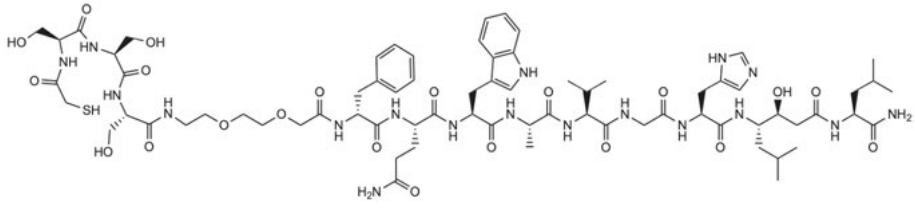

maSES-PEG$_2$-RM26

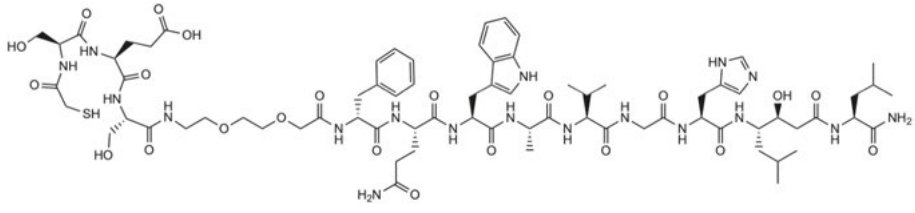

Figure 20. The chemical structures of maSSS-PEG$_2$-RM26 and maSES-PEG$_2$-RM26.

Results and Discussion

The GRPR antagonists maSSS-PEG$_2$-RM26 and maSES-PEG$_2$-RM26 were radiolabelled with technetium-99m with high RCPs, and the radiolabel stability was high with minimal release of technetium-99m under cysteine challenge. The octanol-water distribution coefficient indicated that [^{99m}Tc]Tc-maSSS-PEG$_2$-RM26 had higher lipophilicity than [^{99m}Tc]Tc-maSES-PEG$_2$-RM26 due to the incorporation of glutamic acid in the latter. This result was also reflected by the significantly lower hepatic uptake of [^{99m}Tc]Tc-maSES-PEG$_2$-RM26 (1.1 ± 0.3% IA/g vs. 3 ± 1% IA/g for [^{99m}Tc]Tc-maSSS-PEG$_2$-RM26 at 3 h p.i, $P<0.05$, $n = 4$). Both radiotracers bound to GRPR in PC-3 cells with high specificity, which was also evident in NMRI mice when blocking GRPR led to significantly lower pancreatic (GRPR$^+$) uptake of both radiotracers. The internalisation rate was slow for the radiotracers, and the overall internalised fractions after 24 h of incubation were low. The affinity measurements indicated that while both radiotracers had high affinity for GRPR, [^{99m}Tc]Tc-maSSS-PEG$_2$-RM26 demonstrated higher affinity than [^{99m}Tc]Tc-maSES-PEG$_2$-RM26. While the use of glutamic acid in [^{99m}Tc]Tc-maSES-PEG$_2$-RM26 increased the hydrophilicity, it resulted in lower affinity to GRPR, which led to a significantly lower GRPR-expressing tumour uptake in vivo (2.9 ± 0.7% IA/g vs. 7 ± 2% IA/g for [^{99m}Tc]Tc-maSSS-PEG$_2$-RM26 at 3 h p.i, $P<0.05$, $n = 4$) (the biodistribution is shown in Figure 21), the tumour-to-nontumour ratios were higher for [^{99m}Tc]Tc-maSSS-PEG$_2$-RM26 than for [^{99m}Tc]Tc-maSES-PEG$_2$-RM26. These findings led to the selection of [^{99m}Tc]Tc-maSSS-PEG$_2$-RM26 for further evaluation in vivo.

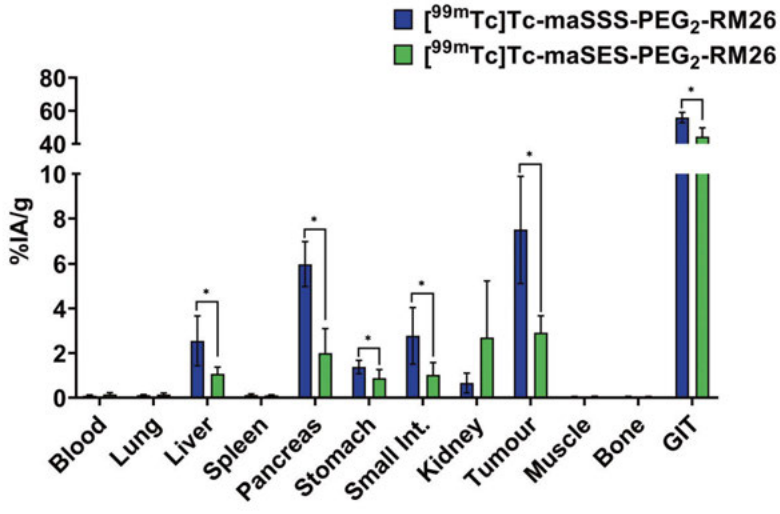

Figure 21. Comparison between the biodistribution of [^{99m}Tc]Tc-maSSS-PEG$_2$-RM26 and [^{99m}Tc]Tc-maSES-PEG$_2$-RM26 in Balb/c nu/nu mice bearing PC-3 (GRPR$^+$) tumours at 3 h p.i. The data are presented as the mean values, and the error bars represent the standard deviation. * Indicates a statistically significant difference with a P value less than 0.05. The values of GIT represent the mean % IA values only.

The in vivo GRPR-targeting specificity of [^{99m}Tc]Tc-maSSS-PEG$_2$-RM26 in PC-3 tumour-bearing Balb/c nu/nu mice (Figure 22) showed significantly lower tumour and pancreatic uptake in the GRPR-blocked groups than in the nonblocked groups.

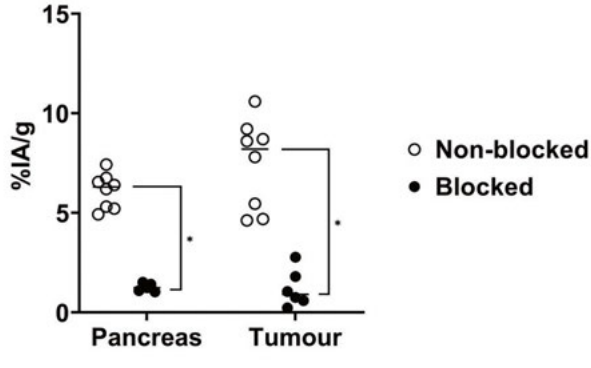

Figure 22. In vivo targeting specificity for [^{99m}Tc]Tc-maSSS-PEG$_2$-RM26 in Balb/c nu/nu mice bearing PC-3 (GRPR$^+$) tumours at 30 min p.i. * Indicates a statistically significant difference with a P value less than 0.05.

The biodistribution of [^{99m}Tc]Tc-maSSS-PEG$_2$-RM26 over time in PC-3 tumour-bearing Balb/c nu/nu mice showed decreased uptake in all studied tissues at 6 h p.i compared with 3 h p.i. Despite this observation, the tumour-to-nontumour ratios were higher at 3 h p.i as a result of the 2-fold higher radioactivity uptake in the tumour at 3 h p.i than at 6 h p.i. Thus, imaging of GRPR-expressing tumours using [^{99m}Tc]Tc-maSSS-PEG$_2$-RM26 is more suitable within a few hours after injection. The microSPECT/CT images (Figure 23) indicated clear visualisation of GRPR-expressing tumours using [^{99m}Tc]Tc-maSSS-PEG$_2$-RM26. The elevated hepatobiliary uptake may be an advantage, as the urinary bladder, which is anatomically in close proximity to the prostate, may have low radioactivity uptake. Additionally, hepatobiliary excretion in humans is slower than that in rodents, which may favour the use of [^{99m}Tc]Tc-maSSS-PEG$_2$-RM26 in the imaging of early-stage GRPR-expressing prostate cancer. The dosimetry estimations, performed using OLINDA, predicted generally low absorbed doses to healthy tissues, and the effective dose was 3.49 $\times$ 10^{-3} mSv/MBq.

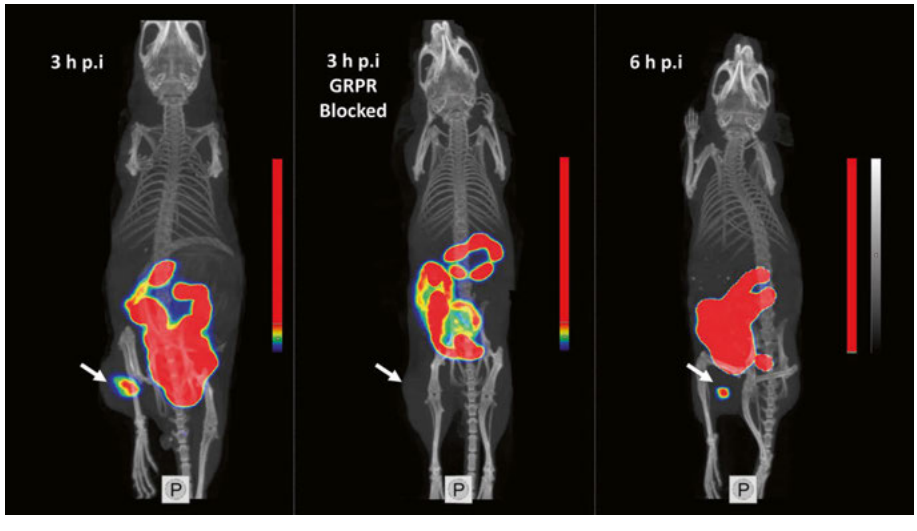

Figure 23. MicroSPECT/CT images of [^{99m}Tc]Tc-maSSS-PEG$_2$-RM26 in Balb/c nu/nu mice bearing PC-3 (GRPR$^+$) tumours. The white arrows point to the tumours.

Conclusion

In conclusion, Paper IV presents the preclinical evaluation of a promising GRPR antagonist that can be radiolabelled with SPECT-suitable technetium-99m via a simple radiolabelling procedure. The radiotracer is able to visualise GRPR-expressing tumours at early time points. A phase I clinical trial, presented in Paper V, was conducted based mainly on the findings in Paper IV.

Paper V

Phase I Trial of [^{99m}Tc]Tc-maSSS-PEG$_2$-RM26, a Bombesin Analogue Antagonistic to Gastrin-Releasing Peptide Receptors (GRPRs) for SPECT Imaging of GRPR Expression in Malignant Tumors

Background and Aim

The targeting of PSMA for detecting prostate cancer has been established in recent years. Two of the most routinely used PSMA-targeting radiotracers are the FDA-approved [^{68}Ga]Ga-PSMA-11 and [^{18}F]DCFPyL. They have optimal sensitivity and specificity in detecting prostate cancer. However, their sensitivity in detecting lymph node metastases is limited[263,264]. Therefore, different molecular targets, such as GRPR, may be more useful in the detection of early-stage prostate cancers.

GRPR is overexpressed in the majority of primary prostate cancers, as well as in the majority of lymph node and bone metastases. In breast cancer, GRPR overexpression is hormone-driven, with most oestrogen receptor-positive breast cancers overexpressing GRPR, while approximately 12% of oestrogen receptor-negative and 7.8% of triple-negative breast cancers overexpress GRPR[265].

In **paper IV**, we conducted a preclinical evaluation of the GRPR antagonist [^{99m}Tc]Tc-maSSS-PEG$_2$-RM26 and demonstrated that it binds to GRPR with high affinity and could visualise GRPR-expressing tumours. A kit formulation can be utilised for one-vial single-step labelling of maSSS-PEG$_2$-RM26 using freshly eluted pertechnetate ($^{99m}TcO_4^-$), taking advantage of the amino-acid-based chelator (maSSS) incorporated in the structure for this purpose. Thus, this study provides a simple and rapid procedure for radiolabelling maSSS-PEG$_2$-RM26 for use in clinical settings.

Our aim in this paper was to evaluate [^{99m}Tc]Tc-maSSS-PEG$_2$-RM26 in a phase I clinical study, with the main objectives of evaluating the safety and tolerability of the radiotracer, studying the biodistribution profile in males and females, estimating the dosimetry, and evaluating the targeting of GRPR-expressing tumours.

Results and Discussion

The six prostate cancer patients and seven breast cancer patients recruited for this study were injected with 40 µg of [^{99m}Tc]Tc-maSSS-PEG$_2$-RM26 (RCP>98%). There were no reported adverse effects, indicating that [^{99m}Tc]Tc-maSSS-PEG$_2$-RM26 is well tolerated and safe at the injected doses. Additionally, the adverse events related to the use of GRPR agonists were averted, as injecting higher doses of our GRPR antagonist than the GRPR agonist doses reported to cause adverse events did not lead to any of these events[266]. After injection, the biodistribution profile of [^{99m}Tc]Tc-maSSS-PEG$_2$-RM26 in male and female patients indicated rapid clearance of the unbound radiotracer from the blood and rapid whole-body elimination. This rapid clearance helps in improving the contrast between the uptake in tumours and background for better detection and visualisation of the target.

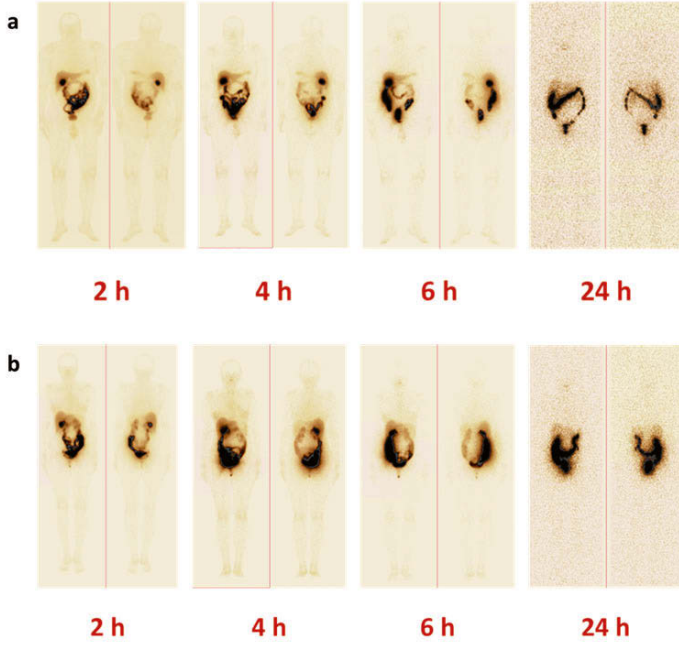

Figure 24. Anterior (left) and posterior (right) images of two patients with (**a**) prostate cancer and (**b**) breast cancer at 2, 4, 6, and 24 h after intravenous injection of [^{99m}Tc]Tc-maSSS-PEG$_2$-RM26.

The close proximity of the prostate to the urinary bladder may impact the visualisation of primary prostatic tumours and regional metastases by radiotracers that are predominantly excreted in urine, resulting in high activity in the urinary bladder shortly after injection. [^{99m}Tc]Tc-maSSS-PEG$_2$-RM26 was

designed to favour hepatobiliary excretion instead of renal excretion to prevent elevated uptake in the urinary bladder. The biodistribution shows elevated hepatobiliary excretion, which is in concordance with the preclinical evaluation of the radiotracer. The images in Figure 24 show the biodistribution of [^{99m}Tc]Tc-maSSS-PEG$_2$-RM26 over time in prostate cancer and breast cancer patients, indicating more efficient radioactivity passage through the gastrointestinal tract in male patients. Despite this, high enterohepatic uptake may impact the visualisation of GRPR-expressing lesions in the lower abdomen, and while liver metastases may prevail in later stages of prostate cancer and in approximately 10% of patients with metastatic disease, approximately 50-70% of metastatic breast cancer patients have liver metastases[267].

At 2 h after injection, it was possible to clearly visualise primary tumours and metastases with elevated [^{99m}Tc]Tc-maSSS-PEG$_2$-RM26 uptake. In prostate cancer patients, [^{99m}Tc]Tc-maSSS-PEG$_2$-RM26 uptake in tumours was identified in four out of six patients. In the seven breast cancer patients, uptake of the radiotracer in primary tumours was identified in all patients. The median sizes of the visualised prostate and breast tumours were 3.22 cm^3 (2.9–16.1) and 13.6 cm^3 (1.6–73.9), respectively. High uptake was additionally detected in the axillary lymph nodes in four breast cancer patients, and the median lesion size was 3.72 cm^3 (1.1–7.8). After 2 h of injecting [^{99m}Tc]Tc-maSSS-PEG$_2$-RM26, the median activity accumulation (SUVmax) in prostate tumours was 1.18 (0.78–1.67), in breast cancer was 0.87 (0.43–1.75), and in breast cancer lymph node metastases was 1.8 (0.58–1.8). The median tumour-to-nontumour value for prostate tumours was 6.85 (4.2–10.9), for breast tumours was 7.8 (2.2–35), and for breast cancer lymph node metastases was 9.2 (6–16.3). The values in all lesions decreased over time. In two of the breast cancer patients, there was no prior evidence of regional metastases. However, the SPECT/CT images showed accumulation of [^{99m}Tc]Tc-maSSS-PEG$_2$-RM26 in the lymph nodes. Morphological examination during surgery detected lymph node metastases, resulting in expanding the surgery to a standard axillary lymphadenectomy. This finding also resulted in restaging one of the patients from N0 to N3 and the other from N0 to N1.

At the two-hour p.i time point, all tumours and metastases with elevated [^{99m}Tc]Tc-maSSS-PEG$_2$-RM26 uptake were clearly visualised. Representative images of prostate and breast tumours are provided in Figures 25 and 26. The results of the immunohistochemical staining indicated positive GRPR expression in 60% of the prostate tumour samples (three out of five samples) and in 71.4% of the breast cancer samples (five out of seven samples). Positive GRPR expression was confirmed in 50% of the samples from breast cancer lymph node metastases (two out of four patients). The highest contrast in the visualised primary prostate tumours was in the patient with the highest PSA value and largest tumour. While all primary tumours in the breast cancer patients were clearly visualised by [^{99m}Tc]Tc-maSSS-PEG$_2$-RM26, it cannot be

confirmed that the lymph nodes investigated by immunohistochemical analysis were detected by [^{99m}Tc]Tc-maSSS-PEG$_2$-RM26 imaging due to the design of the phase I study, which was not designed to determine the sensitivity and specificity.

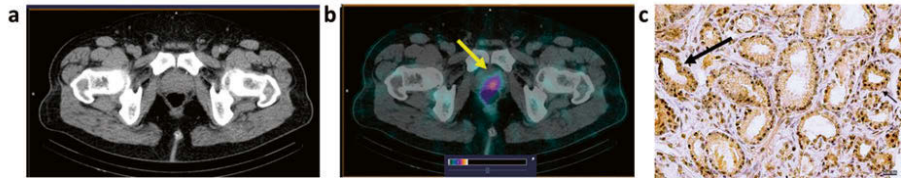

Figure 25. Two hours after IV of [^{99m}Tc]Tc-maSSS-PEG$_2$-RM26 (**a**) CT and (**b**) fused SPECT/CT images of a patient with adenocarcinoma of the prostate. The yellow arrow (**b**) points at a focus of increased [^{99m}Tc]Tc-maSSS-PEG$_2$-RM26 uptake visualised in the prostate (SUVmax = 1.21), and the upper setting of the scale window was adjusted for better visualisation (24% of the maximum number). Immunohistochemical analysis (**c**) of tumour sample showing moderate (2+) GRPR expression in adenocarcinoma cells (black arrow), magnification 40×.

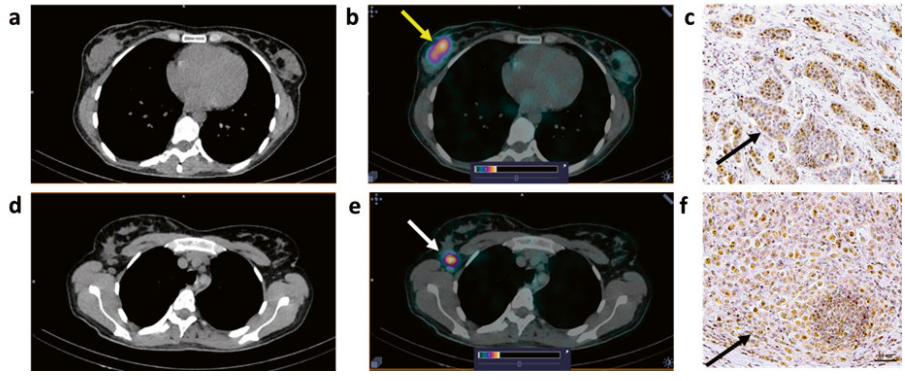

Figure 26. Two hours after IV of [^{99m}Tc]Tc-maSSS-PEG$_2$-RM26 (**a**, **d**) CT and (**b**, **e**) fused SPECT/CT images of a patient with invasive breast carcinoma. The yellow arrow (**b**) points at a focus of increased [^{99m}Tc]Tc-maSSS-PEG$_2$-RM26 uptake visualised in the right breast (SUVmax = 1.75). The white arrow (**e**) points at an enlarged right axillary node (up to 1.3 cm) with elevated [^{99m}Tc]Tc-maSSS-PEG$_2$-RM26 uptake (SUVmax = 1.8), and the upper setting of the scale window was adjusted for better visualisation (24% of the maximum number). Immunohistochemical analysis (**c**) of primary breast tumour and (**f**) of lymph node metastasis showing light (1+) and moderate (2+) GRPR expression, respectively, magnification 40×.

The evaluation of the absorbed doses showed significantly higher absorbed doses in the pancreas and liver of female patients than in the pancreas and liver of male patients. The same pattern was evident for the gallbladder wall. The effective doses for male patients were 0.0053 ± 0.0007 mSv/MBq and for female patients were 0.008 ± 0.003 mSv/MBq, with the radionuclide-associated dose per patient per study being 3–6 mSv.

Conclusion

The administration of the peptide-based GRPR antagonist [^{99m}Tc]Tc-maSSS-PEG_2-RM26 was deemed safe in male and female patients. The injections resulted in low absorbed doses to healthy tissues, with the effective doses being within the same range as for other radiotracers of the same category. SPECT/CT imaging using [^{99m}Tc]Tc-maSSS-PEG_2-RM26 visualised tumours of the prostate and breast, in addition to detecting breast cancer lymph node metastases. Future clinical studies are needed to assess the sensitivity and specificity of [^{99m}Tc]Tc-maSSS-PEG_2-RM26 in detecting GRPR-expressing tumours.

Concluding Remarks

Many men are expected to be diagnosed with prostate cancer during their lifetime. Over the past decades, advances in prostate cancer research have led to a much-improved clinical outcome with diverse options for diagnosis and treatment. Despite the efforts and achievements, more research is needed to further improve the detection rates of the existing diagnostic methods, and there is a need to improve the available treatment options, especially for advanced and aggressive types of prostate cancer.

Targeting PSMA and GRPR shows great promise in improving the existing diagnostic and therapeutic tools, as they are expressed at varying levels during the different stages of prostate cancer.

Papers I-II investigated the dual targeting of PSMA and GRPR by heterodimers that can be labelled with radioiodine or radiometals. We evaluated the effect of linker modification on the pharmacokinetic profile.

- The findings of **Paper I** indicated that a more hydrophilic linker between PSMA-617 and RM26 resulted in a heterodimer, [^{125}I]I-BO530, that retained high specificity for PSMA and GRPR. The heterodimer also showed elevated and well-retained tumour uptake 3 d p.i.

- **Paper II** showed that the incorporation of a phenylalanine and the use of a shorter linker in the structure of [^{111}In]In-BQ7800 resulted in a highly PSMA- and GRPR-specific heterodimer, [^{111}In]In-BQ7812. The structural modifications also resulted in a much-improved affinity for PSMA.

Targeting GRPR for therapeutic purposes may be useful in the management of patients with early-stage or oligometastatic prostate cancer. In Paper III, we investigated the effect of conjugating an albumin-binding domain to the GRPR antagonist RM26 on tumour uptake and the overall pharmacokinetic profile from a therapeutic perspective.

- **Paper III** showed that the conjugation of ABD035 to RM26, [^{111}In]In-DOTA-ABD-RM26, increased the concentration of radi-

oactivity in the blood, which resulted in improved and stable tumour uptake over several days p.i. However, elevated uptake in normal tissues abolishes the use of the conjugate in radionuclide therapy, but perhaps it may be useful in delivering cytotoxic drugs to GRPR-expressing malignant tumours.

The availability of SPECT scanners extends to more countries around the world than PET scanners. This increased SPECT scanner availability necessitates the continuous development of SPECT-suitable radiotracers for targeting prostate cancer cell markers, such as GRPR. The use of amino acid-based chelators and the use of a kit formulation enabled one-vial single-step radiolabelling of molecules with freshly eluted generator-produced $^{99m}TcO_4^-$, which is feasible for use in clinical settings.

- **Paper IV** reported the preclinical evaluation of the GRPR antagonist [^{99m}Tc]Tc-maSSS-PEG$_2$-RM26, which possessed high specificity and affinity for GRPR. Additionally, it had low renal excretion, which may benefit imaging of primary prostate tumours as they are in close proximity to the urinary bladder.

- **Paper V** reported the clinical translation of [^{99m}Tc]Tc-maSSS-PEG$_2$-RM26. Injections of the radiolabelled GRPR antagonist in prostate and breast cancer patients were safe and well tolerated. The dosimetry estimations were in agreement with radiotracers of the same category. [^{99m}Tc]Tc-maSSS-PEG$_2$-RM26 could also visualise GRPR-expressing primary tumours in addition to some lymph node metastases that were not detected using conventional imaging methods.

The findings in this thesis explored different theranostic approaches for the management of prostate cancer through the targeting of two of the most prominent and investigated prostate cancer cell markers: PSMA and GRPR. Our findings warrant the continuation of work to further improve the tools available for diagnosing and treating prostate cancer patients.

Ongoing and Future Studies

The dual targeting of PSMA and GRPR is an attractive approach to build on the existing success of PSMA targeting and the great potential of GRPR targeting. We are continuing to develop more heterodimers with improved tumour uptake and, equally important, reduced kidney uptake. We are developing heterodimers that can be labelled with radiometals such as gallium-68 for PET imaging and lutetium-177 for therapy. The clinical translation of one of the reported heterodimers is to be performed to assess its safety and tolerability in prostate cancer patients and to assess its performance in detecting primary prostate tumours and metastases.

Targeting GRPR with therapeutic intent is still in the early stages with much to be uncovered and learned. We designed modifications to the structure of DOTA-ABD-RM26 with the aim of improving the pharmacokinetic profile and stability. However, there was little success with these modifications, and a future approach is to use an albumin-binding moiety of lower molecular weight in proportion to the size of RM26.

The metabolic stability of peptides is essential to allow for a higher level of binding to the targeted protein on malignant tumour cells. Our group investigated amino acid modifications in the sequence of RM26, conferring high resistance to the action of neprilysin, although the results are not yet published at the time of writing this thesis.

The translation of [^{99m}Tc]Tc-maSSS-PEG$_2$-RM26 into a clinical trial provided insight into the clinical needs and how to design preclinical studies to meet this demand. We are currently working on derivatives of [^{99m}Tc]Tc-maSSS-PEG$_2$-RM26 to slightly improve the hydrophilicity and visualisation of GRPR-expressing breast and prostate primary tumours and metastases.

Appendix

Table A1: ISUP grade group classification system

Grade Group 1	Gleason Score ≤ 6
Grade Group 2	Gleason Score 7 (3 + 4)
Grade Group 3	Gleason Score 7 (4 + 3)
Grade Group 4	Gleason Score 8
Grade Group 5	Gleason Score 9–10

Table A2: TNM clinical classification of prostate cancer

T	Primary Tumour
TX	Tumour cannot be assessed
T0	No evidence of primary tumour
T1	**Impalpable and invisible tumour by imaging (clinically inapparent)**
T1a	Incidental histological finding (≤ 5% of resected tissue)
T1b	Incidental histological finding (≥ 5% of resected tissue)
T1c	Identified by needle biopsy
T2	**Tumour confined within the prostate**
T2a	Involves ½ of one lobe or less
T2b	Involves >½ of one lobe but not both lobes
T2c	Involves both lobes
T3	**Tumour extends through the prostatic capsule**
T3a	Extracapsular extension including microscopic bladder neck involvement
T3b	Tumour invades the seminal vesicle(s)
T4	**Tumour is fixed or invades adjacent structures other than seminal vesicles**
N	**Regional Lymph Nodes**
NX	Regional lymph nodes cannot be assessed
N0	No regional lymph node metastasis
N1	Regional lymph node metastasis
M	**Distant Metastasis**
M0	No distant metastasis
M1	**Distant metastasis**
M1a	Nonregional lymph node(s)
M1b	Bone(s)
M1c	Other site(s)

Acknowledgements

The work in this thesis was done at the Theranostics group, Department of Medicinal Chemistry, Uppsala University. This work would not have been completed without the continuous guidance, help, and support of many people whom I would like to express my endless gratitude and appreciation to:

My main supervisor **Prof**. **Anna Orlova** for believing in me and providing me with the great opportunity to work in the field I pursued for many years before moving to Sweden. You were always helpful, supportive, patient and understanding. There were many difficult situations that you dealt with in a perfect way and I am very grateful for every single time you were quick to intervene and help. I learned a lot from you and I could not have asked for a better supervisor and mentor!

My co-supervisor **Lect**. **Ulrika Rosentsröm** for being there whenever I needed guidance and support. Also, for providing great support in my different projects during my doctoral studies.

My co-supervisor **Assoc**. **Prof**. **Anzhelika Vorobyeva** for your valuable and constructive input in my projects and for your great support and willingness to help whenever I asked you. You always provided the time no matter how busy you were and I truly appreciate that.

My co-supervisor and dear friend **Dr**. **Bogdan Mitran** for your continuous support and help since before I started my doctoral studies. You always guided me to do what is right... and what is wrong. Also, for trusting my navigation skills, which took us to the worst beach in Shanghai. More importantly though, for the terrible choice of movies. I have been impatiently waiting since 2019 to say that I am actually good at playing ping pong, even though it is only evident when you start trash talking.

Prof. **Vladimir Tolmachev**, for being a great mentor despite not being one of my official supervisors. You had great input in all my projects and you always provided time whenever I had questions. It is always fun to discuss science with you! You are always supportive, this provided me with extra confidence especially when presenting at conferences abroad.

Our group members (former and current)

Cheng, you were my first supervisor in our group and you taught me a lot in a short period of time. I will always be grateful for all your kindness and help. **Javad**, thank you for the great talks and I wish you the best with your career. **Maryam**, thank you for being kind and helpful, and for your willingness to talk and share thoughts and ideas. Also, for the great company on the conferences abroad. **Tianqi** and **Yongsheng**, you are very kind and supportive, it is always fun to talk to you and I wish you all the best, and soon to become doctors. **Fanny**, thank you for the fun discussions and for your support. It has been great to work with you.

Panagiotis and **Katya**, it is so nice to work closely with you and have fun discussions. You are very helpful, kind and supportive. I am glad I get to share the office with you. I know I have been away for the most part but I am sure that we have a great team and I wish you the best of luck with your research!

Mohamed Altai, thank you for everything you have taught me and thank you for your continuous guidance and support. You are very helpful, selfless and kind. I cannot say enough to express my gratitude for what I am certain is a lifelong friendship.

Sara, it has been an honour to work with you and share the same office. You are so kind, helpful, intelligent and generous! I can also truly say that I enjoyed our gymnastics talks, even if I understood nothing! Always stay over the bridge.

My dearest friend **Maria**, where do I even begin... I don't know how many topics we have talked about or how many times you were there to push me to do better. Our short walks are literally what kept me going for a long period of time, who needs a therapist when they have a wonderful friend like you! You are the funniest, kindest, and most sincere person I know, even if we're going to hell for all the jokes. You are always here whenever I need help and it's a blessing that you are my closest friend. Tack för allt! ⚽

PPP

Sergio, the world's best padel/ping pong player and the world's best climber! But more importantly (and less debatably), the world's best director! Wherever I go, I always say that we have the best work environment at PPP, which you are responsible for by being so kind to everyone. I am looking forward to losing at padel again.

Veronika, the place collapses if you are away for a few days. You are extremely kind and helpful. I have asked you so many questions and you always had the right answer, without hesitating to help. Thank you for everything!

Ram, my dear friend and neighbour, also world's second-best padel player. You are very generous and you were always there to help and support me whenever I needed anything. Shukriya, Ram!

Ola, how many times did I go to your office and ask if you had a minute for a question? Plenty! Yet you always answered without being bothered and no matter how busy you were, thank you!

TPI

You added a great fun element to our work place! It is so much fun to talk to you and I wish you all the best!

Olof, thank you for all the fun discussions and all the great padel games! **Gry**, you are so kind and it was always fun at the lab when you were there. **Emmi**, you are very kind and smart! Thank you for all the good memories and I wish you the best of luck with your career. **Pierre** (second-best padel player), thank you for always being cool, kind and helpful! Good luck with your career. **Thanos**, you are a great friend, it was always fun to go to the movies, especially if the movie is 🙂. **Francesco**, hands-down the funniest guy at our work place! Also, a great actor/director! Good luck with your doctoral studies. **Olivia**, thank you for your kindness and for being so nice! I wish you good luck with your studies. **Niccoló**, you are one of the nicest and most helpful people I know! Thank you for everything! **Amina**, you are always so nice and kind! I wish you the best of luck with your doctoral studies.

To our collaborators

I would like to thank our dear collaborators at KTH: **Amelie**, **Ábel**, **Hanna**, **Kristina**, **Sophia**, **Jesper**, **Charles, Stefan** and **John**, for your great and continuous help which contributed majorly to my work. I would also like to thank **Mats Larhed**, **Jonas Eriksson**, **Jens Sörensen**, **Vladimir Chernov**, and **Anders Örbom**, for all their help. I am also grateful for all the help of our collaborators in **Tomsk**.

To my friends and colleagues at BMS

Bo, you were the first to give me an opportunity to work in research. I am grateful for all your help and all the encouraging and kind words you said. I also want to thank **Marika**, **Anja**, **Diana**, **Sara**, **Tabassom** and **Mehran**, for all the good discussions and support.

I would also like to thank **Mikael Hedeland**, for always being supportive and helpful, **Rana Refaey**, who was the first to encourage me to take this journey.

Also, thank you, **Gjertrud**, for being such a good friend, we started our studies at the same time in Uppsala and now we finish our doctoral studies in the same year, I am grateful for all your help and support.

To my childhood friends

Mohamed Yasser, the world's best striker! We met in three continents and share so many stories and memories! Thank you for your continuous support throughout everything!

Omar Bahary and **Omar Mamdouh**, my worst and favourite Call of Duty squad! Thank you for all your support and the great memories. Also, thank you for tolerating my anger when you waste time looting empty houses in Al Mazrah 🤌

Amr Khairy and **Ahmed Hilal**, thank you for being great friends and for always being there whenever I needed to talk.

To my beloved family

Tarek, **Sanaa**, **Ahmed** and **Sara**, you are the reason behind every good thing I do. Your guidance and support are endless. You will always be close to my heart even if we are many miles apart. This thesis is dedicated to you.

أحبكم إلى الأبد ❤️

Ayman Abouzayed
Uppsala, 2023

References

1. Sung H, Ferlay J, Siegel RL, et al. Global Cancer Statistics 2020: GLOBOCAN Estimates of Incidence and Mortality Worldwide for 36 Cancers in 185 Countries. *CA Cancer J Clin*. 2021;71(3):209-249. doi:10.3322/caac.21660
2. Ittmann M. Anatomy and Histology of the Human and Murine Prostate. *Cold Spring Harb Perspect Med*. 2018;8(5):a030346. doi:10.1101/cshperspect.a030346
3. McNeal JE. Anatomy of the prostate: an historical survey of divergent views. *Prostate*. 1980;1(1):3-13. doi:10.1002/pros.2990010103
4. McNeal JE. Normal and pathologic anatomy of prostate. *Urology*. 1981;17(Suppl 3):11-16.
5. McNeal JE, Redwine EA, Freiha FS, Stamey TA. Zonal distribution of prostatic adenocarcinoma. Correlation with histologic pattern and direction of spread. *Am J Surg Pathol*. 1988;12(12):897-906. doi:10.1097/00000478-198812000-00001
6. McNeal JE. Origin and development of carcinoma in the prostate. *Cancer*. 1969;23(1):24-34. doi:10.1002/1097-0142(196901)23:1<24::aid-cncr2820230103>3.0.co;2-1
7. Bostwick DG, Brawer MK. Prostatic Intra-Epithelial Neoplasia and Early Invasion in Prostate Cancer. *Cancer*. 1987;59(4):788-794. doi:10.1002/1097-0142(19870215)59:4<788::AID-CNCR2820590421>3.0.CO;2-I
8. Qian J, Wollan P, Bostwick DG. The extent and multicentricity of high-grade prostatic intraepithelial neoplasia in clinically localized prostatic adenocarcinoma. *Hum Pathol*. 1997;28(2):143-148. doi:10.1016/S0046-8177(97)90097-6
9. Gandaglia G, Abdollah F, Schiffmann J, et al. Distribution of metastatic sites in patients with prostate cancer: A population-based analysis: Sites of Metastases in PCa Patients. *The Prostate*. 2014;74(2):210-216. doi:10.1002/pros.22742
10. Hellman S, Weichselbaum RR. Oligometastases. *J Clin Oncol*. 1995;13(1):8-10. doi:10.1200/JCO.1995.13.1.8
11. Chen ME, Johnston DA, Tang K, Babaian RJ, Troncoso P. Detailed mapping of prostate carcinoma foci: Biopsy strategy implications. *Cancer*. 2000;89(8):1800-1809. doi:10.1002/1097-0142(20001015)89:8<1800::AID-CNCR21>3.0.CO;2-D
12. McNeal JE. Normal histology of the prostate. *Am J Surg Pathol*. 1988;12(8):619-633. doi:10.1097/00000478-198808000-00003
13. Lee JJ, Thomas IC, Nolley R, Ferrari M, Brooks JD, Leppert JT. Biologic differences between peripheral and transition zone prostate cancer: Differences Between Peripheral and Transition Zone Prostate Cancer. *The Prostate*. 2015;75(2):183-190. doi:10.1002/pros.22903

14. Aaron L, Franco OE, Hayward SW. Review of Prostate Anatomy and Embryology and the Etiology of Benign Prostatic Hyperplasia. *Urol Clin North Am*. 2016;43(3):279-288. doi:10.1016/j.ucl.2016.04.012
15. Lee CH, Akin-Olugbade O, Kirschenbaum A. Overview of Prostate Anatomy, Histology, and Pathology. *Endocrinol Metab Clin North Am*. 2011;40(3):565-575. doi:10.1016/j.ecl.2011.05.012
16. Sato S, Kimura T, Onuma H, Egawa S, Takahashi H. Transition zone prostate cancer is associated with better clinical outcomes than peripheral zone cancer. *BJUI Compass*. 2021;2(3):169-177. doi:10.1002/bco2.47
17. Bracarda S, de Cobelli O, Greco C, et al. Cancer of the prostate. *Crit Rev Oncol Hematol*. 2005;56(3):379-396. doi:10.1016/j.critrevonc.2005.03.010
18. Nguyen-Nielsen M, Borre M. Diagnostic and Therapeutic Strategies for Prostate Cancer. *Semin Nucl Med*. 2016;46(6):484-490. doi:10.1053/j.semnuclmed.2016.07.002
19. Sekhoacha M, Riet K, Motloung P, Gumenku L, Adegoke A, Mashele S. Prostate Cancer Review: Genetics, Diagnosis, Treatment Options, and Alternative Approaches. *Molecules*. 2022;27(17):5730. doi:10.3390/molecules27175730
20. Carlsson SV, Vickers AJ. Screening for Prostate Cancer. *Med Clin North Am*. 2020;104(6):1051-1062. doi:10.1016/j.mcna.2020.08.007
21. Guo LH, Wu R, Xu HX, et al. Comparison between Ultrasound Guided Transperineal and Transrectal Prostate Biopsy: A Prospective, Randomized and Controlled Trial. *Sci Rep*. 2015;5(1):16089. doi:10.1038/srep16089
22. Mabjeesh NJ, Lidawi G, Chen J, German L, Matzkin H. High detection rate of significant prostate tumours in anterior zones using transper-ineal ultrasound-guided template saturation biopsy. *BJU Int*. 2012;110(7):993-997. doi:10.1111/j.1464-410X.2012.10972.x
23. Stefanova V, Buckley R, Flax S, et al. Transperineal Prostate Biopsies Using Local Anesthesia: Experience with 1,287 Patients. Prostate Cancer Detection Rate, Complications and Patient Tolerability. *J Urol*. 2019;201(6):1121-1126. doi:10.1097/JU.0000000000000156
24. Grummet JP, Weerakoon M, Huang S, et al. Sepsis and "superbugs": should we favour the transperineal over the transrectal approach for prostate biopsy? *BJU Int*. 2014;114(3):384-388. doi:10.1111/bju.12536
25. Gleason DF. The Veteran's Administration Cooperative Urologic Research Group: histologic grading and clinical staging of prostatic carcinoma. In: Tannenbaum M, ed. *Urologic Pathology: The Prostate*. Lea & Febiger; 1977:171-198.
26. Epstein JI, Egevad L, Srigley JR, Humphrey PA. The 2014 International Society of Urological Pathology (ISUP) Consensus Conference on Gleason Grading of Prostatic Carcinoma. *Am J Surg Pathol*. 2016;40(2):244-252. doi:10.1097/PAS.0000000000000530
27. Tsao C kai, Gray KP, Nakabayashi M, et al. Patients with Biopsy Gleason 9 and 10 Prostate Cancer Have Significantly Worse Outcomes Compared to Patients with Gleason 8 Disease. *J Urol*. 2015;194(1):91-97. doi:10.1016/j.juro.2015.01.078
28. Chan TY, Partin AW, Walsh PC, Epstein JI. Prognostic significance of Gleason score 3+4 versus Gleason score 4+3 tumor at radical prostatectomy. *Urology*. 2000;56(5):823-827. doi:10.1016/s0090-4295(00)00753-6
29. Ahmed HU, El-Shater Bosaily A, Brown LC, et al. Diagnostic accuracy of multi-parametric MRI and TRUS biopsy in prostate cancer (PROMIS): a paired validating confirmatory study. *Lancet*. 2017;389(10071):815-822. doi:10.1016/S0140-6736(16)32401-1

30. Turkbey B, Rosenkrantz AB, Haider MA, et al. Prostate Imaging Reporting and Data System Version 2.1: 2019 Update of Prostate Imaging Reporting and Data System Version 2. *Eur Urol*. 2019;76(3):340-351. doi:10.1016/j.eururo.2019.02.033
31. Cash H, Maxeiner A, Stephan C, et al. The detection of significant prostate cancer is correlated with the Prostate Imaging Reporting and Data System (PI-RADS) in MRI/transrectal ultrasound fusion biopsy. *World J Urol*. 2016;34(4):525-532. doi:10.1007/s00345-015-1671-8
32. Kasivisvanathan V, Rannikko AS, Borghi M, et al. MRI-Targeted or Standard Biopsy for Prostate-Cancer Diagnosis. *N Engl J Med*. 2018;378(19):1767-1777. doi:10.1056/NEJMoa1801993
33. Xie J, Jin C, Liu M, et al. MRI/Transrectal Ultrasound Fusion-Guided Targeted Biopsy and Transrectal Ultrasound-Guided Systematic Biopsy for Diagnosis of Prostate Cancer: A Systematic Review and Meta-analysis. *Front Oncol*. 2022;12:880336. doi:10.3389/fonc.2022.880336
34. Kam J, Yuminaga Y, Kim R, et al. Does magnetic resonance imaging–guided biopsy improve prostate cancer detection? A comparison of systematic, cognitive fusion and ultrasound fusion prostate biopsy. *Prostate Int*. 2018;6(3):88-93. doi:10.1016/j.prnil.2017.10.003
35. Ghafoor S, Burger IA, Vargas AH. Multimodality Imaging of Prostate Cancer. *J Nucl Med*. 2019;60(10):1350-1358. doi:10.2967/jnumed.119.228320
36. Metser U, Chua S, Ho B, et al. The Contribution of Multiparametric Pelvic and Whole-Body MRI to Interpretation of 18F-Fluoromethylcholine or 68Ga-HBED-CC PSMA-11 PET/CT in Patients with Biochemical Failure After Radical Prostatectomy. *J Nucl Med*. 2019;60(9):1253-1258. doi:10.2967/jnumed.118.225185
37. Whitmore WFJr. Natural history and staging of prostate cancer. *Urol Clin North Am*. 1984;11(2):205-220.
38. Jewett HJ. The present status of radical prostatectomy for stages A and B prostatic cancer. *Urol Clin North Am*. 1975;2(1):105-124.
39. Schröder FH, Hermanek P, Denis L, Fair WR, Gospodarowicz MK, Pavone-Macaluso M. The TNM classification of prostate cancer. *Prostate Suppl*. 1992;4:129-138. doi:10.1002/pros.2990210521
40. International Union Against Cancer (UICC). Prostate. In: Sobin LH, Gospodarowicz MK, Wittekind C, eds. *TNM Classification of Malignant Tumours*. 7th ed. Wiley-Blackwell; 2009:243-248.
41. Mankoff DA. A definition of molecular imaging. *J Nucl Med*. 2007;48(6):18N-21N.
42. Rahmim A, Zaidi H. PET versus SPECT: strengths, limitations and challenges. *Nucl Med Commun*. 2008;29(3):193-207. doi:10.1097/MNM.0b013e3282f3a515
43. IAEA. IMAGINE, the new IAEA Medical imAGIng and Nuclear mEdicine global resources database. Published 2023. Accessed March 27, 2023. https://humanhealth.iaea.org/HHW/DBStatistics/IMAGINEMaps.html
44. Ware RE, Williams S, Hicks RJ. Molecular Imaging of Recurrent and Metastatic Prostate Cancer. *Semin Nucl Med*. 2019;49(4):280-293. doi:10.1053/j.semnuclmed.2019.02.005
45. Liberti MV, Locasale JW. The Warburg Effect: How Does it Benefit Cancer Cells? *Trends Biochem Sci*. 2016;41(3):211-218. doi:10.1016/j.tibs.2015.12.001
46. Jadvar H. Is There Use for FDG-PET in Prostate Cancer? *Semin Nucl Med*. 2016;46(6):502-506. doi:10.1053/j.semnuclmed.2016.07.004

47. Minamimoto R, Senda M, Jinnouchi S, et al. The current status of an FDG-PET cancer screening program in Japan, based on a 4-year (2006–2009) nationwide survey. *Ann Nucl Med*. 2013;27(1):46-57. doi:10.1007/s12149-012-0660-x
48. Oyama, Nobuyuki, Akino H, Kanamaru H, et al. 11C-acetate PET imaging of prostate cancer. *J Nucl Med*. 2002;43(2):181-186.
49. Ackerstaff E, Glunde K, Bhujwalla ZM. Choline phospholipid metabolism: A target in cancer cells? *J Cell Biochem*. 2003;90(3):525-533. doi:10.1002/jcb.10659
50. Kitajima K, Yamamoto S, Odawara S, et al. Diagnostic Performance of 11C-choline PET/CT and FDG PET/CT in Prostate Cancer. *Acta Med Okayama*. 2018;72(3):289-296. doi:10.18926/AMO/56075
51. De Bari B, Alongi F, Lestrade L, Giammarile F. Choline-PET in prostate cancer management: The point of view of the radiation oncologist. *Crit Rev Oncol Hematol*. 2014;91(3):234-247. doi:10.1016/j.critrevonc.2014.04.002
52. Love C, Din AS, Tomas MB, Kalapparambath TP, Palestro CJ. Radionuclide Bone Imaging: An Illustrative Review. *RadioGraphics*. 2003;23(2):341-358. doi:10.1148/rg.232025103
53. Langsteger W, Rezaee A, Pirich C, Beheshti M. 18F-NaF-PET/CT and 99mTc-MDP Bone Scintigraphy in the Detection of Bone Metastases in Prostate Cancer. *Semin Nucl Med*. 2016;46(6):491-501. doi:10.1053/j.semnuclmed.2016.07.003
54. Bénard F, Harsini S, Wilson D, et al. Intra-individual comparison of 18F-sodium fluoride PET–CT and 99mTc bone scintigraphy with SPECT in patients with prostate cancer or breast cancer at high risk for skeletal metastases (MITNEC-A1): a multicentre, phase 3 trial. *Lancet Oncol*. 2022;23(12):1499-1507. doi:10.1016/S1470-2045(22)00642-8
55. Loeb S, Zhou Q, Siebert U, et al. Active Surveillance Versus Watchful Waiting for Localized Prostate Cancer: A Model to Inform Decisions. *Eur Urol*. 2017;72(6):899-907. doi:10.1016/j.eururo.2017.07.018
56. Zaorsky NG, Davis BJ, Nguyen PL, et al. The evolution of brachytherapy for prostate cancer. *Nat Rev Urol*. 2017;14(7):415-439. doi:10.1038/nrurol.2017.76
57. Mercader C, Musquera M, Franco A, Alcaraz A, Ribal MJ. Primary cryotherapy for localized prostate cancer treatment. *Aging Male*. 2020;23(5):1460-1466. doi:10.1080/13685538.2020.1796960
58. Muto S, Yoshii T, Saito K, Kamiyama Y, Ide H, Horie S. Focal Therapy with High-intensity-focused Ultrasound in the Treatment of Localized Prostate Cancer. *Jpn J Clin Oncol*. 2008;38(3):192-199. doi:10.1093/jjco/hym173
59. Pisansky TM. External-Beam Radiotherapy for Localized Prostate Cancer. *N Engl J Med*. 2006;355(15):1583-1591. doi:10.1056/NEJMct055263
60. Schiller KC, Habl G, Combs SE. Protons, Photons, and the Prostate – Is There Emerging Evidence in the Ongoing Discussion on Particle Therapy for the Treatment of Prostate Cancer? *Front Oncol*. 2016;6. doi:10.3389/fonc.2016.00008
61. Hamdy FC, Donovan JL, Lane JA, et al. 10-Year Outcomes after Monitoring, Surgery, or Radiotherapy for Localized Prostate Cancer. *N Engl J Med*. 2016;375(15):1415-1424. doi:10.1056/NEJMoa1606220
62. Bill-Axelson A, Holmberg L, Garmo H, et al. Radical Prostatectomy or Watchful Waiting in Prostate Cancer — 29-Year Follow-up. *N Engl J Med*. 2018;379(24):2319-2329. doi:10.1056/NEJMoa1807801

63. Bolla M, Van Tienhoven G, Warde P, et al. External irradiation with or without long-term androgen suppression for prostate cancer with high metastatic risk: 10-year results of an EORTC randomised study. *Lancet Oncol*. 2010;11(11):1066-1073. doi:10.1016/S1470-2045(10)70223-0
64. Warde P, Mason M, Ding K, et al. Combined androgen deprivation therapy and radiation therapy for locally advanced prostate cancer: a randomised, phase 3 trial. *The Lancet*. 2011;378(9809):2104-2111. doi:10.1016/S0140-6736(11)61095-7
65. Widmark A, Klepp O, Solberg A, et al. Endocrine treatment, with or without radiotherapy, in locally advanced prostate cancer (SPCG-7/SFUO-3): an open randomised phase III trial. *The Lancet*. 2009;373(9660):301-308. doi:10.1016/S0140-6736(08)61815-2
66. Bolla M, de Reijke TM, Van Tienhoven G, et al. Duration of Androgen Suppression in the Treatment of Prostate Cancer. *N Engl J Med*. 2009;360(24):2516-2527. doi:10.1056/NEJMoa0810095
67. Siegel DA, O'Neil ME, Richards TB, Dowling NF, Weir HK. Prostate Cancer Incidence and Survival, by Stage and Race/Ethnicity — United States, 2001–2017. *MMWR Morb Mortal Wkly Rep*. 2020;69(41):1473-1480. doi:10.15585/mmwr.mm6941a1
68. Scher HI, Fizazi K, Saad F, et al. Increased Survival with Enzalutamide in Prostate Cancer after Chemotherapy. Cabot RC, Harris NL, Rosenberg ES, et al., eds. *N Engl J Med*. 2012;367(13):1187-1197. doi:10.1056/NEJMoa1207506
69. Chi KN, Agarwal N, Bjartell A, et al. Apalutamide for Metastatic, Castration-Sensitive Prostate Cancer. *N Engl J Med*. 2019;381(1):13-24. doi:10.1056/NEJMoa1903307
70. Smith MR, Hussain M, Saad F, et al. Darolutamide and Survival in Metastatic, Hormone-Sensitive Prostate Cancer. *N Engl J Med*. 2022;386(12):1132-1142. doi:10.1056/NEJMoa2119115
71. Auchus RJ, Sharifi N. Sex Hormones and Prostate Cancer. *Annu Rev Med*. 2020;71(1):33-45. doi:10.1146/annurev-med-051418-060357
72. Desai K, McManus JM, Sharifi N. Hormonal Therapy for Prostate Cancer. *Endocr Rev*. 2021;42(3):354-373. doi:10.1210/endrev/bnab002
73. Ryan CJ, Smith MR, Fizazi K, et al. Abiraterone acetate plus prednisone versus placebo plus prednisone in chemotherapy-naive men with metastatic castration-resistant prostate cancer (COU-AA-302): final overall survival analysis of a randomised, double-blind, placebo-controlled phase 3 study. *Lancet Oncol*. 2015;16(2):152-160. doi:10.1016/S1470-2045(14)71205-7
74. Tannock IF, Horti J, Oudard S, James ND, Rosenthal MA. Docetaxel plus Prednisone or Mitoxantrone plus Prednisone for Advanced Prostate Cancer. *N Engl J Med*. 2004;351(15):1502-1512.
75. de Bono JS, Oudard S, Ozguroglu M, et al. Prednisone plus cabazitaxel or mitoxantrone for metastatic castration-resistant prostate cancer progressing after docetaxel treatment: a randomised open-label trial. *The Lancet*. 2010;376(9747):1147-1154. doi:10.1016/S0140-6736(10)61389-X
76. Kantoff PW, Higano CS, Shore ND, et al. Sipuleucel-T Immunotherapy for Castration-Resistant Prostate Cancer. *N Engl J Med*. 2010;363(5):411-422. doi:10.1056/NEJMoa1001294
77. Sartor O, de Bono J, Chi KN, et al. Lutetium-177–PSMA-617 for Metastatic Castration-Resistant Prostate Cancer. *N Engl J Med*. 2021;385(12):1091-1103. doi:10.1056/NEJMoa2107322

78. Fizazi K, Carducci M, Smith M, et al. Denosumab versus zoledronic acid for treatment of bone metastases in men with castration-resistant prostate cancer: a randomised, double-blind study. *The Lancet*. 2011;377(9768):813-822. doi:10.1016/S0140-6736(10)62344-6
79. Parker C, Nilsson S, Heinrich D, et al. Alpha Emitter Radium-223 and Survival in Metastatic Prostate Cancer. *N Engl J Med*. 2013;369(3):213-223. doi:10.1056/NEJMoa1213755
80. Siegel RL, Miller KD, Wagle NS, Jemal A. Cancer statistics, 2023. *CA Cancer J Clin*. 2023;73(1):17-48. doi:10.3322/caac.21763
81. Horoszewicz JS, Kawinski E, Murphy GP. Monoclonal antibodies to a new antigenic marker in epithelial prostatic cells and serum of prostatic cancer patients. *Anticancer Res*. 1987;7(5B):927-935.
82. Leek J, Lench N, Maraj B, et al. Prostate-specific membrane antigen: evidence for the existence of a second related human gene. *Br J Cancer*. 1995;72(3):583-588. doi:10.1038/bjc.1995.377
83. Israeli RS, Powell CT, Corr JG, Fair WR, Heston WD. Expression of the prostate-specific membrane antigen. *Cancer Res*. 1994;54(7):1807-1811.
84. Silver DA, Pellicer I, Fair WR, Heston WD, Cordon-Cardo C. Prostate-specific membrane antigen expression in normal and malignant human tissues. *Clin Cancer Res*. 1997;3(1):81-85.
85. Kinoshita Y, Kuratsukuri K, Landas S, et al. Expression of Prostate-Specific Membrane Antigen in Normal and Malignant Human Tissues. *World J Surg*. 2006;30(4):628-636. doi:10.1007/s00268-005-0544-5
86. Bostwick DG, Pacelli A, Blute M, Roche P, Murphy GP. Prostate specific membrane antigen expression in prostatic intraepithelial neoplasia and adenocarcinoma: A study of 184 cases. *Cancer*. 1998;82(11):2256-2261. doi:10.1002/(SICI)1097-0142(19980601)82:11<2256::AID-CNCR22>3.0.CO;2-S
87. Su SL, Huang IP, Fair WR, Powell CT, Heston WD. Alternatively spliced variants of prostate-specific membrane antigen RNA: ratio of expression as a potential measurement of progression. *Cancer Res*. 1995;55(7):1441-1443.
88. Schmittgen TD, Teske S, Vessella RL, True LD, Zakrajsek BA. Expression of prostate specific membrane antigen and three alternatively spliced variants of PSMA in prostate cancer patients. *Int J Cancer*. 2003;107(2):323-329. doi:10.1002/ijc.11402
89. Wright GL, Haley C, Beckett ML, Schellhammer PF. Expression of prostate-specific membrane antigen in normal, benign, and malignant prostate tissues. *Urol Oncol Semin Orig Investig*. 1995;1(1):18-28. doi:10.1016/1078-1439(95)00002-Y
90. Kawakami M, Nakayama J. Enhanced Expression of Prostate-specific Membrane Antigen Gene in Prostate Cancer as Revealed by in Situ Hybridization. *Cancer Res*. 1997;57(12):2321-2324.
91. Hupe MC, Philippi C, Roth D, et al. Expression of Prostate-Specific Membrane Antigen (PSMA) on Biopsies Is an Independent Risk Stratifier of Prostate Cancer Patients at Time of Initial Diagnosis. *Front Oncol*. 2018;8:623. doi:10.3389/fonc.2018.00623
92. Chang SS, O'Keefe DS, Bacich DJ, Reuter VE, Heston WD, Gaudin PB. Prostate-specific membrane antigen is produced in tumor-associated neovasculature. *Clin Cancer Res*. 1999;5(10):2674-2681.
93. Rajasekaran SA, Anilkumar G, Oshima E, et al. A Novel Cytoplasmic Tail MXXXL Motif Mediates the Internalization of Prostate-specific Membrane

Antigen. *Mol Biol Cell*. 2003;14(12):4835-4845. doi:10.1091/mbc.e02-11-0731
94. Liu H, Rajasekaran A, Moy P, et al. Constitutive and antibody-induced internalization of prostate-specific membrane antigen. *Cancer Res*. 1998;58(18):4055-5060.
95. Troyer JK, Feng Q, Beckett ML, Wright GL. Biochemical characterization and mapping of the 7E11-C5.3 epitope of the prostate-specific membrane antigen. *Urol Oncol*. 1995;1(1):29-37.
96. Kuppermann D, Calais J, Marks LS. Imaging Prostate Cancer: Clinical Utility of Prostate-Specific Membrane Antigen. *J Urol*. 2022;207(4):769-778. doi:10.1097/JU.0000000000002457
97. Liu H, Moy P, Kim S, et al. Monoclonal antibodies to the extracellular domain of prostate-specific membrane antigen also react with tumor vascular endothelium. *Cancer Res*. 1997;57(1):3629-3634.
98. Pandit-Taskar N, O'Donoghue JA, Divgi CR, et al. Indium 111-labeled J591 anti-PSMA antibody for vascular targeted imaging in progressive solid tumors. *EJNMMI Res*. 2015;5(1):28. doi:10.1186/s13550-015-0104-4
99. Pandit-Taskar N, O'Donoghue JA, Durack JC, et al. A Phase I/II Study for Analytic Validation of 89Zr-J591 ImmunoPET as a Molecular Imaging Agent for Metastatic Prostate Cancer. *Clin Cancer Res*. 2015;21(23):5277-5285. doi:10.1158/1078-0432.CCR-15-0552
100. Niaz MJ, Batra JS, Walsh RD, et al. Pilot Study of Hyperfractionated Dosing of Lutetium-177–Labeled Antiprostate-Specific Membrane Antigen Monoclonal Antibody J591 (177Lu-J591) for Metastatic Castration-Resistant Prostate Cancer. *The Oncologist*. 2020;25(6):477-e895. doi:10.1634/theoncologist.2020-0028
101. Subasinghe N, Schulte M, Chan MYM, Roon RJ, Koerner JF, Johnson RL. Synthesis of acyclic and dehydroaspartic acid analogs of Ac-Asp-Glu-OH and their inhibition of rat brain N-acetylated .alpha.-linked acidic dipeptidase (NAALA dipeptidase). *J Med Chem*. 1990;33(10):2734-2744. doi:10.1021/jm00172a009
102. Serval V, Galli T, Cheramy A, Glowinski J, Lavielle S. In vitro and in vivo inhibition of N-acetyl-L-aspartyl-L-glutamate catabolism by N-acylated L-glutamate analogs. *J Pharmacol Exp Ther*. 1992;260(3):1093-1100.
103. Jackson PF, Cole DC, Slusher BS, et al. Design, Synthesis, and Biological Activity of a Potent Inhibitor of the Neuropeptidase N-Acetylated r-Linked Acidic Dipeptidase. *J Med Chem*. 1996;39(2):619-622. doi:10.1021/jm950801q
104. Bařinka C, Rojas C, Slusher B, Pomper M. Glutamate carboxypeptidase II in diagnosis and treatment of neurologic disorders and prostate cancer. *Curr Med Chem*. 2012;19(6):856-870. doi:10.2174/092986712799034888
105. Kozikowski AP, Nan F, Conti P, et al. Design of Remarkably Simple, Yet Potent Urea-Based Inhibitors of Glutamate Carboxypeptidase II (NAALADase). *J Med Chem*. 2001;44(3):298-301. doi:10.1021/jm000406m
106. Kopka K, Benešová M, Bařinka C, Haberkorn U, Babich J. Glu-Ureido–Based Inhibitors of Prostate-Specific Membrane Antigen: Lessons Learned During the Development of a Novel Class of Low-Molecular-Weight Theranostic Radiotracers. *J Nucl Med*. 2017;58(Supplement 2):17S-26S. doi:10.2967/jnumed.116.186775
107. Pomper MG, Musachio JL, Zhang J, et al. 11C-MCG: Synthesis, Uptake Selectivity, and Primate PET of a Probe for Glutamate Carboxypeptidase II

(NAALADase). *Mol Imaging*. 2002;1(2):96-101. doi:10.1162/15353500200202109
108. Foss CA, Mease RC, Fan H, et al. Radiolabeled small-molecule ligands for prostate-specific membrane antigen: in vivo imaging in experimental models of prostate cancer. *Clin Cancer Res*. 2005;11(11):4022-4028. doi:10.1158/1078-0432.CCR-04-2690
109. Davis MI, Bennett MJ, Thomas LM, Bjorkman PJ. Crystal structure of prostate-specific membrane antigen, a tumor marker and peptidase. *Proc Natl Acad Sci USA*. 2005;102(17):5981-5986. doi:10.1073/pnas.0502101102
110. Maresca KP, Hillier SM, Femia FJ, et al. A Series of Halogenated Heterodimeric Inhibitors of Prostate Specific Membrane Antigen (PSMA) as Radiolabeled Probes for Targeting Prostate Cancer. *J Med Chem*. 2009;52(2):347-357. doi:10.1021/jm800994j
111. Hillier SM, Maresca KP, Femia FJ, et al. Preclinical Evaluation of Novel Glutamate-Urea-Lysine Analogues That Target Prostate-Specific Membrane Antigen as Molecular Imaging Pharmaceuticals for Prostate Cancer. *Cancer Res*. 2009;69(17):6932-6940. doi:10.1158/0008-5472.CAN-09-1682
112. Barrett JA, Coleman RE, Goldsmith SJ, et al. First-in-man evaluation of 2 high-affinity PSMA-avid small molecules for imaging prostate cancer. *J Nucl Med*. 2013;54(3):380-387. doi:10.2967/jnumed.112.111203
113. Zechmann CM, Afshar-Oromieh A, Armor T, et al. Radiation dosimetry and first therapy results with a 124I/131I-labeled small molecule (MIP-1095) targeting PSMA for prostate cancer therapy. *Eur J Nucl Med Mol Imaging*. 2014;41(7):1280-1292. doi:10.1007/s00259-014-2713-y
114. Afshar-Oromieh A, Haberkorn U, Zechmann C, et al. Repeated PSMA-targeting radioligand therapy of metastatic prostate cancer with 131I-MIP-1095. *Eur J Nucl Med Mol Imaging*. 2017;44(6):950-959. doi:10.1007/s00259-017-3665-9
115. Lu G, Maresca KP, Hillier SM, et al. Synthesis and SAR of 99mTc/Re-labeled small molecule prostate specific membrane antigen inhibitors with novel polar chelates. *Bioorg Med Chem Lett*. 2013;23(5):1557-1563. doi:10.1016/j.bmcl.2012.09.014
116. Cardinale J, Giesel FL, Wensky C, Rathke HG, Haberkorn U, Kratochwil C. PSMA-GCK01 - A Generator-Based 99mTc-/188Re-Theranostic Ligand for the Prostate-Specific Membrane Antigen. *J Nucl Med*. Published online February 9, 2023:jnumed.122.264944. doi:10.2967/jnumed.122.264944
117. Vallabhajosula S, Nikolopoulou A, Babich JW, et al. ^{99m}Tc-Labeled Small-Molecule Inhibitors of Prostate-Specific Membrane Antigen: Pharmacokinetics and Biodistribution Studies in Healthy Subjects and Patients with Metastatic Prostate Cancer. *J Nucl Med*. 2014;55(11):1791-1798. doi:10.2967/jnumed.114.140426
118. Robu S, Schottelius M, Eiber M, et al. Preclinical Evaluation and First Patient Application of 99mTc-PSMA-I&S for SPECT Imaging and Radioguided Surgery in Prostate Cancer. *J Nucl Med*. 2017;58(2):235-242. doi:10.2967/jnumed.116.178939
119. Werner P, Neumann C, Eiber M, Wester HJ, Schottelius M. [99mTc]Tc-PSMA-I&S-SPECT/CT: experience in prostate cancer imaging in an outpatient center. *EJNMMI Res*. 2020;10(1):45. doi:10.1186/s13550-020-00635-z
120. Urbán S, Meyer C, Dahlbom M, et al. Radiation Dosimetry of ^{99m}Tc-PSMA I&S: A Single-Center Prospective Study. *J Nucl Med*. 2021;62(8):1075-1081. doi:10.2967/jnumed.120.253476

121. Mease RC, Dusich CL, Foss CA, et al. *N* -[*N* -[(*S*)-1,3-Dicarboxypropyl]Carbamoyl]-4-[18F]Fluorobenzyl- L -Cysteine, [18F]DCFBC: A New Imaging Probe for Prostate Cancer. *Clin Cancer Res*. 2008;14(10):3036-3043. doi:10.1158/1078-0432.CCR-07-1517
122. Rowe SP, Gage KL, Faraj SF, et al. ^{18}F-DCFBC PET/CT for PSMA-Based Detection and Characterization of Primary Prostate Cancer. *J Nucl Med*. 2015;56(7):1003-1010. doi:10.2967/jnumed.115.154336
123. Rowe SP, Macura KJ, Mena E, et al. PSMA-Based [18F]DCFPyL PET/CT Is Superior to Conventional Imaging for Lesion Detection in Patients with Metastatic Prostate Cancer. *Mol Imaging Biol*. 2016;18(3):411-419. doi:10.1007/s11307-016-0957-6
124. Morris MJ, Rowe SP, Gorin MA, et al. Diagnostic Performance of 18F-DCFPyL-PET/CT in Men with Biochemically Recurrent Prostate Cancer: Results from the CONDOR Phase 3, Multicenter Study. *Clin Cancer Res*. 2021;27(13):3674-3682.
125. Eder M, Schäfer M, Bauder-Wüst U, et al. 68Ga-complex lipophilicity and the targeting property of a urea-based PSMA inhibitor for PET imaging. *Bioconjug Chem*. 2012;23(4):688-697. doi:10.1021/bc200279b
126. Afshar-Oromieh A, Haberkorn U, Eder M, Eisenhut M, Zechmann CM. [68Ga]Gallium-labelled PSMA ligand as superior PET tracer for the diagnosis of prostate cancer: comparison with 18F-FECH. *Eur J Nucl Med Mol Imaging*. 2012;39(6):1085-1086. doi:10.1007/s00259-012-2069-0
127. Fendler WP, Calais J, Eiber M, et al. Assessment of 68Ga-PSMA-11 PET Accuracy in Localizing Recurrent Prostate Cancer: A Prospective Single-Arm Clinical Trial. *JAMA Oncol*. 2019;5(6):856. doi:10.1001/jamaoncol.2019.0096
128. Maurer T, Gschwend JE, Rauscher I, et al. Diagnostic Efficacy of (68)Gallium-PSMA Positron Emission Tomography Compared to Conventional Imaging for Lymph Node Staging of 130 Consecutive Patients with Intermediate to High Risk Prostate Cancer. *J Urol*. 2016;195(5):1436-1443. doi:10.1016/j.juro.2015.12.025
129. Benešová M, Schäfer M, Bauder-Wüst U, et al. Preclinical Evaluation of a Tailor-Made DOTA-Conjugated PSMA Inhibitor with Optimized Linker Moiety for Imaging and Endoradiotherapy of Prostate Cancer. *J Nucl Med*. 2015;56(6):914-920. doi:10.2967/jnumed.114.147413
130. Rahbar K, Schmidt M, Heinzel A, et al. Response and Tolerability of a Single Dose of 177Lu-PSMA-617 in Patients with Metastatic Castration-Resistant Prostate Cancer: A Multicenter Retrospective Analy-sis. *J Nucl Med*. 2016;57(9):1334-1338. doi:10.2967/jnumed.116.173757
131. Giesel FL, Cardinale J, Schäfer M, et al. 18F-Labelled PSMA-1007 shows similarity in structure, biodistribution and tumour uptake to the theragnostic compound PSMA-617. *Eur J Nucl Med Mol Imaging*. 2016;43(10):1929-1930. doi:10.1007/s00259-016-3447-9
132. Cardinale J, Schäfer M, Benešová M, et al. Preclinical Evaluation of 18F-PSMA-1007, a New Prostate-Specific Membrane Antigen Ligand for Prostate Cancer Imaging. *J Nucl Med*. 2017;58(3):425-431. doi:10.2967/jnumed.116.181768
133. Rahbar K, Weckesser M, Ahmadzadehfar H, Schäfers M, Stegger L, Bögemann M. Advantage of 18F-PSMA-1007 over 68Ga-PSMA-11 PET imaging for differentiation of local recurrence vs. urinary tracer excretion. *Eur J Nucl Med Mol Imaging*. 2018;45(6):1076-1077. doi:10.1007/s00259-018-3952-0

134. Rauscher I, Krönke M, König M, et al. Matched-Pair Comparison of 68Ga-PSMA-11 PET/CT and 18F-PSMA-1007 PET/CT: Frequency of Pitfalls and Detection Efficacy in Biochemical Recurrence After Radical Prostatectomy. *J Nucl Med*. 2020;61(1):51-57. doi:10.2967/jnumed.119.229187
135. Behr SC, Aggarwal R, VanBrocklin HF, et al. Phase I Study of CTT1057, an 18F-Labeled Imaging Agent with Phosphoramidate Core Targeting Prostate-Specific Membrane Antigen in Prostate Cancer. *J Nucl Med*. 2019;60(7):910-916. doi:10.2967/jnumed.118.220715
136. Noto B, Auf der Springe K, Huss S, Allkemper T, Stegger L. Prostate-Specific Membrane Antigen–Negative Metastases—A Potential Pitfall in Prostate-Specific Membrane Antigen PET. *Clin Nucl Med*. 2018;43(6):e186-e188. doi:10.1097/RLU.0000000000002073
137. Bilinski P, Webb M. An exceptional response to 177LuPSMA undermined by neuroendocrine transformation. *Urol Case Rep*. 2021;34:101467. doi:10.1016/j.eucr.2020.101467
138. Bakht MK, Derecichei I, Li Y, et al. Neuroendocrine differentiation of prostate cancer leads to PSMA suppression. *Endocr Relat Cancer*. 2018;26(2):131-146. doi:10.1530/ERC-18-0226
139. Krohn T, Verburg FA, Pufe T, et al. [68Ga]PSMA-HBED uptake mimicking lymph node metastasis in coeliac ganglia: an important pitfall in clinical practice. *Eur J Nucl Med Mol Imaging*. 2015;42(2):210-214. doi:10.1007/s00259-014-2915-3
140. Rischpler C, Beck TI, Okamoto S, et al. 68Ga-PSMA-HBED-CC Uptake in Cervical, Celiac, and Sacral Ganglia as an Im-portant Pitfall in Prostate Cancer PET Imaging. *J Nucl Med*. 2018;59(9):1406-1411. doi:10.2967/jnumed.117.204677
141. Blazak JK, Thomas P. Paget Disease: A Potential Pitfall in PSMA PET for Prostate Cancer. *Clin Nucl Med*. 2016;41(9):699-700. doi:10.1097/RLU.0000000000001296
142. Rowe SP, Deville C, Paller C, et al. Uptake of [18F]DCFPyL in Paget's Disease of Bone, an Important Potential Pitfall in the Clinical Interpretation of PSMA PET Studies. *Tomography*. 2015;1(2):81-84. doi:10.18383/j.tom.2015.00169
143. Müller C, Umbricht CA, Gracheva N, et al. Terbium-161 for PSMA-targeted radionuclide therapy of prostate cancer. *Eur J Nucl Med Mol Imaging*. 2019;46(9):1919-1930. doi:10.1007/s00259-019-04345-0
144. Banerjee SR, Minn I, Kumar V, et al. Preclinical Evaluation of 203/212Pb-Labeled Low-Molecular-Weight Compounds for Targeted Radiopharmaceutical Therapy of Prostate Cancer. *J Nucl Med*. 2020;61(1):80-88. doi:10.2967/jnumed.119.229393
145. Kratochwil C, Bruchertseifer F, Giesel FL, et al. 225Ac-PSMA-617 for PSMA-Targeted α-Radiation Therapy of Metastatic Castra-tion-Resistant Prostate Cancer. *J Nucl Med*. 2016;57(12):1941-1944. doi:10.2967/jnumed.116.178673
146. Zacherl MJ, Gildehaus FJ, Mittlmeier L, et al. First Clinical Results for PSMA-Targeted α-Therapy Using ^{225}Ac-PSMA-I&T in Advanced-mCRPC Patients. *J Nucl Med*. 2021;62(5):669-674. doi:10.2967/jnumed.120.251017
147. Kris RM, Hazan R, Villines J, Moody TW, Schlessinger J. Identification of the bombesin receptor on murine and human cells by cross-linking experiments. *J Biol Chem*. 1987;262(23):11215-11220. doi:10.1016/S0021-9258(18)60946-9

148. Corjay MH, Dobrzanski DJ, Way JM, et al. Two distinct bombesin receptor subtypes are expressed and functional in human lung carcinoma cells. *J Biol Chem*. 1991;266(28):18771-18779. doi:10.1016/S0021-9258(18)55129-2
149. Erspamer V, Erspamer GF, Inselvini M. Some pharmacological actions of alytesin and bombesin. *J Pharm Pharmacol*. 1970;22(11):875-876. doi:10.1111/j.2042-7158.1970.tb08465.x
150. Erspamer V, Erspamer GF, Inselvini M, Negri L. Occurrence of bombesin and alytesin in extracts of the skin of three European discoglossid frogs and pharmacological actions of bombesin on extravascular smooth muscle. *Br J Pharmacol*. 1972;45(2):333-348. doi:10.1111/j.1476-5381.1972.tb08087.x
151. Bertaccini G, Erspamer V, Melchiorri P, Sopranzi N. Gastrin release by bombesin in the dog. *Br J Pharmacol*. 1974;52(2):219-225. doi:10.1111/j.1476-5381.1974.tb09703.x
152. Broccardo M, Erspamer GF, Melchiorri P, Negri L, Castiglione R. Relative potency of bombesin-like peptides. *Br J Pharmacol*. 1975;55(2):221-227. doi:10.1111/j.1476-5381.1975.tb07631.x
153. McDonald TJ, Jörnvall H, Nilsson G, et al. Characterization of a gastrin releasing peptide from porcine non-antral gastric tissue. *Biochem Biophys Res Commun*. 1979;90(1):227-233. doi:10.1016/0006-291X(79)91614-0
154. Wood SM, Jung RT, Webster JD, et al. The effect of the mammalian neuropeptide, gastrin-releasing peptide (GRP), on gastrointestinal and pancreatic hormone secretion in man. *Clin Sci (Lond)*. 1983;65(4):365-371.
155. Gargosky SE, Wallace JC, Upton FM, Ballard FJ. C-terminal bombesin sequence requirements for binding and effects on protein synthesis in Swiss 3T3 cells. *Biochem J*. 1987;247(2):427-432. doi:10.1042/bj2470427
156. Moody TW, Carney DN, Cuttitta F, Quattrocchi K, Minna JD. High affinity receptors for bombesin/GRP-like peptides on human small cell lung cancer. *Life Sci*. 1985;37(2):105-113. doi:10.1016/0024-3205(85)90413-8
157. Scemama JL, Zahidi A, Fourmy D, et al. Interaction of [125I]-Tyr4-bombesin with specific receptors on normal human pancreatic membranes. *Regul Pept*. 1986;13(2):125-132. doi:10.1016/0167-0115(86)90220-X
158. Schubert ML, Hightower J, Coy DH, Makhlouf GM. Regulation of acid secretion by bombesin/GRP neurons of the gastric fundus. *Am J Physiol-Gastrointest Liver Physiol*. 1991;260(1):G156-G160. doi:10.1152/ajpgi.1991.260.1.G156
159. Degen LP, Peng F, Collet A, et al. Blockade of GRP receptors inhibits gastric emptying and gallbladder contraction but accelerates small intestinal transit. *Gastroenterology*. 2001;120(2):361-368. doi:10.1053/gast.2001.21174
160. Niebergall-Roth E, Singer MV. Central and peripheral neural control of pancreatic exocrine secretion. *J Physiol Pharmacol*. 2001;52(4 Pt 1):523-528.
161. Pereira PJS, Machado GDB, Danesi GM, et al. GRPR/PI3Kγ: Partners in Central Transmission of Itch. *J Neurosci*. 2015;35(49):16272-16281. doi:10.1523/JNEUROSCI.2310-15.2015
162. Xiao D, Wang J, Hampton LL, Weber HC. The human gastrin-releasing peptide receptor gene structure, its tissue expression and promoterq. *Gene*. 2001;264(1):95-103. doi:10.1016/s0378-1119(00)00596-5
163. Markwalder R, Reubi JC. Gastrin-releasing peptide receptors in the human prostate: relation to neoplastic transformation. *Cancer Res*. 1999;59(5):1152-1159.
164. Reubi JC, Wenger S, Schmuckli-Maurer J, Schaer JC, Gugger M. Bombesin receptor subtypes in human cancers: detection with the universal radiolig-and

(125)I-[D-TYR(6), beta-ALA(11), PHE(13), NLE(14)] bombesin(6-14). *Clin Cancer Res*. 2002;8(4):1139-1146.
165. Patel O, Shulkes A, Baldwin GS. Gastrin-releasing peptide and cancer. *Biochim Biophys Acta BBA - Rev Cancer*. 2006;1766(1):23-41. doi:10.1016/j.bbcan.2006.01.003
166. Gugger M, Reubi JC. Gastrin-Releasing Peptide Receptors in Non-Neoplastic and Neoplastic Human Breast. *Am J Pathol*. 1999;155(6):2067-2076. doi:10.1016/S0002-9440(10)65525-3
167. Carroll RE, Matkowskyj KA, Chakrabarti S, McDonald TJ, Benya RV. Aberrant expression of gastrin-releasing peptide and its receptor by well-differentiated colon cancers in humans. *Am J Physiol-Gastrointest Liver Physiol*. 1999;276(3):G655-G665. doi:10.1152/ajpgi.1999.276.3.G655
168. Fleischmann A, Waser B, Gebbers JO, Reubi JC. Gastrin-Releasing Peptide Receptors in Normal and Neoplastic Human Uterus: Involvement of Multiple Tissue Compartments. *J Clin Endocrinol Metab*. 2005;90(8):4722-4729. doi:10.1210/jc.2005-0964
169. Sun B, Schally AV, Halmos G. The presence of receptors for bombesin/GRP and mRNA for three receptor subtypes in human ovarian epithelial cancers. *Regul Pept*. 2000;90(1-3):77-84. doi:10.1016/S0167-0115(00)00114-2
170. Sun B, Halmos G, Schally AV, Wang X, Martinez M. Presence of receptors for bombesin/gastrin-releasing peptide and mRNA for three receptor subtypes in human prostate cancers. *The Prostate*. 2000;42(4):295-303. doi:10.1002/(SICI)1097-0045(20000301)42:4<295::AID-PROS7>3.0.CO;2-B
171. Körner M, Waser B, Rehmann R, Reubi JC. Early over-expression of GRP receptors in prostatic carcinogenesis: GRP Receptor in Prostate Carcinogenesis. *The Prostate*. 2014;74(2):217-224. doi:10.1002/pros.22743
172. Ananias HJK, van den Heuvel MC, Helfrich W, de Jong IJ. Expression of the gastrin-releasing peptide receptor, the prostate stem cell antigen and the prostate-specific membrane antigen in lymph node and bone metastases of prostate cancer. *Prostate*. 2009;69(10):1101-1108. doi:10.1002/pros.20957
173. de Visser M, van Weerden WM, Krenning EP, de Jong M. Androgen-Dependent Expression of the Gastrin-Releasing Peptide Receptor in Human Prostate Tumor Xenografts. *J Nucl Med*. 2007;48(1):88-93.
174. Beer M, Montani M, Gerhardt J, et al. Profiling gastrin-releasing peptide receptor in prostate tissues: Clinical implications and molecular correlates: GRPR in Prostate Cancer. *The Prostate*. 2012;72(3):318-325. doi:10.1002/pros.21434
175. Faviana P, Boldrini L, Erba PA, et al. Gastrin-Releasing Peptide Receptor in Low Grade Prostate Cancer: Can It Be a Better Predictor Than Prostate-Specific Membrane Antigen? *Front Oncol*. 2021;11:650249. doi:10.3389/fonc.2021.650249
176. Breeman WAP, Hofland LJ, de Jong M, et al. Evaluation of radiolabelled bombesin analogues for receptor-targeted scintigraphy and radiotherapy. *Int J Cancer*. 1999;81(4):658-665. doi:10.1002/(SICI)1097-0215(19990517)81:4<658::AID-IJC24>3.0.CO;2-P
177. Breeman WAP, De Jong M, Bernard BF, et al. Pre-clinical evaluation of [111In-DTPA-Pro1, Tyr4]bombesin, a new radioligand for bombesin-receptor scintigraphy. *Int J Cancer*. 1999;83(5):657-663. doi:10.1002/(SICI)1097-0215(19991126)83:5<657::AID-IJC15>3.0.CO;2-Y
178. Breeman WAP, de Jong M, Erion JL, et al. Preclinical Comparison of 111In-Labeled DTPA- or DOTA-Bombesin Analogs for Receptor- Targeted Scintigraphy and Radionuclide Therapy. *J Nucl Med*. 2002;43(12):1650-1656.

179. Bauer W, Briner U, Doepfner W, et al. SMS 201-995: a very potent and selective octapeptide analogue of somatostatin with prolonged action. *Life Sci*. 1982;31(11):1133-1140. doi:10.1016/0024-3205(82)90087-x
180. Van de Wiele C, Dumont F, Vanden Broecke R, et al. Technetium-99m RP527, a GRP analogue for visualisation of GRP receptor-expressing malignancies: a feasibility study. *Eur J Nucl Med*. 2000;27(11):1694-1699. doi:10.1007/s002590000355
181. Lantry LE, Cappelletti E, Maddalena ME, et al. 177Lu-AMBA: Synthesis and Characterization of a Selective 177Lu-Labeled GRP-R Agonist for Systemic Radiotherapy of Prostate Cancer. *J Nucl Med*. 2006;47(7):1144-1152.
182. Schroeder RPJ, van Weerden WM, Krenning EP, et al. Gastrin-releasing peptide receptor-based targeting using bombesin analogues is superior to metabolism-based targeting using choline for in vivo imaging of human prostate cancer xenografts. *Eur J Nucl Med Mol Imaging*. 2011;38(7):1257-1266. doi:10.1007/s00259-011-1775-3
183. Prignon A, Nataf V, Provost C, et al. 68Ga-AMBA and 18F-FDG for preclinical PET imaging of breast cancer: effect of tamoxifen treatment on tracer uptake by tumor. *Nucl Med Biol*. 2015;42(2):92-98. doi:10.1016/j.nucmedbio.2014.10.003
184. Baum RP, Prasad V, Mutloka N, Frischnecht M, Maecke H, Reubi J. Molecular imaging of bombesin receptors in various tumors by Ga-68 AMBA PET/CT: First results. *J Nucl Med*. 2007;48(2):79P.
185. Mansi R, Nock BA, Dalm SU, Busstra MB, van Weerden WM, Maina T. Radiolabeled Bombesin Analogs. *Cancers*. 2021;13(22):5766. doi:10.3390/cancers13225766
186. Bodei L, Ferrari M, Nunn A, et al. 177Lu-AMBA bombesin analogue in hormone refractory prostate cancer patients: A phase I escalation study with single-cycle administrations. *Eur J Nucl Med Mol Imaging*. 2007;34:S221.
187. Cuttitta F, Carney DN, Mulshine J, et al. Bombesin-like peptides can function as autocrine growth factors in human small-cell lung cancer. *Nature*. 1985;316(6031):823-826. doi:10.1038/316823a0
188. Preston SR, Miller GV, Primrose JN. Bombesin-like peptides and cancer. *Crit Rev Oncol Hematol*. 1996;23(3):225-238. doi:10.1016/1040-8428(96)00204-1
189. Milovanovic SR, Radulovic S, Groot K, Schally AV. Inhibition of growth of PC-82 human prostate cancer line xenografts in nude mice by bombesin antagonist RC-3095 or combination of agonist [D-Trp6]-luteinizing hormone-releasing hormone and somatostatin analog RC-160. *Prostate*. 1992;20(4):269-280. doi:10.1002/pros.2990200403
190. Miyazaki M, Lamharzi N, Schally AV, et al. Inhibition of growth of MDA-MB-231 human breast cancer xenografts in nude mice by bombesin/gastrin-releasing peptide (GRP) antagonists RC-3940-II and RC-3095. *Eur J Cancer*. 1998;34(5):710-717. doi:10.1016/S0959-8049(97)10123-X
191. Cescato R, Maina T, Nock B, et al. Bombesin Receptor Antagonists May Be Preferable to Agonists for Tumor Targeting. *J Nucl Med*. 2008;49(2):318-326. doi:10.2967/jnumed.107.045054
192. Mansi R, Wang X, Forrer F, et al. Evaluation of a 1,4,7,10-Tetraazacyclododecane-1,4,7,10-Tetraacetic Acid–Conjugated Bombesin-Based Radioantagonist for the Labeling with Single-Photon Emission Computed Tomography, Positron Emission Tomography, and Therapeutic Radionuclides. *Clin Cancer Res*. 2009;15(16):5240-5249. doi:10.1158/1078-0432.CCR-08-3145

193. Wang LH, Coy DH, Taylor JE, et al. des-Met carboxyl-terminally modified analogues of bombesin function as potent bombesin receptor antagonists, partial agonists, or agonists. *J Biol Chem*. 1990;265(26):15695-15703. doi:10.1016/S0021-9258(18)55454-5
194. Nock B, Nikolopoulou A, Chiotellis E, et al. [99mTc]Demobesin 1, a novel potent bombesin analogue for GRP receptor-targeted tumour imaging. *Eur J Nucl Med Mol Imaging*. 2003;30(2):247-258. doi:10.1007/s00259-002-1040-x
195. Maina T, Bergsma H, Kulkarni HR, et al. Preclinical and first clinical experience with the gastrin-releasing peptide receptor-antagonist [68Ga]SB3 and PET/CT. *Eur J Nucl Med Mol Imaging*. 2016;43(5):964-973. doi:10.1007/s00259-015-3232-1
196. Bakker IL, Fröberg AC, Busstra MB, et al. GRPr Antagonist 68Ga-SB3 PET/CT Imaging of Primary Prostate Cancer in Therapy-Naïve Patients. *J Nucl Med*. 2021;62(11):1517-1523. doi:10.2967/jnumed.120.258814
197. Lymperis E, Kaloudi A, Sallegger W, et al. Radiometal-Dependent Biological Profile of the Radiolabeled Gastrin-Releasing Peptide Receptor Antagonist SB3 in Cancer Theranostics: Metabolic and Biodistribution Patterns Defined by Neprilysin. *Bioconjug Chem*. 2018;29(5):1774-1784. doi:10.1021/acs.bioconjchem.8b00225
198. Nock BA, Kaloudi A, Kanellopoulos P, et al. [99mTc]Tc-DB15 in GRPR-Targeted Tumor Imaging with SPECT: From Preclinical Evaluation to the First Clinical Outcomes. *Cancers*. 2021;13(20):5093. doi:10.3390/cancers13205093
199. Heimbrook DC, Saari WS, Balishin NL, et al. Gastrin releasing peptide antagonists with improved potency and stability. *J Med Chem*. 1991;34(7):2102-2107. doi:10.1021/jm00111a027
200. Dalm SU, Bakker IL, de Blois E, et al. 68Ga/177Lu-NeoBOMB1, a Novel Radiolabeled GRPR Antagonist for Theranostic Use in Oncology. *J Nucl Med*. 2017;58(2):293-299. doi:10.2967/jnumed.116.176636
201. Ruigrok EAM, Verhoeven M, Konijnenberg MW, et al. Safety of [177Lu]Lu-NeoB treatment: a preclinical study characterizing absorbed dose and acute, early, and late organ toxicity. *Eur J Nucl Med Mol Imaging*. 2022;49(13):4440-4451. doi:10.1007/s00259-022-05926-2
202. Nock BA, Kaloudi A, Lymperis E, et al. Theranostic Perspectives in Prostate Cancer with the Gastrin-Releasing Peptide Receptor Antagonist NeoBOMB1: Preclinical and First Clinical Results. *J Nucl Med*. 2017;58(1):75-80. doi:10.2967/jnumed.116.178889
203. Llinares M, Devin C, Chaloin O, et al. Syntheses and biological activities of potent bombesin receptor antagonists: Bombesin receptor antagonists. *J Pept Res*. 1999;53(3):275-283. doi:10.1034/j.1399-3011.1999.00028.x
204. Varasteh Z, Åberg O, Velikyan I, et al. In Vitro and In Vivo Evaluation of a 18F-Labeled High Affinity NOTA Conjugated Bombesin Antagonist as a PET Ligand for GRPR-Targeted Tumor Imaging. Gelovani JG, ed. *PLoS ONE*. 2013;8(12):e81932. doi:10.1371/journal.pone.0081932
205. Mitran B, Thisgaard H, Rosenström U, et al. High Contrast PET Imaging of GRPR Expression in Prostate Cancer Using Cobalt-Labeled Bombesin Antagonist RM26. *Contrast Media Mol Imaging*. 2017;2017:6873684. doi:10.1155/2017/6873684
206. Mitran B, Rinne SS, Konijnenberg MW, et al. Trastuzumab cotreatment improves survival of mice with PC-3 prostate cancer xenografts treated with the GRPR antagonist ^{177}Lu-DOTAGA-PEG$_2$-RM26. *Int J Cancer*. 2019;145(12):3347-3358. doi:10.1002/ijc.32401

207. Varasteh Z, Velikyan I, Lindeberg G, et al. Synthesis and Characterization of a High-Affinity NOTA-Conjugated Bombesin Antagonist for GRPR-Targeted Tumor Imaging. *Bioconjug Chem*. 2013;24(7):1144-1153. doi:10.1021/bc300659k
208. Zhang J, Niu G, Fan X, et al. PET Using a GRPR Antagonist ^{68}Ga-RM26 in Healthy Volunteers and Prostate Cancer Patients. *J Nucl Med*. 2018;59(6):922-928. doi:10.2967/jnumed.117.198929
209. Mansi R, Wang X, Forrer F, et al. Development of a potent DOTA-conjugated bombesin antagonist for targeting GRPr-positive tumours. *Eur J Nucl Med Mol Imaging*. 2011;38(1):97-107. doi:10.1007/s00259-010-1596-9
210. Kähkönen E, Jambor I, Kemppainen J, et al. In vivo imaging of prostate cancer using [68Ga]-labeled bombesin analog BAY86-7548. *Clin Cancer Res*. 2013;19(19):5434-5443. doi:10.1158/1078-0432.CCR-12-3490
211. Stoykow C, Erbes T, Maecke HR, et al. Gastrin-releasing Peptide Receptor Imaging in Breast Cancer Using the Receptor Antagonist (68)Ga-RM2 And PET. *Theranostics*. 2016;6(10):1641-1650. doi:10.7150/thno.14958
212. Minamimoto R, Sonni I, Hancock S, et al. Prospective Evaluation of 68Ga-RM2 PET/MRI in Patients with Biochemical Recur-rence of Prostate Cancer and Negative Findings on Conventional Imaging. *J Nucl Med*. 2018;59(5):803-808. doi:10.2967/jnumed.117.197624
213. Touijer KA, Michaud L, Alvarez HAV, et al. Prospective Study of the Radiolabeled GRPR Antagonist BAY86-7548 for Positron Emission Tomography/Computed Tomography Imaging of Newly Diagnosed Prostate Cancer. *Eur Urol Oncol*. 2019;2(2):166-173. doi:10.1016/j.euo.2018.08.011
214. Fassbender TF, Schiller F, Mix M, et al. Accuracy of [68Ga]Ga-RM2-PET/CT for diagnosis of primary prostate cancer compared to histopathology. *Nucl Med Biol*. 2019;70:32-38. doi:10.1016/j.nucmedbio.2019.01.009
215. Morgat C, Schollhammer R, Macgrogan G, et al. Comparison of the binding of the gastrin-releasing peptide receptor (GRP-R) antagonist 68Ga-RM2 and 18F-FDG in breast cancer samples. Ahmad A, ed. *PLOS ONE*. 2019;14(1):e0210905. doi:10.1371/journal.pone.0210905
216. Kurth J, Krause BJ, Schwarzenböck SM, Bergner C, Hakenberg OW, Heuschkel M. First-in-human dosimetry of gastrin-releasing peptide receptor antagonist [177Lu]Lu-RM2: a radiopharmaceutical for the treatment of metastatic castration-resistant prostate cancer. *Eur J Nucl Med Mol Imaging*. 2020;47(1):123-135. doi:10.1007/s00259-019-04504-3
217. Lau J, Rousseau E, Zhang Z, et al. Positron Emission Tomography Imaging of the Gastrin-Releasing Peptide Receptor with a Novel Bombesin Analogue. *ACS Omega*. 2019;4(1):1470-1478. doi:10.1021/acsomega.8b03293
218. Minamimoto R, Hancock S, Schneider B, et al. Pilot Comparison of ^{68}Ga-RM2 PET and ^{68}Ga-PSMA-11 PET in Patients with Biochemically Recurrent Prostate Cancer. *J Nucl Med*. 2016;57(4):557-562. doi:10.2967/jnumed.115.168393
219. Iagaru A. Will GRPR Compete with PSMA as a Target in Prostate Cancer? *J Nucl Med*. 2017;58(12):1883-1884. doi:10.2967/jnumed.117.198192
220. Schollhammer R, De Clermont Gallerande H, Yacoub M, et al. Comparison of the radiolabeled PSMA-inhibitor 111In-PSMA-617 and the radiolabeled GRP-R antagonist 111In-RM2 in primary prostate cancer samples. *EJNMMI Res*. 2019;9(1):52. doi:10.1186/s13550-019-0517-6
221. Baratto L, Song H, Duan H, et al. PSMA- and GRPR-Targeted PET: Results from 50 Patients with Biochemically Recurrent Prostate Cancer. *J Nucl Med*. 2021;62(11):1545-1549. doi:10.2967/jnumed.120.259630

222. Gao X, Tang Y, Chen M, et al. A prospective comparative study of [68Ga]Ga-RM26 and [68Ga]Ga-PSMA-617 PET/CT imaging in suspicious prostate cancer. *Eur J Nucl Med Mol Imaging*. Published online 2023. doi:10.1007/s00259-023-06142-2
223. Eder M, Schäfer M, Bauder-Wüst U, Haberkorn U, Eisenhut M, Kopka K. Preclinical evaluation of a bispecific low-molecular heterodimer targeting both PSMA and GRPR for improved PET imaging and therapy of prostate cancer. *The Prostate*. 2014;74(6):659-668. doi:10.1002/pros.22784
224. Bandari RP, Jiang Z, Reynolds TS, et al. Synthesis and biological evaluation of copper-64 radiolabeled [DUPA-6-Ahx-(NODAGA)-5-Ava-BBN(7-14)NH2], a novel bivalent targeting vector having affinity for two distinct biomarkers (GRPr/PSMA) of prostate cancer. *Nucl Med Biol*. 2014;41(4):355-363. doi:10.1016/j.nucmedbio.2014.01.001
225. Mitran B, Varasteh Z, Abouzayed A, et al. Bispecific GRPR-Antagonistic Anti-PSMA/GRPR Heterodimer for PET and SPECT Diagnostic Imaging of Prostate Cancer. *Cancers*. 2019;11(9):1371. doi:10.3390/cancers11091371
226. Liolios C, Schäfer M, Haberkorn U, Eder M, Kopka K. Novel Bispecific PSMA/GRPr Targeting Radioligands with Optimized Pharmacokinetics for Improved PET Imaging of Prostate Cancer. *Bioconjug Chem*. 2016;27(3):737-751. doi:10.1021/acs.bioconjchem.5b00687
227. Bandari RP, Carmack TL, Malhotra A, et al. Development of Heterobivalent Theranostic Probes Having High Affinity/Selectivity for the GRPR/PSMA. *J Med Chem*. 2021;64(4):2151-2166. doi:10.1021/acs.jmedchem.0c01785
228. Ye S, Li H, Hu K, et al. Radiosynthesis and biological evaluation of 18F-labeled bispecific heterodimer targeted dual gastrin-releasing peptide receptor and prostate-specific membrane antigen for prostate cancer imaging. *Nucl Med Commun*. 2022;43(3):323-331. doi:10.1097/MNM.0000000000001520
229. Rivera-Bravo B, Ramírez-Nava G, Mendoza-Figueroa MJ, et al. [68Ga]Ga-iPSMA-Lys3-Bombesin: Biokinetics, dosimetry and first patient PET/CT imaging. *Nucl Med Biol*. 2021;96-97:54-60. doi:10.1016/j.nucmedbio.2021.03.005
230. Mitran B, Varasteh Z, Selvaraju RK, et al. Selection of optimal chelator improves the contrast of GRPR imaging using bombesin analogue RM26. *Int J Oncol*. 2016;48(5):2124-2134. doi:10.3892/ijo.2016.3429
231. Chitneni SK, Koumarianou E, Vaidyanathan G, Zalutsky MR. Observations on the Effects of Residualization and Dehalogenation on the Utility of N-Succinimidyl Ester Acylation Agents for Radioiodination of the Internalizing Antibody Trastuzumab. *Molecules*. 2019;24(21):3907. doi:10.3390/molecules24213907
232. Hoffman TJ, Gali H, Smith CJ, et al. Novel Series of 111In-Labeled Bombesin Analogs as Potential Radiopharmaceuticals for Specific Targeting of Gastrin-Releasing Peptide Receptors Expressed on Human Prostate Cancer Cells. *J Nucl Med*. 2003;44(5):823-831.
233. Varasteh Z, Rosenström U, Velikyan I, et al. The Effect of Mini-PEG-Based Spacer Length on Binding and Pharmacokinetic Properties of a 68Ga-Labeled NOTA-Conjugated Antagonistic Analog of Bombesin. *Molecules*. 2014;19(7):10455-10472. doi:10.3390/molecules190710455
234. Dijkgraaf I, Liu S, Kruijtzer JAW, et al. Effects of linker variation on the in vitro and in vivo characteristics of an 111In-labeled RGD peptide. *Nucl Med Biol*. 2007;34(1):29-35. doi:10.1016/j.nucmedbio.2006.10.006

235. Jamous M, Tamma ML, Gourni E, et al. PEG spacers of different length influence the biological profile of bombesin-based radiolabeled antagonists. *Nucl Med Biol*. 2014;41(6):464-470. doi:10.1016/j.nucmedbio.2014.03.014
236. Lee S, Xie J, Chen X. Peptide-Based Probes for Targeted Molecular Imaging. *Biochemistry*. 2010;49(7):1364-1376. doi:10.1021/bi901135x
237. Boerman OC, Oyen WJG, Corstens FHM. Radio-labeled receptor-binding peptides: A new class of radiopharmaceuticals. *Semin Nucl Med*. 2000;30(3):195-208. doi:10.1053/snuc.2000.7441
238. Dreher MR, Liu W, Michelich CR, Dewhirst MW, Yuan F, Chilkoti A. Tumor Vascular Permeability, Accumulation, and Penetration of Macromolecular Drug Carriers. *JNCI J Natl Cancer Inst*. 2006;98(5):335-344. doi:10.1093/jnci/djj070
239. Reubi JC, Maecke HR. Peptide-Based Probes for Cancer Imaging. *J Nucl Med*. 2008;49(11):1735-1738. doi:10.2967/jnumed.108.053041
240. Kratz F. Albumin as a drug carrier: Design of prodrugs, drug conjugates and nanoparticles. *J Controlled Release*. 2008;132(3):171-183. doi:10.1016/j.jconrel.2008.05.010
241. Wang Z, Tian R, Niu G, et al. Single Low-Dose Injection of Evans Blue Modified PSMA-617 Radioligand Therapy Eliminates Prostate-Specific Membrane Antigen Positive Tumors. *Bioconjug Chem*. 2018;29(9):3213-3221. doi:10.1021/acs.bioconjchem.8b00556
242. Benešová M, Umbricht CA, Schibli R, Müller C. Albumin-Binding PSMA Ligands: Optimization of the Tissue Distribution Profile. *Mol Pharm*. 2018;15(3):934-946. doi:10.1021/acs.molpharmaceut.7b00877
243. Deberle LM, Benešová M, Umbricht CA, et al. Development of a new class of PSMA radioligands comprising ibuprofen as an albumin-binding entity. *Theranostics*. 2020;10(4):1678-1693. doi:10.7150/thno.40482
244. van Kalmthout LWM, Lam MGEH, de Keizer B, et al. Impact of external cooling with icepacks on 68Ga-PSMA uptake in salivary glands. *EJNMMI Res*. 2018;8(1):56. doi:10.1186/s13550-018-0408-2
245. Bushara KO. Sialorrhea in amyotrophic lateral sclerosis: a hypothesis of a new treatment - botulinum toxin A injections of the parotid glands. *Med Hypotheses*. 1997;48(4):337-339. doi:10.1016/S0306-9877(97)90103-1
246. Rodwell K, Edwards P, Ware RS, Boyd R. Salivary gland botulinum toxin injections for drooling in children with cerebral palsy and neurodevelopmental disability: a systematic review: BoNT for Drooling in CP and Neurodevelopmental Disability. *Dev Med Child Neurol*. 2012;54(11):977-987. doi:10.1111/j.1469-8749.2012.04370.x
247. Baum RP, Langbein T, Singh A, et al. Injection of Botulinum Toxin for Preventing Salivary Gland Toxicity after PSMA Radioligand Therapy: an Empirical Proof of a Promising Concept. *Nucl Med Mol Imaging*. 2018;52(1):80-81. doi:10.1007/s13139-017-0508-3
248. Kratochwil C, Giesel FL, Leotta K, et al. PMPA for Nephroprotection in PSMA-Targeted Radionuclide Therapy of Prostate Cancer. *J Nucl Med*. 2015;56(2):293-298. doi:10.2967/jnumed.114.147181
249. Borgna F, Deberle LM, Cohrs S, Schibli R, Müller C. Combined Application of Albumin-Binding [177Lu]Lu-PSMA-ALB-56 and Fast-Cleared PSMA Inhibitors: Optimization of the Pharmacokinetics. *Mol Pharm*. 2020;17(6):2044-2053. doi:10.1021/acs.molpharmaceut.0c00199
250. Comper WD, Glasgow EF. Charge selectivity in kidney ultrafiltration. *Kidney Int*. 1995;47(5):1242-1251. doi:10.1038/ki.1995.178

251. Hammond P, Wade A, Gwilliam M, et al. Amino acid infusion blocks renal tubular uptake of an indium-labelled somatostatin analogue. *Br J Cancer*. 1993;67(6):1437-1439. doi:10.1038/bjc.1993.266
252. Arano Y. Renal brush border strategy: A developing procedure to reduce renal radioactivity levels of radiolabeled polypeptides. *Nucl Med Biol*. 2021;92:149-155. doi:10.1016/j.nucmedbio.2020.03.001
253. Altai M, Membreno R, Cook B, Tolmachev V, Zeglis BM. Pretargeted Imaging and Therapy. *J Nucl Med*. 2017;58(10):1553-1559. doi:10.2967/jnumed.117.189944
254. Verhoeven, Seimbille, Dalm. Therapeutic Applications of Pretargeting. *Pharmaceutics*. 2019;11(9):434. doi:10.3390/pharmaceutics11090434
255. Ramnaraign B, Sartor O. PSMA-Targeted Radiopharmaceuticals in Prostate Cancer: Current Data and New Trials. *The Oncologist*. Published online February 18, 2023:oyac279. doi:10.1093/oncolo/oyac279
256. Jonsson A, Dogan J, Herne N, Abrahmsen L, Nygren PA. Engineering of a femtomolar affinity binding protein to human serum albumin. *Protein Eng Des Sel*. 2008;21(8):515-527. doi:10.1093/protein/gzn028
257. Tolmachev V, Orlova A, Pehrson R, et al. Radionuclide Therapy of HER2-Positive Microxenografts Using a 177Lu-Labeled HER2-Specific Affibody Molecule. *Cancer Res*. 2007;67(6):2773-2782. doi:10.1158/0008-5472.CAN-06-1630
258. Frejd FY, Kim KT. Affibody molecules as engineered protein drugs. *Exp Mol Med*. 2017;49(3):e306. doi:10.1038/emm.2017.35
259. Van den Wyngaert T, Elvas F, De Schepper S, Kennedy JA, Israel O. SPECT/CT: Standing on the Shoulders of Giants, It Is Time to Reach for the Sky! *J Nucl Med*. 2020;61(9):1284-1291. doi:10.2967/jnumed.119.236943
260. Blok D, Feitsma HIJ, Kooy YMC, et al. New chelation strategy allows for quick and clean 99mTc-labeling of synthetic peptides. *Nucl Med Biol*. 2004;31(6):815-820. doi:10.1016/j.nucmedbio.2004.02.009
261. Ahlgren S, Andersson K, Tolmachev V. Kit formulation for 99mTc-labeling of recombinant anti-HER2 Affibody molecules with a C-terminally engineered cysteine. *Nucl Med Biol*. 2010;37(5):539-546. doi:10.1016/j.nucmedbio.2010.02.009
262. Engfeldt T, Tran T, Orlova A, et al. 99mTc-chelator engineering to improve tumour targeting properties of a HER2-specific Affibody molecule. *Eur J Nucl Med Mol Imaging*. 2007;34(11):1843-1853. doi:10.1007/s00259-007-0474-6
263. Pienta KJ, Gorin MA, Rowe SP, et al. A Phase 2/3 Prospective Multicenter Study of the Diagnostic Accuracy of Prostate Specific Membrane Antigen PET/CT with 18F-DCFPyL in Prostate Cancer Patients (OSPREY). *J Urol*. 2021;206(1):52-61. doi:10.1097/JU.0000000000001698
264. von Eyben FE, Picchio M, von Eyben R, Rhee H, Bauman G. 68Ga-Labeled Prostate-specific Membrane Antigen Ligand Positron Emission Tomography/Computed Tomography for Prostate Cancer: A Systematic Review and Meta-analysis. *Eur Urol Focus*. 2018;4(5):686-693. doi:10.1016/j.euf.2016.11.002
265. Morgat C, MacGrogan G, Brouste V, et al. Expression of Gastrin-Releasing Peptide Receptor in Breast Cancer and Its Association with Pathologic, Biologic, and Clinical Parameters: A Study of 1,432 Primary Tumors. *J Nucl Med*. 2017;58(9):1401-1407. doi:10.2967/jnumed.116.188011
266. Bertaccini G, Impicciatore M. Action of bombesin on the motility of the stomach. *Naunyn Schmiedebergs Arch Pharmacol*. 1975;289(2):149-156. doi:10.1007/BF00501302

267. Rashid NS, Grible JM, Clevenger CV, Harrell JC. Breast cancer liver metastasis: current and future treatment approaches. *Clin Exp Metastasis*. 2021;38(3):263-277. doi:10.1007/s10585-021-10080-4

Acta Universitatis Upsaliensis

Digital Comprehensive Summaries of Uppsala Dissertations from the Faculty of Pharmacy 335

Editor: The Dean of the Faculty of Pharmacy

A doctoral dissertation from the Faculty of Pharmacy, Uppsala University, is usually a summary of a number of papers. A few copies of the complete dissertation are kept at major Swedish research libraries, while the summary alone is distributed internationally through the series Digital Comprehensive Summaries of Uppsala Dissertations from the Faculty of Pharmacy. (Prior to January, 2005, the series was published under the title "Comprehensive Summaries of Uppsala Dissertations from the Faculty of Pharmacy".)

Distribution: publications.uu.se
urn:nbn:se:uu:diva-501391

ACTA UNIVERSITATIS
UPSALIENSIS
2023